The Lomfjorden Fault Zone in eastern Spitsbergen (Svalbard)

NOT FINAL

Karsten Piepjohn[1], Winfried Dallmann[2], and Synnøve Elvevold[3]

[1]*Federal Institute for Geosciences and Natural Resources, Stilleweg 2, 30655 Hannover, Germany, Karsten.Piepjohn@bgr.de*

[2]*Institute of Geosciences, UiT The Arctic University of Norway, P.O.Box 5060 Langnes, 9037 Tromsø, Norway, winfried.dallmann@uit.no*

[3]*Norsk Polarinstitutt, Framsenteret, Hjalmar Johansens gate 14, 9296 Tromsø, Norway, elvevold@npolar.no*

ABSTRACT

The Lomfjorden Fault Zone in the eastern part of Spitsbergen is one of the prominent structures in Svalbard oriented parallel to the continental margin of the Barents Shelf. It consists of a network of three N–S striking major faults (Veteranen, Lomfjorden, and Agardhbukta faults), two N–S striking reverse faults (Lomfjella and Bjørnfjellet reverse faults), and a number of NE–SW and NNW–SSE striking normal, reverse, and strike-slip faults. Structural data collected during fieldwork in the northern and central segments of the fault zone, in combination with published data from the southernmost segment, indicate that N–S striking reverse faults in the Lomfjorden Fault Zone were caused by convergence transferred from the West Spitsbergen Fold-and-Thrust Belt eastwards along detachments during an initial phase of the Eurekan deformation in the early Eocene. The W–E contraction was followed by sinistral and dextral strike-slip tectonics along the Lomfjorden Fault Zone during a later phase of the Eurekan deformation in the late Eocene. The NNW–SSE striking reverse and normal faults are oriented obliquely between the N–S striking, en-échelon Lomfjorden and Agardhbukta faults. Shortening and extension across these, respectively, can be explained by left-stepping contractional overstep or left-stepping wrench faults in an overall dextral and left-stepping extensional overstep or left-stepping wrench faults in an overall sinistral, N–S trending strike-slip system. It was not possible

to determine if the sinistral phase pre-dated the dextral one or vice versa. The presence of a large granite massif, the Newtontoppen Granite, is suspected to influence or even control the course of the faults and their transfer systems. The involvement and reactivation of pre-existing Carboniferous and even older structures and the superimposition of convergent and lateral movements along the Lomfjorden Fault Zone is similar to large fault zones in North Greenland and on Ellesmere Island, indicating that it represents an important element of the Eurekan Orogeny during the final break-up of Laurasia.

INTRODUCTION

The archipelago of Svalbard is located at the northwestern margin of the Barents Shelf (Fig. 1). In the eastern part of the main island of Spitsbergen, two major N–S striking fault zones are exposed. The western one is the Billefjorden Fault Zone in central-eastern Spitsbergen (e.g., Harland et al., 1974; Manby, 1990; Manby et al., 1994; McCann and Dallmann, 1996; Harland, 1997; Maher and Braathen, 2011; Braathen et al., 2011; Dallmann, 2015), separating the Northeastern Basement Province and the Devonian Andrée Land Basin (Old Red Sandstone) (Fig. 2A). The eastern one is the Lomfjorden Fault Zone, which consists of three N–S striking major faults (Dallmann, 2015). The western fault is represented by the Veteranen Fault or 'Veteranen Line' (Harland et al., 1992; Harland, 1997), which sub-divides the Northeastern Basement Province into the Western Ny-Friesland Terrane in the W and the Nordaustlandet Terrane in the E (e.g., Gee et al., 1995; Harland, 1997; Gee and Teben'kov, 2004; Fig. 2A). The central fault is the Lomfjorden Fault, which separates Neoproterozoic rocks in the W, partly overlain by Early Carboniferous deposits, from middle Carboniferous and younger sedimentary rocks in the E (Figs. 2B and 3). The eastern fault of the Lomfjorden Fault Zone is the Agardhbukta Fault (Akademikarbreen Fault in Dallmann, 2015; Fig. 2B), which continues southwards to Agardhdalen W of Storfjorden (Miloslavskij et al., 1993b). Prior to this study, the Lomfjorden and Agardhbukta faults were shown as a single, curved fault on most geological overview maps (Nathorst, 1910; Odell, 1927; Frebold, 1935; Hjelle and Lauritzen, 1982; Harland, 1979, 1997; Dallmann et al., 2002). Another fault exists E of the Lomfjorden Fault Zone: the Storfjorden Fault Zone was detected by seismic observations in Storfjorden between

Spitsbergen in the W and Barentsøya and Edgeøya in the E (Eiken, 1985; Fig. 2A). It is suggested to continue northward along the glacier Hinlopenbreen (Fig. 3) with a northward-decreasing offset (Dallmann, 2015).

Most authors agree that the dominant tectonic activity in the southern segment of the Lomfjorden Fault Zone occurred in the Paleogene (e.g., Kellogg, 1975; Harland, 1979; Andresen et al., 1988, 1992, 1994; Larsen, 1988; Nøttvedt et al., 1988; Miloslavskij et al., 1993b). During that time, the western part of Spitsbergen was affected by significant folding and thrusting related to the formation of the West Spitsbergen Fold-and-Thrust Belt (e.g., Harland, 1969, 1973a, b, 1997; Birkenmajer, 1972a, b, 1981; Harland and Horsfield, 1974; Maher and Craddock, 1988; Dallmann et al., 1993; Braathen et al., 1995; Bergh et al., 1997; Tessensohn, 2001; Bergh and Grogan, 2003; Leever et al., 2011; Dallmann, 2015: Fig. 2A). Equivalent fold-and-thrust belt structures occur in North Greenland (e.g., Soper et al., 1982; Soper and Higgins, 1991; von Gosen and Piepjohn, 1999, 2003; Piepjohn and von Gosen, 2001; Tegner et al., 2011) and in the Canadian Arctic Archipelago where they are considered as a consequence of the Eurekan Orogeny (e.g., Thorsteinsson and Tozer, 1970; Higgins and Soper, 1983; Okulitch and Trettin, 1991; Piepjohn et al., 2000b, 2008; Saalmann et al., 2005, 2008; Harrison, 2008; Tessensohn et al., 2008; von Gosen et al., 2008).

The southernmost segment of the Lomfjorden Fault Zone (Fig. 2B) displays orthogonal contraction during the Paleogene formation of the West Spitsbergen Fold-and-Thrust Belt (Kellogg, 1975; Andresen et al., 1988, 1992, 1994; Larsen, 1988; Nøttvedt et al., 1988; Miloslavskij et al., 1993b). Until now, little is known about the structural architecture, kinematics, and age of deformations along the northern and central segments of the Lomfjorden Fault Zone (Fig. 2B). Before, it was interpreted either as a down-to-the-east normal fault on previous geological maps (Hjelle and Lauritzen, 1982; Harland, 1997) or as dominated by reverse faults due to W–E shortening (Bergh et al., 1994).

In this paper, we describe results of structural fieldwork during the 2001-2009 Norwegian mapping program (Dallmann et al., 2009, 2011) in the northern and central segments of the Lomfjorden Fault Zone. The main study area was situated in the eastern part of Ny-Friesland between Kapp Fanshawe in the N and Andromedafjellet in the S (Fig. 3). In addition, some outcrops were studied in Olav V Land between Pachtusovfjellet and Malte Brunfjellet (Fig. 2B). Our results lead to kinematic interpretations of the brittle fault tectonics in the area, which support previously documented convergent tectonics across the fault zone (Andresen et al., 1988, 1992, 1994; Haremo and Andresen, 1992; Miloslavskij et al., 1993b; Bergh et al., 1994). In addition, field observations show that the northern and central segments of the Lomfjorden Fault Zone were also affected by strike-slip deformation. The convergent and lateral displacements can be linked to movements along the southernmost segment of the fault zone and to the West Spitsbergen Fold-and-Thrust Belt.

GEOLOGIC SETTING

The basement in northeastern Spitsbergen consists of Meso- and Paleoproterozoic high-grade metamorphic rocks of the Atomfjella Complex in the W (Western Ny-Friesland Terrane) and low-grade metamorphic to unmetamorphosed Neoproterozoic to Early Paleozoic sedimentary rocks of the Lomfjorden Supergroup in the E (Nordaustlandet Terrane; Fig. 2A). These terranes are separated by the Eolussletta Shear Zone (see below) with the 'Veteranen Line' (Harland et al., 1992; Harland, 1997) or Veteranen Fault marking the eastern boundary of the ductile shear zone (Figs. 3 and 4).

The more than 5 km thick succession of unmetamorphosed to low-grade sedimentary rocks E of the Veteranen Fault is subdivided into the Neoproterozoic Veteranen, Akademikarbreen, Polarisbreen, and the Cambro-Ordovician Oslobreen groups (Harland et al., 1966; Harland, 1997). The succession was folded during the main phase of the Caledonian Orogeny (e.g., Harland et al., 1992; Harland, 1997; Dallmann, 2015). The structural architecture is dominated by km-scale, NNW–SSE to N–S trending anticlines and synclines and some steeply W-dipping reverse faults (Figs. 3 and 4). The Caledonian F_1-folds are characterized by moderately to steeply WSW- and ENE-dipping limbs, subvertical axial planes, subvertical cleavage planes S_1, and approximately N–S trending δ_1-intersection lineations parallel to B_1-fold axes (Fig. 5).

The late Caledonian development was characterized by ductile to brittle sinistral shearing along the Billefjorden Fault Zone in Late Silurian and Early Devonian times (Manby et al., 1994) and by the juxtaposition of the Western Ny-Friesland and the Nordaustlandet terranes along the Eolussletta Shear Zone (Manby, 1990; Manby and Lyberis, 1992; Manby et al., 1994; Lyberis and Manby, 1999; Figs. 3 and 4). The latest phase of the Caledonian Orogeny is represented by the intrusion of undeformed, post-tectonic granitoids of the Chydeniusbreen Granitoid Suite, consisting mainly of the Newtontoppen Granite (Fig. 3) with Silurian to Devonian ages of 385 – 406 Ma (K-Ar, Gayer et al., 1966), 432 ± 10 Ma (Rb-Sr, Teben'kov et al., 1996), and 430 ± 0.7 Ma (U-Pb, Myhre, 2005).

The Caledonian Orogeny was followed by the development of the Old Red Sandstone basin W of the Billefjorden Fault Zone during the latest Silurian (?) and entire Devonian (e.g., Suess, 1888; Frebold, 1935; Orvin, 1940; Friend, 1961; Gee and Moody-Stuart, 1966; Murašov and Mokin, 1979; Piepjohn et al., 2000a; Piepjohn and Dallmann, 2014; Fig. 2A). The sedimentary succession of the Old Red Sandstone basin was deformed during the Svalbardian (=Ellesmerian) Event (e.g., Vogt, 1928; Friend and Moody-Stuart, 1972; Piepjohn, 1994, 2000; McCann, 2000; Piepjohn et al., 2000a). It is still a matter of debate whether the Svalbardian deformation was caused by sinistral strike-slip or by E–W shortening (e.g., Harland et al., 1974; Lamar et al., 1986; Manby et al., 1994; Piepjohn, 1994, 2000; McCann and Dallmann, 1996; Bergh et al., 2011). It should be noted that no Svalbardian structures have been found so far in the Northeastern Basement Province E of the Billefjorden Fault Zone (Dallmann, 2015).

The Svalbardian Event was followed by the deposition of the Viséan to possibly lowermost Serpukhovian Billefjorden Group (Playford, 1962/63; Cutbill and Challinor, 1965; Scheibner et al., 2012). Deposits of this unit occur on the mountain plateau of Lomfjella to the W of the Lomfjorden Fault (Fig. 3), where they unconformably overly Neoproterozoic rocks of the Veteranen Group. An isolated and small occurrence of coaly shales and approximately 100 m of poorly exposed red clastic sedimentary rocks within a NNE–SSW striking fault-bounded slice within a branch of the Lomfjorden Fault located S of Kapp Fanshawe (Dallmann et al., 2009), has yielded a similar palynological age (Scheibner et al., 2012; Fig. 3). Apart from this exposure, the Billefjorden Group does not occur E of the Lomfjorden Fault. This suggests that the

Lomfjorden Fault was already active in the early Carboniferous (Bergh et al., 1994; Dallmann, 2015).

In the middle to late Carboniferous, Spitsbergen was a site of halfgraben formation, such as the St. Jonsfjorden and Billefjorden troughs (Cutbill and Challinor, 1965; Steel and Worsley, 1984; Dallmann, 1999, 2015, and references therein; Braathen et al., 2011). Red sandstone and shale of the middle Carboniferous Malte Brunfjellet Formation occur in the vicinity of the Lomfjorden Fault with a possible extent eastwards to Nordaustlandet – collectively assigned to the Lomfjorden Basin (Dallmann, 2015). After the Moscovian, most of the large fault zones in Svalbard were apparently more or less inactive until the beginning of the break-up of the Arctic and North Atlantic oceans.

The youngest deposits in the study area are mostly horizontal strata of late Carboniferous to Permian limestones of the Gipsdalen Group (Wordiekammen and Gipshuken formations) and sandstones and cherts of the Tempelfjorden Group (Kapp Starostin Formation). They unconformably overlie the folded Neoproterozoic sedimentary successions E of the Lomfjorden Fault (Dallmann et al., 2009, 2011; Fig. 4) and also the middle Carboniferous rocks. The Carboniferous and Permian sedimentary units are intruded by a number of dolerite sills (e.g., Gayer et al., 1966; Halvorsen, 1974; Dallmann et al., 2009, 2011) of Early Cretaceous age (Corfu et al., 2013; Senger et al., 2014) in connection with the volcanic activity of the HALIP (High Arctic Large Igneous Province; e.g., Maher, 2001). Svalbard was subjected to mutiple deformational events in connection with the North-Atlantic and Eurasian Basin rift development during the Cenozoic including the formation of the West Spitsbergen Fold-and-Thrust Belt and a number of subsequent reverse, transform-related and extensional fault systems (e.g., Talwani and Eldholm, 1977; Srivastava, 1978, 1985; Vink, 1982; Srivastava and Tapscott, 1986; De Paor et al., 1989; Tessensohn and Piepjohn, 2000; Faleide et al., 2010; Døssing et al., 2013; Dallmann, 2015; Doré et al., 2016; Piepjohn et al., 2015, 2016; Gion et al., 2017; Figs. 1 and 2).

THE OBSERVED LOMFJORDEN FAULT NETWORK

Our geological mapping in the study area has shown that the northern und central segments of the Lomfjorden Fault Zone are composed of different sets of faults with different orientations (Dallmann et al., 2009, 2011; Fig. 3):

(1) The main direction is represented by three approximately N–S striking major faults. The westernmost Veteranen Fault can be traced from northern Ny-Friesland towards the nunatak Terrierfjellet NE of Billefjorden in the S (Dallmann et al., 2002, 2004, 2009, 2010, 2011; Elvevold and Dallmann, 2011; Fig. 2B). It separates the Eolussletta Shear Zone in the W and sedimentary rocks of the Veteranen Group in the E. The late Caledonian age of the Veteranen Fault is supported in the S at Terrierfjellet, where the juxtaposed West Ny-Friesland and Nordaustlandet terranes are overlain by middle Carboniferous and younger sedimentary rocks (Dallmann et al., 2004; Fig. 2B). In the northern segment, a post-Carboniferous reactivation of the Lomfjorden Faut is indicated by downfaulted early Carboniferous strata SE of Lomfjella (Fig. 3). The central Lomfjorden Fault is exposed at the W-coast of Lomfjordhalvøya S of Kapp Fanshawe and E of the mountains Geren and Freken (Fig. 3). Its southern continuation can be assumed SSW of Glintbreen and SW of Vinkelen due to the large stratigraphic jump between both sides of the glacier valleys. Mostly, it separates Neoproterozoic sedimentary rocks in the W from down-faulted Carboniferous to Permian deposits in the E. Towards the S, the Lomfjorden Fault continues either on the W-side or E-side of the Silurian/Devonian Newtontoppen Granite (Fig. 3). In the E, the Agardhbukta Fault (Fig. 3) can be followed with some certainty from Oslobreen southward to and along Akademikarbreen with exposures at Kirtonryggen (northern segment) (Fig. 3), Vivienberget, Malte Brunfjellet (central segment), and in the Agardhdalen area in the southern segment (Fig. 2B). It mostly separates Neoproterozoic and Paleozoic sedimentary rocks of the Lomfjorden Group in the W from downfaulted Carboniferous to Permian deposits in the E (Figs. 2B and 3). North of Oslobreen, it is not a straight fault line, but a fault system with variably oriented strands seen at Ditlovtoppen and Raudberget. Most segments of the Agardhbukta Fault are covered by glaciers, but its existence can be inferred from high mountain areas with Neoproterozoic and Paleozoic rocks in the W (Dracofjella, Andromedafjellet, Golitsynfjellet) and lower mountains with horizontal Carboniferous and Permian strata in the E (Emblafjellet, Rotfjellet, Kassiopeiafjellet, Pachtusovfjellet; Figs. 3, 4,

and 6). The Carboniferous unconformity and underlying Neoproterozoic rocks are nowhere exposed E of the Agardhbukta Fault except for a small area at Oslobreen (Figs. 3, 4, and 15).

(2) Important structural elements of the Lomfjorden Fault Zone are N–S striking reverse faults. Bergh et al. (1994) reported that the northern segment of the fault zone consists of a set of subparallel, partly curved and variably E- and W-dipping, basement-involved reverse faults. Between the Veteranen and Lomfjorden faults, two steeply ENE-dipping, 7 and 20 km long, reverse faults are exposed at Lomfjella W of Lomfjorden (Lomfjella Reverse Faults) (Fig. 3). South of Lomfjorden, the 15 km long and steeply W-dipping Bjørnfjellet Reverse Fault is exposed E of Bjørnfjellet and at Løveryggen (Fig.3). Bergh et al. (1994) concluded that both reverse faults represent a pop-up structure above an E-directed thrust (Bjørnfjellet Reverse Fault) and a W-directed back thrust (Lomfjella Reverse Faults). Both reverse faults have carried Neoproterozoic rocks over Carboniferous deposits and early Cretaceous dikes. The revserse faults have reactivated inherited Carboniferous normal faults, steeply dipping Neoproterozoic strata and Caledonian thrusts (Bergh et al., 1994). No cross-cutting relationships of these reverse faults with the N–S striking master faults were found. The Lomfjella Reverse Faults and the Bjørnfjellet Reverse Fault do not continue across Lomfjordbotnen towards the SSE or NNW, respectively, but are probably limited by the NE–SW striking Geren Fault (Fig. 3).

(3) Several NE–SW striking faults with lengths of hundreds-of-meters up to 15 km (Fig. 3) mostly follow the major NE–SW valleys and glaciers and are not exposed, although needed to explain the outcrop patterns. Between the Veteranen and Lomfjorden faults in the northern part of the study area, three NE–SW striking faults could be mapped along the valleys of Gullfaksebreen and Faksebreen, and through Lomfjordbotnen at the southern end of Lomfjorden (Geren Fault; Fig. 3). The faults at Gullfaksebreen and Faskebreen cut through NNW–SSE trending km-scale Caledonian anticlines and synclines and the Western Lomfjella Reverse Fault with dextral offsets in the range of 1 to 2 km (Fig. 3). This is supported by the occurrence of small-scale NE–SW striking faults visible on aerial photographs with right-lateral offsets of steeply inclined Neoproterozoic rocks and Caledonian structures. The NE–SW striking Geren Fault between the Veteranen Fault and the Lomfjorden Fault through Lomfjordbotnen is indicated by the offset of different Caledonian structures between Lomfjella and Bjørnfjellet. It is

exposed onshore at Geren and Freken mountains (Fig. 3). Farther S, NE–SW striking faults are documented between the Lomfjorden Fault and the Agardhbukta Fault (Fig. 3). There, the largest fault follows the glacier Chydeniusbreen. Although not exposed, the trace of the fault can be inferred from the jump of the Carboniferous unconformity from 500 m above sea level in the NW to more than 800 m in the SE. The NNW–SSE trending Caledonian Ursafonna Anticline in the Neoproterozoic rock units is dextrally offset by apparently ca. 3 km along the fault (Fig. 3). In addition, there are a number of minor NE–SW striking faults in the Dracoisen area (Fig. 3).

(4) Between the Lomfjorden and Agardhbukta faults, some NNW–SSE striking faults are exposed in the Oslobreen area (Fig. 3). There, the Dolerittfjellet Reverse Fault carries Neoproterozoic rock units ENE-wards over Carboniferous sedimentary rocks and Cretaceous dolerite sills. Farther E, the parallel Sillhøgda Fault is characterized by a normal, down-to-the-SW sense of displacement. Both faults are only locally exposed at Sillhøgda. Their continuations to the NNW and SSE and relationships to the N–S striking master faults are uncertain. Another NNW–SSE striking fault is locally exposed at Raudberget where it separates Neoproterozoic rocks in the ENE from Carboniferous and underlying Neoproterozoic rocks in the WSW (Fig. 3).

STRUCTURES AND THEIR INTERPRETATION

Below, we describe and interpret, from N to S, structural field observations from different outcrops along the Lomfjorden and Agardhbukta faults. The locations are shown in Figure 6. Most of the structural data were not measured in outcrops directly on a fault or within a fault zone because most parts of the fault segments are covered by water or glaciers and exposures are rare (Figs. 3 and 6). Therefore, most structures were observed and measured as close as possible to the faults or fault zones or in blocks between them. In some figures we have inserted schematic diagrams showing pure shear-ellipses and ideal fault and shear plane orientations in strike-slip regimes to provide a reference for configurations of structural elements in the various possible scenarios discussed here.

Kapp Fanshawe

Observations. At the coastal cliffs SSW of Kap Fanshawe, a NNE–SSW striking strand of the northernmost segment of the Lomfjorden Fault is exposed within Neoproterozoic rocks of the Akademikarbreen Group (Figs. 6 and 7A). East of the major fault, the Neoproterozoic rocks dip gently towards the E and are cut by a brittle NE–SW striking fault zone with fault breccias. This fault zone is characterized by left-lateral offsets of the E-dipping bedding planes with displacements up to a few dm (Fig. 7B). This is supported by sinistral slickenside lineations along cm-scale shear planes in the vicinity of the fault (Fig. 7C).

To the W of the NNE–SSW striking fault, Neoproterozoic rocks are affected by a NNE-dipping thrust with NE-dipping strata in the hanging wall and an anticline-syncline pair in the footwall (Fig. 7B). The rocks are folded around gently E-plunging F_2-folds (Fig. 7C) with fold axes perpendicular to the general N–S trend of the Caledonian F_1-anticlines and synclines (compare Fig. 5). The E-plunging fold structures and the NNE-dipping thrust fault in the outcrop are truncated by the NNE–SSW striking fault.

Interpretation. The NE–SW striking cm-scale shear planes with primarily sinistral slickenside lineations and faults with dm-scale sinistral offsets (Fig. 7B and C) indicate sinistral strike-slip along the NNE–SSW striking fault in the centre of the outcrop. This is supported by the presence of sinistral NE–SW striking shear planes and faults subparallel to the master fault (Fig. 7C), and E–W trending F_2-folds and a NNE-dipping thrust, with their inferred N–S shortening direction. These data imply sinistral strike-slip movements along this northernmost segment of the Lomfjorden Fault. A few dextral slickenside lineations on cm-scale NNE–SSW shear planes (Fig. 7C) have been observed also in this area. Because only Neoproterozoic rocks are affected by the brittle strike-slip deformation, a precise timing in this outcrop cannot be determined. However, the slice of Viséan deposits of the Billefjorden Group within the parallel fault in the E (Fig. 7A) suggests that a post-Carboniferous age of the strike-slip deformation in the Neoproterzoic rocks is also possible.

Mjølnerfjellet

Observations. In the coastal outcrops at Mjølnerfjellet along the E-coast of Lomfjorden (Fig. 6), carbonate rocks of the Akademikarbreen Group are exposed underneath the Carboniferous unconformity (Fig. 3). The bedding planes dip moderately towards the SSW and are affected by NE-dipping fault planes with reverse and normal senses of displacements (Fig. 8A). Lateral movements are indicated by WNW–ESE striking cm-scale shear planes with a few sinistral slickenside lineations and NNE–SSW striking faults with dextral offsets of the Neoproterozoic strata up to a few cm (Fig. 8A).

In the W-facing cliffs of Mjølnerfjellet above the limestones of the Akademikarbreen Group, massive Late Carboniferous limestones of the Wordiekammen Formation exhibit a hundreds-of-meters-scale structure, which is dominated by a gently SSW-dipping basal thrust ramp with horizontal limestones in the footwall and folded limestones in the hanging wall (Fig. 8C). At the top, the F_2-folds are truncated by a gently NNE-dipping thrust fault overlain by unfolded planar limestones and cherts (Fig. 8C). In outcrop scale, several m-scale F_2-folds have gently SSW-dipping long limbs and steeply NNE-dipping to partly overturned short limbs indicating a NNE-vergence of the folds. Tectonic transport to the NNE to NE is supported by reverse slickenside lineations on NE-dipping back thrusts (Fig. 8B). The NNE–SSW shortening is consistent with the orientation of the pole of the best-fit great circle defined by the poles to bedding planes S_0 with a WNW–ESE trend of the F_2-folds (Fig. 8B). Evidence for lateral-slip movements in the Carboniferous limestones is poor. Only a few NE–SW striking dextral and WNW–ESE striking sinistral fault planes with slickenside lineations were found (Fig. 8B).

Interpretation. The local character of the F_2-folds and thrust ramp and the oblique orientation of their NNE−SSW shortening directions with respect to the N–S striking Lomfjorden Fault make it possible that the local shortening was controlled by dextral strike-slip motions along the nearby Lomfjorden Fault (Fig. 8D). This is supported by SW-dipping shear planes with reverse slickensides in the Neoproterozoic and Carboniferous rocks, dextral offsets of limestones of the Akadamikarbreen Group along NNE–SSW striking faults (Fig. 8A) and some cm-scale NE–SW striking shear planes with dextral slickenside lineations in Carboniferous limestones (Fig. 8B), which most likely represent synthetic shear planes (Fig. 8D). In addition, WNW–ESE striking sinistral shear planes can be interpreted as antithetic P'-shears (Tchalenko and Ambraseys, 1970;

Bartlett et al., 1981) with respect to possible dextral movements along the Lomfjorden Fault (Fig. 8D). However, it is also possible that the NE–SW striking dextral and WNW–ESE striking sinistral shear planes represent a conjugate set of shear planes related to W–E contraction (see below). NE-dipping cm-scale shear planes with normal slickenside lineations in the Akademikarbreen limestones cannot be correlated with a dextral N–S regime (Fig. 8A). It is possible that they represent the NE–SW extension direction within a N–S striking sinistral regime or a phase of later extension. However, the dominant kinematics at Mjølnerfjellet can be interpreted as N–S striking dextral strike-slip along the Lomfjorden Fault (Fig. 8D).

Geren and Freken

Observations. East of Geren and Freken mountains, about 10 km S of Mjølnerfjellet, the Lomfjorden Fault crops out onshore between Neoproterozoic rocks in the W and Carboniferous strata and a thick Cretaceous dolerite sill in the E (Dallmann et al., 2009; Figs. 3, 6, and 9A). There, moderately ENE-dipping Neoproterozoic rocks of the Veteranen, Akademikarbreen, and Polarisbreen groups are affected by three brittle NE–SW striking faults (Fig. 9A), which represent the exposed strands of the Geren Fault between Lomfjella in the N and Bjørnfjellet in the S (see Fig. 3). It should be noted that these faults do not continue into the Carboniferous limestones and the Cretaceous dolerite sill E of the Lomfjorden Fault (Fig. 9A). Mapping and interpretation of aerial photographs show that the NE–SW faults display lateral dextral offsets of the Neoproterozoic rocks units in the order of some hundreds of m (Fig. 9A). In spite of the dextral offsets of the Neoproterozoic strata, slickenside lineations on subvertical, NE–SW striking, m-scale faults and cm-scale shear planes indicate also sinstral movements (compare Fig. 9A and B). Dextral slickensides have been observed on both NNE–SSW striking and some NW–SE striking cm-scale shear planes, and sinistral shear has also been documented on NNW–SSE striking cm-scale shear planes (Fig. 9B). Reverse slickenside lineations on cm-scale shear planes and dm-scale fault planes indicate both E–W and NW–SE shortening (Fig. 9B).

At Geren and Freken, only Neoproterozoic rocks are affected, while Carboniferous rocks and the dolerite sill to the E of the fault are unaffected. Therefore, a precise timing of the deformations in this area is not possible.

Interpretation. The nonuniform distribution and orientation of the tectonic fabric elements and kinematic indicators at Geren and Freken cannot be explained by only one deformation. The field observations show that three tectonic scenarios and combinations of them are possible:

(a) In a W–E shortening scenario, the mapped NE–SW faults and measured NNE–SSW striking shear planes with dextral slickensides (Fig. 9B) possibly represent the dextral set of a conjugate set of shear planes and faults (Fig. 9C_1). This would also include the possibility that the apparent right-lateral dextral offsets in the map can be partly caused by SE-side-down displacements. NNW–SSE striking shear planes with sinistral slickensides are the sinistral part of the conjugate set of shear planes and faults (Fig. 9B and C_1). This W–E shortening scenario is supported by steeply E- and W-dipping shear planes with reverse slickensides (Fig. 9B and C_1).

The other two possible scenarios are related to N–S trending strike-slip movements:

(b) NNE–SSW striking dextral and ENE–WSW striking sinistral shear planes and faults can be interpreted as synthetic and antithetic shears, respectively, of dextral movements along the Lomfjorden Fault (Fig. 9B and C_2).

(c) However, a sinistral N–S scenario is also possible and indicated by NNW–SSE striking sinistral shear planes (synthetic shears), the NE–SW striking dextral faults (P'-shears), by some NW–SE striking dextral shear planes (antithetic shears), and by some SE- and NW-dipping shear planes with reverse slickensides (Fig. 9B and C_3).

Lomfjella Reverse Faults

Observations. Between the Veteranen Fault in the W and Lomfjorden in the E, the two steeply ENE-dipping Lomfjella Reverse Faults are exposed (Figs. 3 and 4A). The western reverse fault runs from Valhallfonna in the NNW towards Lomfjella in the SSE, and the eastern one is located in the steep coastal cliffs of Lomfjorden E of Lomfjella (Figs. 3 and 10A). The position of both reverse faults was most likely controlled by the orientation of bedding in the km-thick eastern limb of the Caledonian anticline (Fig. 4A) and by reactivation of pre-existing Carboniferous normal faults (Bergh et al., 1994). In the S, the Eastern Lomfjella Reverse Fault is truncated by the NE–SW striking Geren Fault and does not appear again in the mountain areas S of Lomfjordbotnen (Fig. 3).

The 70° E-dipping, 7 km long, Eastern Lomfjella Reverse Fault carries Neoproterozoic rocks over Early Carboniferous strata and Early Cretaceous dolerites (compare Bergh et al., 1994; Figs. 3, 4, 6, and 10). The geological relationships in the field suggest that the displacement is in the range of at least 150 m. The sedimentary rocks above the reverse fault are affected by almost subvertical reverse faults with transports towards the W and by W- and E-dipping back thrusts (Fig. 10B). The amounts of displacement along the reverse faults and back thrusts show displacements of several m. The partly gypsiferous layers of the Veteranen Group exhibit a number of dm- to m-scale duplex structures and imbricates (Fig. 10B and C) supporting a tectonic transport upwards to the W.

Interpretation. The N–S trending F_2-folds related to W-directed reverse faults and E-directed, W- and E-dipping back thrusts support E–W contraction along the Eastern Lomfjella Reverse Fault (Fig. 10A and B). In the Veteranen deposits in the hanging wall, no evidence for strike-slip deformation was found. Some NE–SW striking cm-scale faults and shear planes with dextral slickenside lineations can be interpreted as the dextral set of conjugate shear planes related to W–E shortening (Fig. 10C and D). The second NW–SE striking sinistral set could not be found in this outcrop. This situation is similar to Geren and Freken on the opposite side of Lomfjorden (see above), where the dextral NE–SW faults dominate. Therefore, and following Bergh et al. (1994), we suggest that the Lomfjella Reverse Faults were formed during W–E contraction.

Bjørnfjellet Reverse Fault

Observations. The Bjørnfjellet Reverse Fault is a N–S striking, approximately 15 km long and W-dipping fault between Lomfjordbotnen in the N and Løveryggen in the S (Fig. 3). It represents the dominating structural element in this area W of the Lomfjorden Fault (Bergh et al., 1994; Dallmann et al., 2009). The northern end of the reverse fault is truncated by the Geren

Fault (Fig. 3). Its continuation to the S and its cutting relationship with the Lomfjorden Fault is unclear, because it disappears under the icecap S of Løveryggen. The Bjørnfjellet Reverse Fault carried red beds of the Neoproterozoic Veteranen Group sandstones eastwards on top of flat-lying horizontal middle Carboniferous to Early Permian limestones and Early Cretaceous dolerite sills (Figs. 3, 11A, and B) (Bergh et al., 1994). At Løveryggen, the reverse fault dips about 45° towards the W (Fig. 11B). In the footwall, the base of the Carboniferous can be estimated at about 400 to 450 m a.s.l. underneath the ice of the glacier. In the hanging wall, the Carboniferous is eroded above the 700 m high peak of Løveryggen. This relationship allows to calculate a minimum displacement of 500 m towards the E.

Interpretation. The transport of Neoproterozoic rock units on Carboniferous limstones and Cretaceous sills towards the E along a W-dipping fault supports the orthogonal, convergent character of the Bjørnfjellet Reverse Fault S of Lomfjordbotnen as suggested by Bergh et al. (1994). Local minor structures are a few NW-SE striking cm-scale shear planes with dextral slickenside lineations and dextral faults with lateral offsets of the Neoproterozoic strata in the range of a few cm (Fig. 11C).

Vinkelen

Observations. The SW-facing 50 m high cliff of the nunatak Vinkelen NW of Chydeniusbreen (Figs. 3 and 6) exposes a 100-meters-scale thrust ramp in middle Carboniferous to Early Permian limestones and dolomites of the Gipsdalen Group (Fig. 12). Along the structure with its flat-ramp geometry, folded and thrust-faulted sedimentary rocks were carried towards the NW on top of unfolded limestones (Fig. 12). As the outcrop is inaccessible, bedding planes, faults and folds could not been measured. The thrust ramp was estimated to dip towards SE, and the B_2-fold axes were estimated to trend NE–SW. The thrust displacement is in the range of a few tens-of-meters, assuming that the reddish weathering limestones in the footwall of the ramp and within the fold in the hanging wall are correlated. The structure is local and could not be traced farther across the glacier SW of Vinkelen.

Interpretation. The estimated SE-dip of the thrust ramp and the NE–SW trend of the F_2-folds (Fig. 12) indicate approximately NW–SE shortening, oblique to the NNW–SSE striking faults in the area, e.g., the Lomfjorden Fault farther to the SW (Fig. 3). This sense of obliquity is compatible with an interpretation of sinistral kinematics in an overall N–S to NNW–SSE tectonic regime, provided the shortening at Vinkelen is related to strike-slip deformation.

Raudberget

Observations. Another local thrust is exposed in and restricted to the SW-cliff of Raudberget (Figs. 3, 6, and 13). There, steeply NE-dipping Neoproterozoic rocks of the Veteranen Group and unconformably overlying horizontal limestones of the Carboniferous Wordiekammen Formation are carried towards NW on top of steeply NW-dipping Carboniferous deposits. The thrust displacement is approximately 50 m (Fig. 13A). The folds related to the thrust are estimated to trend NE–SW, which is similar to the situation at Vinkelen (compare Fig. 12). In an outcrop near the upper edge of the cliff in the hanging wall of the thrust, the Carboniferous strata are folded around m-scale folds with NW–SE trending axes, which are perpendicular to the axes of the thrust-related folds (Fig. 13B). The tectonic transport direction of the SW-vergent fold is supported by a brittle, m-scale thrust with a flat-ramp geometry (Fig. 13B).

Interpretation. The deformation in the Neoproterozoic and Carboniferous rocks at Raudberget is characterized by two perpendicular, superimposed shortening phases with a NW-directed thrust ramp and SW-vergent folds. These shortening directions do not coincide with the E–W contraction across the Lomfjella and Bjørnfjellet reverse faults. In addition, regional tectonic events characterized by SE–NW and NE–SW shortening directions are unknown in East Spitsbergen, and the thrust and folds at Raudberget represent local structures. On the other hand, the oblique orientations of the two shortening directions with respect to the N–S striking master faults of the Lomfjorden Fault Zone make it possible that the two deformation phases at Raudberget were caused by strike-slip tectonics, similar to the interpreted situation at Mjölnerfjellet (Fig. 8) and Vinkelen (Fig. 12). If so, the phase with oblique NE–SW shortening can be related to an overall N–S trending dextral regime (Fig. $13D_1$), and the phase with SE–NW shortening can be related to an overall N–S trending sinistral strike-slip regime (Fig. $13D_2$), provided the shortening at Raudberget is related to strike-slip deformation. As we could not find cutting relationships between the structures of the two phases, the relative timing of the two deformation phases remains unclear.

Polarisbreen

Observations. Between Chydenuisbreen and Ursafonna, the ENE-limb of the major Caledonian Ursafonna Anticline exhibits km-thick deposits of the Neoproterozoic to Cambrian Lomfjorden Supergroup (Figs. 3 and 6). The bedding planes of the different units strike NNW–SSE and dip towards the ENE with mostly 30 – 45° (Fig. 14A and B). The entire F_1 fold limb of the anticline is truncated by a number of NE–SW striking, subvertical faults parallel to the assumed fault along the axis of Chydeniusbreen (Figs. 3 and 14A). Similar to the area at Geren, the faults exhibit dextral offsets of the sedimentary layers and the boundaries of the major rock units with magnitudes of up to some hundreds of m (Fig. 14A). The field observations are supported by interpretations of aerial photographs, which indicate that individual rock units are stepwise dextrally offset along the NE–SW striking faults, especially in the fault swarm on the nunatak Vettene S of Polarisbreen (Fig. 14A). At Dracofjella S of Dracoisen, a minor WNW–ESE striking fault indicates a sinistral offset of the strata of approximately 100 m (Fig. 14A).

At the northeastern part of the Grovtoppane mountain ridge SE of Chydenuisbreen (outcrops A925 and A946; Figs. 3, 6, and 14A), ENE-dipping Neoproterozoic to Cambrian sedimentary rocks display cm-scale shear planes with slickenside lineations that support the interpretation of dextral displacement along the NE–SW striking faults (compare Fig. 14A and C). In addition, NW–SE striking shear planes with sinistral slickenside lineations are exposed at outcrop scale (Fig. 14C). Steeply SSE-dipping cm-scale shear planes with reverse slickenside lineations show NNW–SSE shortening (Fig. 14C).

Interpretation. Owing to the difference in elevation of the Carboniferous unconformity on opposite sides of the glacier valley between Grovtoppane and Cepheusfjellet (Fig. 14B) and the truncation of the NE–SW striking faults in that valley, we have inferred the presence there of a N–S striking fault, likely to be the northward continuation of the Agardhbukta Fault (Fig. 14A).

The exposed NE–SW striking dextral strike-slip faults and shear planes are dominant between Chydeniusbreen and around Dracoisen (Fig. 14A and C). As in the Geren and Freken area (compare Fig. 9A), their cutting relationships to the northern segment of the Agardhbukta Fault are unclear. However, they cannot be traced into the Carboniferous and Permian strata E of the fault (Fig. 14A). Another subordinate set is represented by the small, WNW–ESE striking sinistral fault at Dracofjella (Fig. 14B) and NW–SE striking sinistral shear planes (Fig. 14C). Compared with the area at Geren, both sets can be interpreted as conjugate sets of sinistral and dextral shear planes and faults, related to an overall E–W contraction (Fig. 14D). This is supported by approximately E–W striking extension joints. The only set of shear planes, which does not fit into this picture, is represented by steeply SSE-dipping shear planes with reverse slickensides (Fig. 14C).

Oslobreen

The Oslobreen area is dominated by a number of NNW–SSE striking faults at Dolerittfjellet and Sillhøgda and a segment of the N–S striking Agardhbukta Fault at Kirtonryggen (Figs. 3, 6, and 15B). As the nature of the relationship between the faults is obscured by the ice of Oslobreen (Figs. 3 and 15B), it is not possible to see whether the NNW–SSE faults turn southwards into a N–S direction and merge with the Agardhbukta Fault. In any case, the faults do not continue SE-wards into either the area with horizontal Carboniferous and Permian successions at Rotfjellet and Kassiopeiafjellet or the Paleozoic rocks at Kirtonryggen (Figs. 3 and 15B), indicating that the NNW–SSE faults are limited to the E by the N–S striking Agardhbukta Fault.

Observations at Kirtonryggen. A key outcrop in this area is located SW of Kirtonryggen. There, two N–S striking strands of the Agardhbukta Fault separate horizontal Carboniferous/Permian strata and Cretaceous dolerite sills in the W from E-dipping Early Paleozoic rocks of the Oslobreen Group in the E (outcrops A949–951; Fig. 15B). Between the two strands of the fault, a local hundreds-of-meters-scale WNW-vergent F_2-fold is developed in Carboniferous limestones, with a moderately ESE-dipping long limb and an overturned, steeply ESE-dipping short limb (Fig. 15C). ENE-dipping cm-scale shear planes with normal slickenside lineations and approximately N–S striking shear planes with oblique sinistral slickenside lineations were also observed in this area (Fig. 15D).

Interpretation. The WNW–ESE contraction in this outcrop is supported by the NNE–SSW orientation of the B_2-fold axis, cm-scale shear planes with oblique, ESE-directed reverse slickenside lineations and by normal shear planes indicating an ENE–WSW extension direction (Fig. 15D). The oblique orientation of the local F_2-fold structure and the WNW–ESE shortening direction with respect to the two strands of the Agardhbukta Fault suggest that the deformation in this outcrop area can be related to sinistral strike-slip along the N–S striking Agardhbukta Fault imposing a transpressional stress regime on the block between the fault strands (compare Fig. $16D_3$). This is supported by a number of cm-scale N–S striking shear planes with oblique sinistral slickenside lineations (compare Figs. 15D and $16D_3$).

Observations at the Sillhøgda Fault. Northwest of Oslobreen, the NNW–SSE striking Sillhøgda Fault separates horizontal Carboniferous and Permian deposits with Early Cretaceous dolerite sills in the WSW from E-dipping Neoproterozoic rocks of the Akademikarbreen Group and the Cambrian Oslobreen Group in the ENE and unconformably overlying horizontal Carboniferous (Fig. 15A and B). The fault dips steeply to the WSW and the stratigraphic offset across it indicates a normal down-to-the-WSW sense of displacement. The bending of the horizontal Carboniferous/Permian deposits across a monoclinal drag fold into a steeply WSW-dipping position (Fig. 15A) supports this interpretation. Further NE, at the eastern end of Ditlovtoppen, another NNW–SSE striking fault is exposed (Fig. 15A and B). A normal down-to-the-ENE sense of displacement for this fault is confirmed by downthrow of the Carboniferous unconformity to the ENE of about 100 m (Fig. 15A).

Observations at the Dolerittfjellet Reverse Fault. Subparallel to the Sillhøgda Fault (normal dip-slip), the 45° WSW-dipping Dolerittfjellet Reverse Fault (Figs. 15B and 16A) carries SSW-dipping Neoproterozoic limestones over horizontal Carboniferous/Permian rocks and Early Cretaceous dolerite sills (Figs. 15A and 16A) with a minimum displacement of 150 m. Cm-scale SW-dipping brittle shear planes with reverse slickenside lineations in the Neoproterozoic limestones (Fig. 16B) support the ENE–WSW shortening across the reverse fault.

In the southwestern hanging wall of the Dolerittfjellet Reverse Fault, SW-dipping rock units of the Neoproterozoic Polarisbeen and Akademikarbreen groups are locally truncated by ENE–WSW striking faults with dextral offsets of the strata in the range of a hundred m (Fig. 15B). In addition, the limestones are cut by minor NE–SW striking shear planes with sinistral slickenside lineations (Fig. 16B). The Carboniferous deposits in the footwall display minor NE–SW and WNW–ESE striking shear planes with dextral and sinistral slickenside lineations, respectively (Fig. 16C).

Interpretation. Mapping and structural observations indicate that the Dolerittfjellet Reverse Fault is a result of ENE–WSW contraction. This is further supported by an ENE–WSW striking sinistral fault and a N–S striking dextral fault on the small, 780 m high, nunatak N of Dolerittfjellet (Fig. 15B), which can be interpreted as a conjugate set of faults related to the local ENE–WSW shortening across the reverse fault (Fig. 16D_1).

A correlation of the Bjørnfjellet Reverse Fault and Dolerittfjellet Reverse Fault is improbable, because both faults are separated by 30 km of glaciers and have distinctly different orientations (Fig. 3). The oblique NNW–SSE orientation of the Dolerittfjellet Reverse Fault with respect to the N–S striking Lomfjorden and Agardhbukta faults suggests that this local reverse fault was the result of strike-slip deformation. The ENE–WSW shortening direction coincides with a dextral strike-slip system along the N–S striking major faults (Fig. 16D_1 and D_2).

However, the parallel orientation of the normal Sillhøgda Fault to the contractional Dolerittfjellet Reverse Fault must be explained as well (Fig. 15B). If the Sillhøgda Fault also was caused by strike-slip movements, the oblique ENE–WSW extension direction with respect to the master faults is compatible with a N–S oriented sinistral strike-slip system (Fig. 16D_3). This scenario is supported by the tectonic fabric elements in the outcrop SW of Kirtonryggen, which show a WNW–ESE shortening direction and an ENE–WSW extension direction as along the Sillhøgda Fault (compare Figs. 15D and 16D_3). Provided the shortening and extension directions in the Oslobreen area are related to superimposed strike-slip deformation, then the Dolerittfjellet Reverse Fault (ENE–WSW shortening; Fig. 16D_1 and D_2) was formed during dextral, transpressional and the Sillhøgda Fault and the deformation in the Carboniferous strata SW of Kirtonryggen (WNW-ESE shortening; ENE-WSW extension; Figs. 15D and $16D_3$) during sinistral, transtensional strike-slip movements along the N–S striking Lomfjorden Fault Zone.

Pachtusovfjellet

Observations. At Pachtusovfjellet (Figs. 2B and 6B), Carboniferous and Permian deposits are folded into a hundreds-of-meters-scale F_2-flexure or monocline with a gently E-dipping to horizontal eastern limb and a western limb dipping steeply towards the Agardhbukta Fault (Fig. 17A and B). This flexure runs parallel to the Agardhbukta Fault and re-occurs more than 20 km farther S, E of Vivienberget (Fig. 6B). The Carboniferous and Permian deposits are affected by a number of ENE- and steeply WSW-dipping cm-scale shear planes with reverse and sinistral slickenside lineations (Fig. 17A). Similarly oriented cm-scale shear planes also show slickenside lineations with normal senses of displacement. Additionally, some cm-scale NE–SW striking shear planes are characterized by oblique dextral slickenside lineations.

Interpretation. The kinematics in this outcrop are dominated by orthogonal E–W shortening across and by minor sinistral movements parallel to the Agardhbukta Fault. E–W contraction E of the Agardhbukta Fault is supported by the hundreds-of-meters-scale, N–S trending flexure and by ENE- and WSW-dipping shear planes with reverse slickenside lineations in the Carboniferous strata (Fig. 17A and B). Some NE–SW striking dextral shear planes (Fig. 17A) could be either interpreted as part of a conjugate set related to E–W shortening across or as synthetic shear planes related to dextral strike-slip movements along the Agardhbukta Fault (Fig. $17D_1$). In addition, N–S striking shear planes with sinistral slickenside lineations are compatible with sinistral displacements along the Agardhbukta Fault (Fig. 17A). One problem is that the shape of the flexure with a western short limb indicates transport direction to the W (Fig. 17B). Usually, the rock units in the footwall of a reverse fault are younger than the rocks in the hanging wall. Here, the hanging wall consists of Carboniferous and the footwall of Neoproterozoic rocks. This suggests that the Carboniferous and Permian strata were carried westwards across the Agardhbukta Fault during a first phase of W-E contraction. Later, the Agardhbukta Fault was reactivated as a normal fault downfaulting the Carboniferous/Permian strata in the E against the

Neoproterozoic rocks in the W. This is supported by some E- and W-dipping shear planes with extensional slickenside lineations can probably be related to a later extensional reactivation along the Agardhbukta Fault (Fig. 17A). It is, however, not possible to determine the relative timing of the strike-slip movements with respect to the phases of contraction and extension.

Vivienberget

Observations. The mountain Vivienberget (Figs. 2B and 6B) consists of Neoproterozoic rocks in the W, folded during the Caledonian Orogeny, and Early Permian deposits of the Gipshuken Formation in the E, separated by the Agardhbukta Fault (Fig. 2B). A ridge connecting the Permian and Neoproterozoic outcrops exhibits several subvertical fault strands parallel to the master fault, with slices of various, stratigraphically disturbed Neoproterozoic rock units in between. Exposure conditions do, however, not allow for detailed structural observations. The nunatakk Brekkeknausen between Vivienberget and Malte Brunfjellet shows an E-directed thrust and normal faults in the Neoproterozoic (Miloslavskij et al., 1996; Dallmann, 2015). Two moderately W-dipping, E-directed thrusts with transport directions towards the E are exposed in Permian strata at Chimkovfjellet E of the Agardhbukta Fault NE of Vivienberget (Larsen, 1988; Miloslavskij et al., 1996; Fig. 2B). This indicates that also this segment of the Lomfjorden Fault Zone was affected by W–E contraction E of the Agardhbukta Fault. The well-exposed Neoproterozoic units to the W of the fault zone are affected by cm-scale NNE–SSE striking shear planes with dextral slickenside lineations, ESE–WNW striking shear planes with sinistral oblique slickenside lineations, and dm- to m-scale NE-directed reverse faults (Fig. 17C).

Interpretation. The NNE–SSW striking brittle shear planes with dextral displacements, SW-dipping reverse faults, and NE-dipping shear planes with reverse slickenside lineations (Fig. 17C) are compatible with an overall NNE–SSW dextral strike-slip regime with an approximately NE–SW shortening direction (Fig. 17D_2). Because the tectonic fabric elements have only been observed in Neoproterozoic rocks, a precise timing of the deformation is difficult. However, the brittle character and the orientation of the dextral shear planes parallel to the nearby Agardhbukta Fault in the E indicate that a post-Carboniferous deformation along the Agardhbukta Fault is also possible.

Malte Brunfjellet

Observations. Malte Brunfjellet is a nunatak directly W of the Agardhbukta Fault, NE of Tempelfjorden (Figs. 2B and 6B). There, Neoproterozoic deposits (Polarisbreen Group) are unconformably overlain by horizontal Carboniferous strata. As can be seen by the stratigraphy in adjacent nunataks, the eastern side of the fault has apparently dropped by at least 200 m (Miloslavskij et al., 1996). The analyses of shear planes, faults, and slickenside lineations show a complex distribution and orientation of the structures indicating a superposition of various tectonic events (Fig. 18A and B). The Carboniferous and Early Permian strata are cut by a number of dm- to m-scale, steeply NW-dipping reverse faults (Fig. 18B). An irregular set of cm-scale shear planes with reverse slickenside lineations show transport directions ranging from towards the NNE (Fig. 18A), across N, to NW (Fig. 18B). Extensional kinematics are indicated by NE–SW (Fig. 18A) and NNW–SSE striking (Fig. 18B) cm-scale shear planes with normal slickenside lineations and extension joints. Lateral displacements are indicated by cm-scale fault planes with E–W trending sinistral and NW–SE trending dextral (Fig. 18A), and NNE–SSW trending dextral and sinistral slickenside lineations (Fig. 18A and B).

Interpretation. The Carboniferous/Permian sedimentary rocks at Malte Brunfjellet are affected by post-Carboniferous deformation and comprise a number of faults, shear planes, and extension joints with heterogeneous kinematic indications (Fig. 18A and B). This nonuniform distribution can only be explained by the superposition of different tectonic events with different kinematics. A post-Caledonian E–W shortening scenario in the Carboniferous to Permian rock units at Malte Brunfjellet can be excluded: corresponding tectonic elements like W- or E-directed reverse faults and a conjugate set of NW–SE striking sinistral and NE–SW striking dextral faults and shear planes are not developed here (compare Fig. 18A, B, and C_1). The different faults, shear planes and extension joints at Malte Brunfjellet can be explained by lateral movements along the nearby Agardhbukta Fault:

A sinistral N–S strike-slip scenario (Fig. 18B and C_2) is supported by: (a) NNE–SSW striking shear planes with sinistral slickenside lineations with being sinistral synthetic shears in a N–S trending sinistral regime; (b) NNE–SSW striking shear planes with sinistral slickenside lineations (Fig. 18B) compatible with being secondary synthetic shears; (c) NNW–SSE striking extension joints and shear planes with normal slickenside lineations showing an ENE–WSW extension direction (Fig. 18B); (d) steeply NW-dipping reverse faults and SE-dipping shear planes with reverse slickenside lineations in the Carboniferous/Permian rocks indicating a NW–SE orientation of the shortening direction (Fig. 18B).

A dextral N–S strike-slip scenario (Fig. 18A and C_3) is supported by: (a) NNE–SSW striking dextral faults and shear planes compatible with being synthetic structures in a N–S striking dextral regime (Fig. 18A); (b) local NW–SE striking dextral shear planes, which are compatible with being secondary synthetic shears (Fig. 18A); (c) E–W striking shear planes with sinistral slickenside lineations (Fig. 18A); (d) NE–SW striking extension joints indicating a NW–SE extension direction (Fig. 18A); (e) steeply SSW-dipping shear planes with reverse slickenside lineations (Fig. 18A) compatible with a N–S striking dextral regime (Fig. 18C_2). These interpretations support the assumption that the Carboniferous/Permian rocks at Malte Brunfjellet were affected by superimposed sinistral and dextral movements along a N–S striking master fault, although the relative succession of the two phases cannot be determined based on the observed structures.

DISCUSSION

Deformational phases and timing

Structural fieldwork in the exposed outcrops along the faults has shown that the Neoproterozoic-Permian sedimentary rocks and the Early Cretaceous dolerite intrusions were affected by convergent tectonic movements. On the other hand, the appearance of many heterogeneous and overlapping structures and tectonic fabric elements with different orientations and kinematics in a number of observed outcrops suggests that the deformations along the Lomfjorden Fault Zone cannot be only related to a single W–E contraction but to a succession of tectonic phases, which were also controlled by lateral movements.

N–S striking reverse faults. Convergent kinematics across the Lomfjorden Fault Zone are clearly documented by the steep N–S striking Lomfjella and Bjørnfjellet reverse faults between the Veteranen and Lomfjorden faults in the northern segment (Figs. 3, 10, and 11). In the central segment, the 40 km long flexure in Carboniferous to Permian deposits E of the Agardhbukta Fault can be correlated to the same E–W shortening event (Fig. 17). Another convergent structure is the Dolerittfjellet Reverse Fault in the Oslobreen area, however, due to its isolated occurrence and different orientation, a correlation with the N–S striking reverse faults in the Lomfjorden area and at Agardhbukta is not considered.

The Lomfjella und Bjørnfjellet reverse faults have affected early Carboniferous to early Permian deposits and can be separated from Caledonian thrusts in Neoproterozoic rocks. More important is that both reverse faults have also carried Neoproterozoic rocks over dolerite sills at Lomfjella, Bjørnfjellet and Løveryggen, which indicates that the E–W shortening along the reverse faults took place after the intrusion of the dolerite sills from ca. 125–78 Ma ago (Corfu et al., 2013; Senger et al., 2014). The long flexure E of the Agardhbukta Fault in the central segment, for instance observed at Pachtusovfjellet, has involved Carboniferous and Permian rocks and can be correlated with the post-Early Cretaceous Lomfjella and Bjørnfjellet reverse faults. Apart from the clearly convergent structures along the Lomfjella and Bjørnfjellet reverse faults and the flexure at Pachtusovfjellet, we have not found clear evidence for W–E shortening in the observed outcrops along the Veteranen, Lomfjorden and Agardhbukta faults, like E- or W-dipping faults or shear planes with reverse slickensides, except for the outcrops at Geren (Fig. 9B).

NE–SW striking dextral faults. As clear cutting relations to the N–S major faults are not exposed and always covered by scree or glacier ice, it is difficult to interpret the affiliation of the NE–SW striking dextral faults to other structures along the Lomfjorden Fault Zone. There are three possible tectonic explanations:

(a) One distinctive feature is the observation that the NE–SW faults have not affected the Carboniferous and younger rocks in the study area (compare Fig. 3). This could be an argument for a pre-Carboniferous age of these faults. The Caledonian deformation in this area is dominated by km-scale, N–S trending folds (Fig. 5) and E- and W-dipping reverse faults. On this account, the dextral NE–SW faults can represent one part of a conjugate set related to Caledonian E–W contraction. On the other hand, it is also obvious that these faults are not developed in the basement areas W of the Veteranen Fault and the southern part of the Lomfjorden Fault (Fig. 3). In addition, the E–W faults cut through and displace the Lomfjella and Bjørnfjellet reverse faults, which themselves have affected Carboniferous and younger rocks. This makes a pre-Carboniferous age of the NE–SW faults improbable.

(b) The NE–SW striking dextral faults can also be interpreted as a part of a conjugate set of faults that accommodated the last gasp of shortening during the formation of the Lomfjella and Bjørnfjellet reverse faults (compare Fig. 10D). It is conspicuous that there is no or little sinistral equivalent of this conjugate set, except for a small sinistral WNW–ESE fault at Dracoisen (Fig. 14A) and outcrop-scale sinistral shear planes with a similar orientation (Figs. 8A, B, 14C, and 16C). If the dextral NE–SW faults can be attributed to the W–E shortening between the Veteranen and Lomfjorden faults, they also post-date the intrusion of the dolerite sills and do not represent Caledonian structures. In this case, they should also have affected the basement areas W of the Veteranen Fault and the Carboniferous and younger rocks E of the Lomfjorden Fault, either cutting through or being offset by them.

(c) Another possibility is that the NE–SW striking dextral faults are related to strike-slip movements along the major faults of the Lomfjorden Fault Zone. Although it cannot be seen in the field whether the dextral faults are truncated by the N–S master faults or if they merge with them, it is obvious that they are limited to the areas between the Veteranen, Lomfjorden and Agardhbukta faults (Fig. 3). It is, therefore, possible that they can also represent synthetic dextral faults within a large-scale dextral strike-slip regime along the N–S Lomfjorden Fault Zone. In summary, a final conclusion on the origin and tectonic reason of the NE–SW striking dextral faults cannot be suggested here and needs more field data.

The N–S striking major faults of the Lomfjorden Fault Zone. At first sight, large-scale strike-slip along the N–S striking master faults is not as obvious as, for example, the convergent structures, because especially the Lomfjorden and Agardhbukta faults are submerged under fjords and glaciers, and outcrops are rare. In addition, often nonuniform and irregular orientations and relationships of tectonic fabric elements and their kinematic evidence in the limited number of accessible outcrops make it difficult to gain clear and direct indication and evidence for strike-slip movements along the N–S striking faults of the Lomfjorden Fault Zone. The structural observations in the outcrop areas have shown that the rock units in many outcrops are characterized by NE–SW and NW–SE oriented shortening and extension directions, respectively, and are often combined with lateral faults and shear planes, which, altogether, do not coincide with the W–E shortening across the Lomfjella and Bjørnfjellet reverse faults discussed above. The structural diversity found in these outcrops can be explained as a consequence of local strain produced by strike-slip movements along the Lomfjorden and Agardhbukta faults. Assuming that the N–S striking major faults represent the actual zones of tectonic movements and displacements, the oblique orientations of local convergent or extensional structures with respect to the major faults are important for the interpretation of possible strike-slip movements.

The best exposure with the most reliable indications for strike-slip movements along the N–S striking major faults can be found along the Agardhbukta Fault at Kirtonryggen. There, a hundred m scale, NNE–SSW trending F_2-fold in Carboniferous strata is pinched between the two strands of the superior N–S fault. The fold-structure with WNW–ESE shortening and ENE–WSW extension directions is most likely related to sinistral movements along the Agardhbukta Fault (compare Figs. 15D and 16D_3). This is supported by N–S striking shear planes with sinistral slickenside lineations (Fig. 15D). Another outcrop with a thrust in Carboniferous limestones at Vinkelen depicts a similar NW–SE shortening direction (Fig. 12), which also may indicate a sinistral scenario parallel to the N–S master faults. At Pachtusovfjellet, sinistral movements along the nearby Agardhbukta Fault are directly observed by some shear planes with sinistral slickenside lineations (Fig. 17A). In another case, the oblique orientation of the NNE–SSW shortening orientation in Carboniferous limestones at Mjølnerfjellet is compatible with dextral strike-slip motions along the Lomfjorden Fault. This supposition is supported by NNE–SSW striking dextral and WNW–ESE striking sinistral faults and shear planes, which can be interpreted as synthetic and antithetic shears, respectively, in a N–S oriented dextral strike-slip regime (Fig. 8A, B, and D_1).

There are two outcrop areas, which are more complex and characterized by a superposition of perpendicular, NW–SE and NE–SW oriented shortening directions. At Raudberget, thrusting and folding displays NW–SE and NE–SW shortening directions in Neoproterozoic and Carboniferous rocks (Fig. 13) indicating possible local sinistral and dextal strike-slip deformation within a N–S trending system. A similar situation is shown by shear planes with sinistral, dextral and reverse slickenside lineations and extension joints at Malte Brunfjellet (Fig. 18). The distribution of the tectonic fabric elements depicting NE–SW and NW–SE shortening directions and NW–SE and ENE–WSW extension directions can be explained by a superposition of dextral and sinistral strike-slip movements, respectively, along the Agardhbukta Fault.

In the above mentioned outcrops, Neoproterozoic and Carboniferous to Permian sedimentary rocks are affected by NE–SW and NW–SE shortening and extension and combined systems of strike-slip faults and shear planes indicting that the deformations took place after the Permian. Additionally, outcrops in Neoproterozoic sedimentary rocks are interpreted to be affected by NNE–SSW striking sinistral strike-slip movement at Kapp Fanshawe (Fig. 7) and by dextral movements along the Agardhbukta Fault at Vivienberget (Fig. 17C) and at Geren and Freken (Fig. 9B). Because the tectonic fabric elements in these outcrops have only affected Neoproterozoic rocks, a more precise timing is not possible. However, the similarity to the structures described above and the close location to the Lomfjorden Fault and Agardhbukta Fault, respectively, make it possible that the deformation in these outcrops is also related to post-Permian strike-slip deformations.

Sillhøgda Fault and Dolerittfjellet Reverse Fault. Between Balderfonna and Andromedafjellet, the NNW–SSE striking Dolerittfjellet Reverse Fault and the parallel, normal Sillhøgda Fault are obliquely oriented with respect to the master N–S faults. In this context, the en-échelon arrangement of the two major faults is an important observation: the Lomfjorden Fault can be traced from Kapp Fanshawe in the N to the highly glaciated areas around the Newtontoppen Granite in the S, whereas the Agardhbukta Fault starts under the ice of Balderfonna in the N and can be traced towards Agardhbukta in the S (Figs. 2B, 3, and 19) indicating a left-stepping arrangement of the two faults (Fig. 19). The kinematics and geometries of fault orientations in the overlap area suggest that this area underwent strike-slip deformation characterized by zones of contraction and extension in the overlap area between the overstepping Lomfjorden and Agardhbukta faults (Fig. 19). In this scenario, two possible strike-slip scenarios are possible:

(a) The Dolerittfjellet Reverse Fault can be related to a left-stepping contractional overstep or to left-stepping wrench faults with NNW–SSE striking reverse faults in the overstep zone (McClay, 1987; Fig. 19A_1) or dextral restraining offsets (Woodcock and Fischer, 1986; Fig. 19A). This situation is comparable with the local NE–SW shortening directions in Carboniferous and younger rocks at Mjølnerfjellet, Raudberget, Malte Brunfjellet, and in Neoproterozoic rocks at Vivienberget (Fig. 19A). These geometries are compatible with a N–S trending dextral strike-slip deformation.

(b) The Sillhøgda Fault and parallel oriented normal faults can be related to a left-stepping extensional overstep or to left-stepping wrench faults with NNW–SSE striking extensional faults in the overstep zone (McClay, 1987; Fig. 19B_1) or sinistral releasing offsets (Woodcock and Fischer, 1986; Fig. 19B). This situation is comparable with the local NE–SW extension directions in Carboniferous and younger rocks at Kirtonryggen and Malte Brunfjellet and is supported by NW–SE oriented shortening directions in Carboniferous and younger rocks at Vinkelen, Raudberget, Kirtonryggen and Malte Brunfjellet (Fig. 19B). These geometries are compatible with a N–S trending sinistral strike-slip deformation.

It should be noted that the large intrusion of the Newtontoppen Granite is situated just SW of the overlap area between the Lomfjorden and Agardhbukta faults (Fig. 19). The intrusive body has most probably acted as a buttress during strike-slip deformation and is responsible for the en-échelon offset between the two major faults and the location of the releasing and restraining offsets in the overlap area. Teben'kov et al. (1996) described the Newtontoppen Granite as an asymmetric lopolith or harpolith-like body with a steep root in its southwestern part and extended elongations towards the N and E. This may be a reason that strike-slip along the Lomfjorden fault could not penetrate through the granite at its western side.

From the cutting relations described above, the following relative succession of post-Early Cretaceous tectonic phases along the northern and central segments of the Lomfjorden Fault Zone can be expected:

(1) The older deformation phase 1 is characterized by the N–S striking contractional structures. Between the Veteranen and Lomfjorden faults in the northern segment, the steep Lomfjella and Bjørnfjellet reverse faults are characterized by W–E shortening (Figs. 3 and 19A). In the central segment, the 40 km long flexure in Carboniferous to Permian deposits E of the Agardhbukta Fault indicates that this section of the fault was also affected by E–W shortening (Fig. 19A).

(2) The second phase of deformation is characterized by strike-slip deformation along the major N–S striking faults characterized by opposing NE–SW and NW–SE shortening and extension directions in local outcrops and by left-stepping contractional and extensional oversteps in the transfer area between the en-échelon Lomfjorden and Agardhbukta faults at a larger scale. It was not possible in the field to determine a relative timing of the dextral and sinistral phases of lateral motions, respectively, because we could not find clear cutting relationships of structures of the two phases.

The significance of the N–S trending strike-slip movements along the Lomfjorden Fault Zone cannot be estimated because the large-scale, N–S striking master faults are oriented almost parallel to the orientation of the Neoproterozoic rock units and the km-scale Caledonian F_1-folds, and the Carboniferous sedimentary rocks are always sub-horizontal, except for some folded areas in the vicinity of the faults. Therefore, it is not possible to calculate or establish any amounts of lateral displacements along the northern and central segments of the Lomfjorden Fault Zone.

Extensional structures. Apart from convergent and lateral structures along the Lomfjorden Fault Zone, there is also evidence for normal faulting. The profile in Figure 4B shows that the Carboniferous and younger sedimentary cover is already eroded and removed in the high mountain areas W of the Lomfjorden Fault. East of it, the Carboniferous unconformity is located below sea level or a little bit higher. Along the Lomfjorden Fault Zone, the following down-to-east offsets can be estimated: In the northern segment, the downthrow across the Lomfjorden

Fault exceeds 600 m between Lomfjella and Lomfjordhalvøya (Fig. 4A) and about 900m between Jakobitoppen and Klumpen (Fig. 4B). Farther E, the downthrow across the Agardhbukta Fault between Raudberget and Mertonryggen is at least 600 m (Fig. 4B). This is a difference of more than 1,500 m between the high mountains W of Chydeniusbreen and the E-coast of Lomfjordhalvøya across the entire fault zone. In the central segment, downthrows of 500-600 m can be estimated between Golitsynfjellet and Pachtusovfjellet and at Vivienberget (Fig. 6B). In the southern segment, Miloslavskij et al. (1993b) have estimated amounts of normal displacements from 400-450 m at Eistraryggen N of Agardhdalen decreasing to 100 m at Rurikfjellet S of Agardhdalen. The timing of the extensional movements remains difficult. Apatite fission track analyses by Dörr et al. (2012) suggested that post-Early Jurassic uplift led to removal of the Triassic, Jurassic and possibly younger sequences in the study area by erosion, and the exhumation of the Newtontoppen Granite took place in latest Cretaceous to Paleocene times. It is also possible, that vertical movements, apart from the W–E contraction along the Lomfjella and Bjørnfjellet reverse faults, were caused by oblique lateral movements, or by young extension following the strike-slip movements along the Lomfjorden Fault Zone.

Lateral variation in the Lomfjorden Fault Zone

South of Malte Brunfjellet, the southern section of the Agardhbukta Fault runs through Mesozoic sedimentary rocks and has affected Triassic and Jurassic strata (Miloslavskij et al., 1993a, b; Fig. 2B). North and S of Agardhdalen, the exposed fault zone constitutes a single, asymmetric E-facing, disrupted anticline in Mesozoic and probably Permian rocks (Kellogg, 1975; Andresen et al., 1988, 1992, 1994; Larsen, 1988; Nøttvedt et al., 1988; Haremo and Andresen, 1992; Miloslavskij et al., 1993a, b; Figs. 2B and 20). The deformation between the Billefjorden and Lomfjorden fault zones is characterized by a combination of thin-skinned and thick-skinned tectonics. Both the Billefjorden and Lomfjorden fault zones are pre-existing, steep, E- and W-dipping, respectively, basement-involved faults, which were reactivated during the Paleogene contraction causing inversion and uplift of the Ny-Friesland Block between the two fault zones (e.g., Nøttvedt et al., 1988; Haremo and Andresen, 1992; Fig. 20).

Although the southern segment of the Lomfjorden Fault Zone seems to be dominated by E–W shortening, the geological map (Miloslavskij et al., 1993a) shows a number of faults, monoclines, and anticline-syncline pairs approaching the main fault zone near Agardhdalen at acute angles from the NE (Fig. 2B). These oblique, amalgamating orientations with respect to the main fault, which are typical structures in strike-slip zones, indicate that lateral displacements may have affected the Lomfjorden Fault Zone also in its southernmost segment. The oblique orientations of the syncline and anticline axes with respect to the Agardhbukta Fault in this area (Miloslavskij et al., 1993a, b) are compatible with sinistral displacements along the Agardhbukta Fault and possibly the Storfjorden Fault in the E (Fig. 2B).

In contrast to the southernmost segment, the Lomfjorden Fault Zone N of Malte Brunfjellet (Fig. 2B) has affected Neoproterozoic and Paleozoic, but no Mesozoic rock units, except for the Early Cretaceous dolerite sills (Figs. 2B and 3). While the southernmost segment is dominated by contractional movements along detachment zones and thrusts, but only little strike-slip components (see citations above), the northern and central segments are characterized by both E–W shortening along steep reverse faults during a first and by strike-slip movements during a second tectonic phase.

The apparent structural difference between the northern/central and southernmost segments of the Lomfjorden Fault Zone can be explained by the different levels of exposure. Andresen et al. (1988, 1992), Nøttvedt et al. (1988) and Miloslavskij et al. (1993b) suggested that the contractional deformation at Agardhbukta was caused by a steep, pre-existing fault in the Neoproterozoic basement underneath the Mesozoic and upper Paleozoic sedimentary succession (Fig. 20). Possible candidates for such basement-rooted faults are exposed in the northern (Lomfjella and Bjørnfjellet reverse faults) and in the central segment of the fault zone (flexure E of the Agardhbukta Fault). These observations in combination with the results presented here suggest that the northern segment of the Lomfjorden Fault Zone represents the basement involved deeper level of the fault zone, which is covered by a Mesozoic succession in the S. It should be noted that the assumed steep faults in the southern segment and the steep reverse faults in the northern segment represent pre-existing, probably Carboniferous (and maybe older) faults, which have been reactivated during the E–W shortening after the intrusion of the Early

Cretaceous dolerite sills along the entire Lomfjorden Fault Zone, as suggested by Bergh et al. (1994).

Relationship of the Lomfjorden Fault Zone to the West Spitsbergen Fold-and-Thrust Belt

The relationship between the West Spitsbergen Fold-and-Thrust Belt and the Lomfjorden Fault Zone at Agardhdalen in the E is documented by the detachment zones in Triassic and Jurassic strata underneath the Central Tertiary Basin (Fig. 20). The observed deformation along the Lomfjorden Fault Zone was transferred from the W-coast of Spitsbergen eastwards along at least three detachment zones localized in Permian gypsum and middle Triassic and late Jurassic organic-rich shales (Andresen et al., 1988, 1992, 1994; Nøttvedt et al., 1988; Haremo and Andresen, 1992; Braathen et al., 1995; Bergh et al., 1997; Blinova et al., 2012, 2013; Fig. 20). The sedimentary successions hosting the three detachment zones in the southern segment of the Lomfjorden Fault Zone are already eroded and removed in the northern and central segments. This suggests that a much deeper detachment horizon is required for the contraction in the northern and central segments of the fault zone, that generated or reactivated reverse faults in the Neoproterozoic rocks in the N, but also the assumed basement-rooted faults in the S. A possible candidate is an Ellesmerian/Svalbardian detachment assumed in the pre-Devonian basement underneath the deformed Old Red Sandstone basin by Piepjohn (1994, 2000) and Piepjohn et al. (2015). Similar sub-Ellesmerian detachments are known from North Greenland and Ellesmere Island (Soper and Higgins, 1987; Klaper, 1990; Piepjohn et al., 2008; Piepjohn and von Gosen, 2017; Stephenson et al., 2017). On Ellesmere Island, they were reactivated during the Paleogene Eurekan Orogeny (Harrison, 2008; Piepjohn et al., 2008; Piepjohn and von Gosen, 2017). It is possible that such an Ellesmerian deep-seated detachment on Spitsbergen was reactivated during the Eurekan convergent movements and responsible for the convergence across the post-Early Cretaceous reverse faults between the Veteranen and Lomfjorden faults in the northern segment.

This model may explain the differences between the northern/central and southernmost segments: the Mesozoic cover rocks including the convergent Eurekan detachment zones are located in a crustal level that is already eroded in the northern segment. The Lomfjella and Bjørnfjellet reverse faults in the northern segment can possibly be related to the same orthogonal convergence. As the detachment zones are related to the formation of the West Spitsbergen Fold-and-Thrust Belt, the age of the post-Early Cretaceous deformation phases in the northern and central segments can be estimated as follows: The age of the West Spitsbergen Fold-and-Thrust Belt is estimated to be Paleogene by most authors (e.g., Kellogg, 1975; Andresen et al., 1988, 1992; Larsen, 1988; Nøttvedt et al., 1988; Maher et al., 1989; Gion et al., 2017). K–Ar whole rock ages of 49 Ma in ductilely deformed Carboniferous sediments at the E-coast of Forlandsundet Graben (Tessensohn et al., 2001) and $^{40}Ar/^{39}Ar$ muscovite ages of 55–44 Ma in the basement rocks of Prins Karls Forland (Faehnrich et al., 2017; Schneider et al., this volume, chapter 8) indicate that the culmination of the Eurekan Orogeny took place in the early Eocene. This is supported by Kleinspehn and Teyssier (2016), Piepjohn et al. (2016), and Barnes and Schneider (this volume, chapter 7) who suggest a structural change from convergent tectonics during a first phase (53–47 Ma) to strike-slip tectonics during a second stage (47–34 Ma) of the Eurekan Orogeny. The convergent E–W contraction was transferred to the E durng the first Eurekan phase (re-)activating the steep reverse faults along the Lomfjorden Fault Zone. Therefore, an Early Eocene age for the E–W shortening across the Lomfjella and Bjørnfjellet reverse faults in the northern and across the Agardhbukta Fault in the central and southern segments of the Lomfjorden Fault can be inferred, as supported by Bergh et al. (1994). The strike-slip movements along the Lomfjorden Fault Zone post-date the E–W contraction and can be therefore correlated with the second Eurekan phase of strike-slip faulting at the W-coast of Spitsbergen in the Late Eocene.

The Lomfjorden Fault Zone within the Arctic framework

The formation of the West Spitsbergen Fold-and-Thrust Belt and the dextral translation along and parallel to the Hornsund Fault Complex at the W-coast of Spitsbergen (Riis & Vollset, 1988; Sigmond, 2002; Dallmann, 2015) (including the Lomfjorden Fault Zone; Fig. 21) is closely connected with the Paleocene/Eocene plate-tectonic reconfiguration during the opening of the Eurasian Basin, Labrador Sea/Baffin Bay, and the North Atlantic Ocean (e.g., Talwani and Eldholm, 1977; Srivastava, 1978, 1985; Vink, 1982; Srivastava and Tapscott, 1986; De Paor et al., 1989; Tessensohn and Piepjohn, 2000; Gaina et al., 2009; Faleide et al., 2010; Tsikalas et al., 2012; Døssing et al., 2013; Dallmann, 2015; Doré et al., 2016; Piepjohn et al., 2015, 2016; Gion et al., 2017; Sømme et al., 2018). The orientation parallel to the continental margin of Svalbard and the succession of tectonic structural events indicate that the Lomfjorden Fault Zone, together with the Billefjorden Fault Zone and possibly the Svartfjella-Eidembukta-Daudmannsodden Lineament at the W-coast of Spitsbergen (Maher et al., 1997), represent major structural elements of the Eurekan Orogeny and the resulting movements between Greenland and Svalbard during the final separation of North America and Eurasia. In this context it should be noted that many faults in the Eurekan deformation zones on Ellesmere Island are characterized by two or multiphase, often staggered opposing sinistral and dextral strike-slip regimes (Fig. 21). On Ellesmere Island, sinistral strike-slip movements along the Wegener Fault were followed by contraction or oblique-sinistral movements along the Wegener Fault (Piepjohn et al., 2000b, 2013, 2016; Saalmann et al., 2005, 2008; Tessensohn et al., 2008; von Gosen et al., 2008, 2012, this volume, chapter 18; Fig. 21). The fault zones parallel to the continental margin of North America (e.g., Mount Rawlinson Fault, Feilden Fault Zone) are characterized by both dextral and sinistral strike-slip movements (Piepjohn et al., 2013; Fig. 21). In Svalbard NE of the Hornsund Fault Complex, orthogonal contraction and formation of the West Spitsbergen Fold-and-Thrust Belt was followed by dextral strike-slip tectonics (CASE Team, 2001; Piepjohn et al., 2015, 2016; Kleinspehn and Teyssier, 2016; Barnes and Schneider, this volume, chapter 7). The structural development along Lomfjorden Fault Zone shows a similar structural development with W-E contraction in an early deformation phase (possibly associated with the Eurekan stage 1 by Piepjohn et al., 2016) and a later phase of dextral and sinistral strike-slip deformation, possibly associated with the Eurekan stages 1 and 2 by Piepjohn et al. (2016), respectively.

It remains unclear how the sinistral strike-slip movements in the northern/central segment of the Lomfjorden Fault Zone developed in the general dextral plate-tectonic setting between Northeast Greenland and Svalbard (see Fig. 21). But it should be noted that Ohta (1988), Maher et al. (1997), and Bergh et al. (2000) also assumed or observed sinistral strike-slip displacement at the NE-margin of Forlandsundet along the Svartfjella-Eidembukta-Daudmansodden lineament (SEDL; Fig. 2A). Maher et al. (1997) and Bergh et al. (2000) suggested two basic possibilities: (a) the sinistral motion is a local phenomenon in an overall dextral transpressive setting or (b) the sinistral motion reflects a short period of sinistral motion between Greenland and Svalbard (Barents Shelf) as proposed by Skilbrei and Srivastava (1993).

It is not possible to determine amounts of lateral dispacements long the Lomfjorden Fault Zone, because the faults are located almost parallel to the pre-Carboniferous Caledonian sturctures in the Neoproterotzoic rocks and the strike-slip faults cut through horizontal Carboniferous and younger rocks. This is similar to many other Eurekan strike-slip fault zones on Ellesmere Island, where the structural trends of the Ellesmerian and Eurekan deformations are more or less parallel, and often, structures of the Ellesmerian orogeny are affected or reactivated by Eurekan deformation (e.g., Piepjohn et al., 2008, 2015). It is also characteristic that the Carboniferous faults, which were generated during the formation of the St. Jonsfjorden, Billefjorden and Lomfjorden basins, were reactivated during the contractional and lateral movements of the Eurekan deformation: similar to the Lomfjorden Fault Zones, Early Carboniferous fault zones have been reactivated in North Greenland (Depot Bugt Conglomerate; Piepjohn and von Gosen, 2001) and on Ellesmere Island ("Okse Bay Group"; Beauchamp et al., this volume, chapter 13). The locations of Paleogene Eurekan contractional and lateral faults paralleling the continental margins of Barents Shelf and North America were controlled by the pre-existing zones of crustal weakness from Carboniferous or even older tectonic events.

CONCLUSIONS

The N–S striking Lomfjorden Fault Zone in eastern Spitsbergen consists of three master faults, the Veteranen, Lomfjorden, and Agardhbukta faults, which are linked up by a complex network of NE–SW and NW–SE striking strike-slip, reverse and normal faults. The fault zone cuts through Neoproterozoic, Carboniferous, and Permian sedimentary rocks and Early Cretaceous dolerite sills in the northern and central segments, while it also affects Mesozoic successions in the southernmost segment. Early deformation along the zone is represented by steep reverse faults and convergent flexures parallel to the major fault strands indicating that the Lomfjorden Fault Zone was affected by Eurekan E–W shortening during a first phase in the early Eocene, most probably coeval with the development of the West Spitsbergen Fold-and-Thrust Belt. The reverse faults in the northern and central segments of the Lomfjorden Fault Zone correspond to the deep-seated, basement-involved and reactivated faults in the southern segment, which have there been suggested to occur under the Mesozoic successions. The detachment zones, which controlled the structural development in the southern segment, must have been eroded farther N. There instead, a much deeper detachment horizon is required in the basement, which may be a reactivated Ellesmerian detachment.

This convergent deformation was, in conformity with the transform plate margin development to the W, followed by strike-slip movements along the Lomfjorden Fault Zone during a second Eurekan phase in the late Eocene. The relative temporal succession of the two superimposed, dextral and sinistral, strike-slip regimes remains uncertain. Strike-slip deformation included transpressional and transtensional structures between the main fault strands. A particularly prominent feature is a transfer zone between the Lomfjorden and Agardhbukta faults just N of a major granite body (Newtontoppen Granite), which seems to control the position of the faults by deflecting them around it. The location of the Lomfjorden Fault Zone and its main fault strands is most likely inherited from Caledonian and/or Carboniferous structures. Being zones of crustal weakness, these were reactivated during the Eurekan deformation and the break-up of Laurasia.

ACKNOWLEDGMENTS

Structural fieldwork in eastern Ny-Friesland was carried out during joint expeditions of the Norwegian Polar Institute (NP) and the German Federal Institute for Geosciences and Natural Resources (BGR) in 2001, 2005, 2006, and 2009. The expeditions were embedded in the Norway's mapping program and BGR’s research program CASE (Circum-Arctic Structural Events) in cooperation with the universities of Bremen, Idaho, Munich, Tromsø, and the natural museums of Berlin and Oslo. Winfried Dallmann is thankful to the Norwegian Polar Institute for long-term fieldwork support during the years 2005 to 2009. We would also like to thank Donald C. Murphy, Werner von Gosen, and the volume editors William C. McClelland and Lutz Reinhardt for many suggestions and comments on the manuscript, and Science Editor Christian Koeberl for handling this submission. Alvar Braathen's, Justin Strauss’ and one anonymous reviewer's comments and suggestions helped to considerably improve the manuscript.

REFERENCES CITED

Andresen, A., Bergh, S.G., and Haremo, P., 1994, Basin inversion and thin-skinned deformation associated with the Tertiary transpressional West Spitsbergen Orogen, in Thurston, D.K., and Fujita, K., eds., 1992 proceedings, International Conference on Arctic Margins, Anchorage, Alaska, September 1992: U.S. Deptartment of the Interior, Minerals Management Service, Alaska Outer Continental Shelf Region, p. 161–166.

Andresen, A., Haremo, P., and Bergh, S.G., 1988, The southern termination of the Lomfjorden Fault Zone; evidence for Tertiary compression on East-Spitsbergen, *in* Dallmann, W.K., Ohta, Y., and Andresen, A., eds., Tertiary Tectonics of Svalbard, Extended abstracts from Symposium held in Oslo 26 and 27 April 1988: Norsk Polarinstitutt Rapportserie, v. 46, p. 75–78.

Andresen, A., Haremo, P., Swensson, E., and Bergh, S.G., 1992, Structural geology around the southern termination of the Lomfjorden Fault Complex, Agardhdalen, east Spitsbergen, *in* Dallmann, W.K., Andresen, A., and Krill, A., eds., Post-Caledonian Tectonic Evolution of Svalbard, Proceedings from an International Conference held in Oslo 15-16 November 1990: Norsk Geologisk Tidsskrift, v. 72, p. 83–91.

Barnes, C.J., and Schneider, D.A., 2018, this volume, chapter 7, Late Cretaceous−Paleogene burial and exhumation history of the Southwestern Basement Province, Svalbard, revealed by zircon (U-Th)/He thermochronology, *in* Piepjohn, K., Strauss, J.V., Reinhardt, L., and McClelland, W.C., eds., Circum-Arctic Structural Events: Tectonic Evolution of the Arctic Margins and Trans-Arctic Links with Adjacent Orogens: Geological Society of America Special Paper, v. 541, Chapter 7, https://doi.org/10.1130/2018.2541(07).

Bartlett, W.L., Friedman, M., and Logan, J.M., 1981, Experimental folding and faulting of rocks under confining pressure. Part IX. Wrench faults in limestone layers: Tectonophysics, v. 79, p. 255–277.

Beauchamp, B., Alonso-Torres, D., Piepjohn, K., Thériault, P., and Grasby, S.E., 2018, this volume, chapter 13, Early Carboniferous syn-rift sedimentation in the Sverdrup Basin (Yelverton Pass area, northern Ellesmere Island, Arctic Canada): A solution to the Okse Bay problem, *in* Piepjohn, K., Strauss, J.V., Reinhardt, L., and McClelland, W.C., eds., Circum-Arctic Structural Events: Tectonic Evolution of the Arctic Margins and Trans-Arctic Links with Adjacent Orogens: Geological Society of America Special Paper 541, https://doi.org/10.1130/2018.2541(13).

Bergh, S.G., and Grogan, P., 2003, Tertiary structure of the Sørkapp-Hornsund Region, South Spitsbergen, and implications for the offshore southern extension of the fold-thrust belt: Norwegian Journal of Geology, v. 83, p. 43–60.

Bergh, S.G., Braathen, A., and Maher Jr., H.D., 1994, The Lomfjorden fault zone: basement-controlled Carboniferous subsidence and Tertiary contractional reactivation in the Svalbard Foreland, East Spitsbergen: Tectonics and Structural Geology Studies Group of Norwegian Geological Society, (Nov. 10-11 1994), abstract, p. 20.

Bergh, S.G., Braathen, A., and Andresen, A., 1997, Interaction of basement-involved and thin-skinned tectonism in the Tertiary Fold-Thrust belt of central Spitsbergen, Svalbard: American Association of Petroleum Geologists Bulletin, v. 81, p. 637–661.

Bergh, S.G., Maher Jr., H.D., and Braathen, A., 2000, Tertiary divergent thrust directions from partitioned transpression, Brøggerhalvøya, Spitsbergen: Norsk Geologisk Tidsskrift, v. 80, p. 63–82.

Bergh, S.G., Maher Jr., H.D., and Braathen, A., 2011, Late Devonian transpressional tectonics in Spitsbergen, Svalbard, and implications for basement uplift of the Sørkapp-Hornsund High: Journal of the Geological Society, v. 168, p. 441–456.

Birkenmajer, K., 1972a, Tertiary history of Spitsbergen and continental drift: Acta Geologica Polonica, v. 22, no. 2, p. 200–218.

Birkenmajer, K., 1972b, Alpine fold belt of Spitsbergen: International Geological Congress, 24th Session, p. 282–292.

Birkenmajer, K., 1981, The Geology of Svalbard, the western part of the Barents Sea, and the continental margin of Scandinavia, *in* Nairn, A.E.M., Churkin, M., and Stehli, F.G., eds., The Ocean Basins and Margins. The Arctic Ocean: Plenum Press, v. 5, p. 265–329.

Blinova, M., Faleide, J.I., Gabrielsen. R.H., and Mjelde, R., 2012, Seafloor expression and shallow structure of a fold-and-thrust system, Isfjorden, west Spitsbergen: Polar Research, v. 31, 11209, http://dx.doi.org/10.3402/polar.v31i0.11209.

Blinova, M., Faleide, J.I., Gabrielsen. R.H., and Mjelde, R., 2013, Analysis of structural trends of sub-sea-floor strata in the Isfjorden area of the West Spitsbergen Fold-and-Thrust Belt based on multichannel seismic data: Journal of the Geological Society, London, v. 170, p. 657–668. doi: 10.1144/jgs2012-109.

Braathen, A., Bergh, S.G., and Maher Jr., H.D., 1995, Structural outline of a Tertiary basement-cored uplift/inversion structure in western Spitsbergen, Svalbard: Kinematics and controlling factors: Tectonics, v. 14, no. 1, p. 95–119.

Braathen, A., Bælum, K., Maher Jr., H.D., and Buckley, S.J., 2011, Growth of extensional faults and folds during deposition of an evaporite-dominated half-graben basin; the Carboniferous Billefjorden Trough, Svalbard: Norwegian Journal of Geology, v. 91, p. 137–161.

CASE Team, 2001, The evolution of the West Spitsbergen Fold-and-Thrust Belt, *in* Tessensohn, F., ed., Intra-Continental Fold Belts. CASE 1: West Spitsbergen: Geologisches Jahrbuch (Polar Issue No. 7) B 91, p. 733–773.

Christie-Blick, N., and Biddle, K.T., 1985, Deformation and Basin Formation along Strike-Slip Faults, *in* Biddle, K.T., and Christie-Blick, N., eds., Strike-slip deformation, basin formation, and sedimentation: Society of Economic Paleontologists and Mineralogists, Special Publications, v. 37, p. 1–34.

Corfu, S.P., Polteau, S., Planke, S., Faleide, J.I., Svensen, H., Zayoncheck, A., and Stolbov, N., 2013, U–Pb geochronology of Cretaceous magmatism on Svalbard and Franz Josef Land, Barents Sea Large Igneous Province: Geological Magazine, v. 150, no. 6, p. 1127–1135, doi: 10.1017/S0016756813000162.

Cutbill, J.L., and Challinor, A., 1965, Revision of the stratigraphical scheme of the Carboniferous and Permian rock of Spitsbergen and Bjørnøya: Geological Magazine, v. 102, p. 418–439.

Dallmann, W.K., ed., 1999, Lithostratigraphic Lexicon of Svalbard - Review and recommendations for nomenclature use. Upper Palaeozoic to Quaternary Bedrock: Stratigrafisk Komité for Svalbard (SKS) - Committée on the Stratigraphy of Svalbard. Norsk Polarinstitutt, p. 1–318.

Dallmann, W.K., ed., 2015, Geoscience Atlas of Svalbard: Norsk Polarinstitutt Rapport Series, v. 148, p. 1–292.

Dallmann, W. K., Andresen, A., Bergh, S. G., Maher Jr., H. D., and Ohta, Y., 1993, Tertiary fold-and-thrust belt of Spitsbergen, Svalbard: Norsk Polarinstitutt Meddelelser, v. 128, p. 1–46.

Dallmann, W.K., Ohta, Y., Elvevold, S., and Blomeier, D., 2002, Bedrock map of Svalbard and Jan Mayen, scale 1:750,000: Norsk Polarinstitutt Temakart 33.

Dallmann, W.K., Ohta, Y., Birjukov, A.S., Karnoušenko, E.P., Sirotkin, A.N., and Piepjohn, K., 2004, Geological map of Svalbard 1:100 000, sheet C7G Dicksonfjorden: Norsk Polarinstitutt Temakart 35.

Dallmann, W.K., Piepjohn, K., Elvevold, S., and Blomeier, D., 2009, Geological map of Svalbard 1:100 000, sheet D5G Lomfjordhalvøya: Norsk Polarinstitutt Temakart 44.

Dallmann, W.K., Elvevold, S., Piepjohn, K., and Blomeier, D., 2010, Geological map of Svalbard 1:100 000, sheet C5G Åsgårdfonna: Norsk Polarinstitutt Temakart 46.

Dallmann, W.K., Piepjohn, K., Halverson, G.P., Elvevold, S., and Blomeier, D., 2011, Geological map of Svalbard 1:100 000, sheet D6G Vaigattbogen: Norsk Polarinstitutt Temakart 48.

De Paor, D., Bradley, D., Eisenstadt, G., and Phillips, S., 1989, The Arctic Eurekan orogen: A most unusual fold-and-thrust belt: Geological Society of America Bulletin, v. 101, no. 7, p. 952–967.

Dörr, N., Lisker, F., Clift, P.D., Carter, A., Gee, D.G., Teben'kov, A.M., and Spiegel, C., 2012, Late Mesozoic-Cenozoic exhumation history of northern Svalbard and its regional significance: Constraints from apatite fission track analysis: Tectonophysics, v. 514-517, p. 81–92, doi:10.1016/j.tecto.2011.10.007.

Doré, A.G., Lundin, E.R., Gibbons, A., Sømme, T.P., and Tørudbakken, B.O., 2016, Transform margins of the Arctic: a synthesis and re-evaluation, *in* Nemčok, M., Rybar, S., Sinhar, S.T., Hermeston, S.A., and Ledvényiová, L., eds., Transform Margins: Development, Controls and Petroleum Systems: Geological Society of London, Special Publications, v. 431, p. 63–94.

Døssing, A., Hopper, J.R., Olesen, A.V., Rasmussen, T.M., and Halpenny J., 2013, New aero-gravity results from the Arctic Ocean: Linking the latest Cretaceous-early Cenozoic plate kinematics of the North Atlantic and Arctic Ocean: Geochemistry, Geophysics. Geosystems, v. 14, doi:10.1002/ggge.20253.

Eiken, O., 1985, Seismic mapping of the post-Caledonian strata in Svalbard: Polar Research, v. 3, p. 167–176.

Elvevold, S., and Dallmann, W.K., 2011, Geological map of Svalbard 1:100 000, sheet C4G Mosselhalvøya: Norsk Polarinstitutt Temakart 47.

Faehnrich, K., Schneider, D., Manecki, M., Czerny, J., Myhre, P.I., Majka, J., Kośmińska, K., Barnes, C., and Maraszewska, M., 2017, Eurekan deformation on Prins Karls Forland, Svalbard – new insights from Ar40/Ar39 muscovite dating: EGU General Assembly 2017, v. 19, p. 642.

Faleide, J.I., Bjorlykke, K., and Gabrielsen, R.H.O., 2010, Geology of the Norwegian Continental Shelf, *in* Bjorlykke, K., ed., Petroleum Geoscience: From Sedimentary Environments to Rock Physics, Springer, Berlin, p. 467–499.

Frebold, H., 1935, Geologie von Spitzbergen, der Bäreninsel, des König Karl- und Franz-Joseph-Landes, *in* Krenkel, E., ed., Geologie der Erde: Gebrüder Borntraeger Berlin, 195 p.

Friend, P.F., 1961, The Devonian stratigraphy of north and central Vestspitsbergen: Proceedings of the Yorkshire Geological Society, v. 33, p. 77–118.

Friend, P. F., and Moody-Stuart, M., 1972, Sedimentation of the Wood Bay Formation (Devonian) of Spitsbergen: a regional analysis of a late orogenic basin: Norsk Polarinstitutt Skrifter, v. 157, p. 1–77.

Gaina, C., Gernigon, L., and Ball, P., 2009, Palaeocene–Recent plate boundaries in the NE Atlantic and the formation of the Jan Mayen microcontinent: Journal of the Geological Society, London, v. 166, p. 601–616, http://dx.doi.org/10.1144/0016-76492008-112.

Gayer, R.A., Gee, D.G., Harland, W.B., Miller, J.A., Spali, H.R., Wallis, H.R., and Winsnes, T.S., 1966, Radiometric age determinations on rocks from Spitsbergen: Norsk Polarinstitutt Skrifter, v. 137, p. 1–39.

Gee, D.G., and Moody-Stuart, M., 1966, The base of the Old Red Sandstone in central north Haakon VII Land, Vestspitsbergen: Norsk Polarinstitutt Årbok 1964, p. 57–68.

Gee, D.G., and Teben'kov, A.M., 2004, Svalbard: A fragment of the Laurentian margin, *in* Gee, D.G., and Pease, V., eds., The Neoproterozoic Timanide Orogen of Eastern Baltica: Geological Society, London, Memoir, v. 30, p. 191–206.

Gee, D.G., Johansson, A., Ohta, Y., Teben'kov, A.M., Krasil'ščhikov, A.A., Balashov, Y.A., Larionov, A.N., Gannibal, L.F., and Ryungenen, G.I., 1995, Grenvillian basement and a major unconformity within the Caledonides of Nordaustlandet, Svalbard: Precambrian Research, v. 70, no. 3-4, p. 215–234.

Gion, A.M., Williams, S.E., and Müller, R.D., 2017, A reconstruction of the Eurekan Orogeny incorporating deformation constraints: Tectonics, v. 36, p. 304–320, doi:10.1002/2015TC004094.

Halvorsen, E., 1974, The magnetic fabric of some dolerite intrusions, Northeast Spitsbergen; Implications for their mode of emplacement: Earth and Planetary Science Letters, v. 21, p. 127–-133.

Haremo, P., and Andresen, A., 1992, Tertiary decollement thrusting and inversion structures along Billefjorden and Lomfjorden fault zones, East Central Spitsbergen, *in* Larsen, R.M., Brekke, H., Larsen, B.T., and Talleras, E., eds., Structural and tectonic modelling and its application to petroleum geology: Norwegian Petroleum Society Special Publications, v. 1, p. 481–494, https://doi.org/10.1016/B978-0-444-88607-1.50038-3.

Haremo, P., Andresen, A., Dypvik, H., Nagy, J., Elverhoi, A., Eikeland, T.A., and Johansen, H., 1990, Structural development along the Billefjorden Fault Zone in the area between Kjellstromdalen and Adventdalen/Sassendalen, central Spitsbergen: Polar Research, v. 8, p. 195–216.

Haremo, P., Swensson, E., and Andresen, A., 1992, Evidence of Mesozoic extension along the Lomfjorden Fault Zone, Agardhbukta: Norsk Geologisk Tidsskrift, v. 136, p. 137.

Harland, W.B., 1969, Contribution of Spitsbergen to understanding of tectonic evolution of North Atlantic region: American Association of Petroleum Geologists Memoir, v. 12, p. 817–-851.

Harland, W.B., 1973a, Mesozoic geology of Svalbard, *in* Pitcher, M.G., ed., Arctic Geology: American Association of Petroleum Geologists Memoir, v. 19, p. 135–148.

Harland, W.B., 1973b, Tectonic evolution of Barents Shelf and related plates, *in* Pitcher, M.G., ed., Arctic Geology: American Association of Petroleum Geologists Memoir, v. 19, p. 599–608.

Harland, W.B., 1979, A review of major faults in Svalbard, *in* Speed, R., Sharp, R., and Evernden, J.F., Proceedings of Conference VIII - Analysis of actual fault zones in bedrock, 1-5 April 1979: Open File Report of the United States Geological Survey, v. 79-1239, p. 157–180.

Harland, W.B., 1997, The Geology of Svalbard: Geological Society, London, Memoir, v. 17, 521 p.

Harland, W.B., and Horsfield, W.T., 1974, West Spitsbergen Orogen, *in* Spencer, A.M., ed., Cenozoic Orogenic Belts, Data for orogenic Studies: Geological Society, London, Special Publications, v. 4, p. 747–755.

Harland, W.B., Wallis, R.H., and Gayer, R.A., 1966, A revision of the lower Hecla Hoek succession in central north Spitsbergen and correlation elsewhere: Geological Magazine, v. 193, p. 70–97.

Harland, W.B., Cutbill, J.L., Friend, P.F., Gobbett, D.J., Holliday, D.W., Maton, P.I., Parker, J.R., and Wallis, R.H., 1974, The Billefjorden Fault Zone, Spitsbergen. The long history of a major tectonic lineament: Norsk Polarinstistutt Skrifter, v. 161, 72 p.

Harland, W.B., Scott, R.A., Auckland, K.A., and Snape, I., 1992, The Ny-Friesland Orogen, Spits-Bergen: Geological Magazine, v. 129, no. 6, p. 679–708.

Harrison, J.C., 2008, Regional variation in structural style, deformation kinematics, and summary of tectonic history, northeast Ellesmere Island, *in* Mayr, U., ed., Geology of northeast Ellesmere Island adjacent to Kane Basin and Nares Strait, Nunavut: Geological Survey of Canada Bulletin, v. 592, p. 245–284.

Harrison, J.C., Brent, T.A., and Oakey, G.N., 2006, Sheet 1 of 2, Bedrock Geology, Nares Strait, scale 1:1,000,000. Bedrock geology of the Nares Strait region of Arctic Canada and Greenland, with explanatory text and GIS content: Geological Survey of Canada Open-File Report 5278.

Håkansson, E., Heinberg, C., and Stemmerik, L., 1991, Mesozoic and Cenozoic history of the Wandel Sea Basin area, North Greenland, *in* Peel, J.S., and Sønderholm, M., eds., Sedimentary basins of North Greenland: Rapport Grønlands geologiske Undersøgelse, v. 160, p. 153–164.

Henriksen, N., 1992, Geological Map of Greenland 1:500,000, Sheet 7 Nybøe Land, Sheet 8 Peary Land: Grønlands Geologiske Undersøgelse, 40 p.

Higgins, A.K., and Soper, N.J., 1983, The Lake Hazen fault zone: a transpresional upthrust? Current Research, Part B. Geological Survey of Canada, Paper 83-1B, p. 215–221.

Hjelle, A., 1993, Geology of Svalbard: Norsk Polarinstitutt Polarhåndbok, v. 7, 162 p.

Hjelle, A., and Lauritzen, Ø., 1982, Geological map of Svalbard 1:500,000, sheet 3G, Spitsbergen northern part: Norsk Polarinstitutt Skrifter, v. 154c, p. 1–15.

Hoeppener, R., 1955, Tektonik im Schiefergebirge. Eine Einführung: Geologische Rundschau, v. 44, p. 26–58.

Kellogg, H.E., 1975, Tertiary stratigraphy and tectonism in Svalbard and continental Drift: American Association of Petroleum Geologists Bulletin, v. 59, p. 465–485.

Klaper, E.M., 1990, The mid-Paleozoic deformation in the Hazen fold belt, Ellesmere Island, Arctic Canada: Canadian Journal of Earth Sciences, v. 27, p. 1359–1370.

Kleinspehn, K.L., and Teyssier, C., 2016, Oblique rifting and the Late Eocene–Oligocene demise of Laurasia with inception of Molloy Ridge: Deformation of Forlandsundet Basin, Svalbard: Tectonophysics. http://dx.doi.org/10.1016/j.tecto.2016.05.010.

Lamar, D.L., Reed, W.E., and Douglass, D.N., 1986, The Billefjorden Fault Zone, Spitsbergen: is it part of a major Late Devonian transform? Geological Society of Amerca Bulletin, v. 97, p. 1083–108.

Larsen, B.T., 1988, Tertiary Thrust Tectonics in the east of Spitsbergen, and implications for the plate-tectonic development of the North-Atlantic, *in* Dallmann, W.K., Ohta, Y., and Andresen, A., eds., Tertiary Tectonics of Svalbard, extended abstracts from Symposium held in Oslo 26 and 27 April 1988: Norsk Polarinstitutt Rapportserie, v. 46, p. 85–88.

Leever, K.A., Gabrielsen, R.H., Faleide, J.I., and Braathen, A., 2011, A transpressional origin for the West Spitsbergen fold-and-thrust belt: Insight from analog modeling: Tectonics, v. 30, TC2014. doi: 10.1029/2010TC002753.

Lyberis, N., and Manby, G.M., 1999, Continental collision and lateral escape deformation in the lower and upper crust: An example from Caledonide Svalbard: Tectonics, v. 18, p. 40–63.

Maher Jr., H.D., 2001, Manifestations of the Cretaceous High Arctic Large Igneous Province in Svalbard: Journal of Geology, v. 109, p. 91-104, https://doi.org /10.1086/317960.

Maher Jr., H.D., and Craddock, C., 1988, Decoupling as an alternate model for transpression during the initial opening of the Norwegian-Greenland Sea: Polar Research, v. 6, p. 137–140.

Maher Jr., H.D., and Braathen, A., 2011, Løvehovden fault and Billefjorden rift basin segmentation and development, Spitsbergen: Geological Magazine, v. 148, no. 1, p. 154–170, doi:10.1017/S0016756810000567.

Maher Jr., H.D., Ringset, N., and Dallmann, W.K., 1989, Tertiary structures in the platform cover strata of Nordenskiold Land, Svalbard: Polar Research, v. 7, p. 83–93.

Maher Jr., H.D., Bergh, S.G., Braathen, A., and Ohta, Y., 1997, Svartfjella, Eidembukta, and Daudmannsodden lineament: Tertiary orogen-parallel motion in the crystalline hinterland of Spitsbergen's fold-thrust belt: Tectonics, v. 16, no. 1, p. 88–106.

Manby, G. M., 1990, The geology of the Harkerbreen Group, Ny-Friesland, Svalbard: protoliths and tectonic significance: Geological Magazine, v. 127, p. 129–146.

Manby, G.M., and Lyberis, N., 1992, Tectonic evolution of the Devonian Basin of northern Svalbard, *in* Dallmann, W.K., Andresen, A., and Krill, A., eds., Post-Caledonian Tectonic Evolution of Svalbard, Proceedings from an International Conference held in Oslo 15-16 November 1990: Norsk Geologisk Tidsskrift, v. 72, p. 7–19.

Manby, G.M., Lyberis, N., Chorowicz, J., and Thiedig, F., 1994, Post-Caledonian tectonics along the Billefjorden fault zone, Svalbard, and its implications for the Arctic region: Geological Society of America Bulletin, v. 105, p. 201–216.

McCann, A.J., 2000, Deformation of the Old Red Sandstone of NW Spitsbergen; links to the Ellesmerian and Caledonian orogenies, *in* Friend, P.F., and Williams, B.P.J., eds., New Perspectives on the Old Red Sandstone: Geological Society, London, Special Publications, v. 180, p. 567–584.

McCann, A.J., and Dallmann, W.K., 1996, Reactivation history of the long-lived Billefjorden Fault Zone in north central Spitsbergen, Svalbard: Geological Magazine, v. 133, no. 1, p. 63–84.

McClay, K.R., 1987, The Mapping of Geological Structures. Geological Society of London Handbook, vi + 161 p. Milton Keynes: Open University Press; New York, Toronto: Halsted Press, John Wiley. ISBN 0 335 15096 9(OUP); 0 470 20355 2 (Halstead).

Miloslavskij, M.J., Birjukov, A.S., Šlënskij, S.N., Hansen, S., Larsen, B.T., Dallmann, W.K., and Andresen, A., 1993a, Geological map of Svalbard 1:100 000, sheet D9G Agardhfjellet - Map: Norsk Polarinstitutt Temakart 21.

Miloslavskij, M.J., Dallmann, W.K., Dypvik, H., Krasil´čšikov, A.A., Birkeland, Ø., and Salvigsen, O., 1993b, Geological Map of Svalbard 1:100,000, sheet D9G Agardhfjellet - Text: Norsk Polarinstitutt Temakart, v. 21, p. 1–41.

Miloslavskij, M.J., Birjukov, A.S., Šlënskij, S.N., Krasil´čšikov, A.A., and Dallmann, W.K., 1996, Geological map of Svalbard 1:100 000, sheet D8G Negribreen: Norsk Polarinstitutt Temakart 25.

Murašov, L.G., and Mokin, J.I., 1979, Stratigraphic subdivision of the Devonian deposits of Spitsbergen: Norsk Polarinstitutt Skrifter, v. 167, p. 49–261.

Myhre, P.I., 2005, The tectonomagmatic evolution of Svalbard's northwestern terrane: U/Pb ages from Proterozoic crust and Caledonian magmatic evolution in Spitsbergen. Unpublished Master-thesis, University of Oslo, pp.

Nathorst, A. G., 1910, Beiträge zur Geologie der Bären-Insel, Spitzbergens und des König-Karl-Landes: Bulletin of the Geological Institution of the University of Uppsala, v. 10, p. 261–416.

Nøttvedt, A., Livbjerg, F., and Midbøe, P., 1988, Tertiary deformation on Svalbard – various models and recent advances, *in* Dallmann, W.K., Ohta, Y., and Andresen, A., eds., Tertiary Tectonics of Svalbard, Extended abstracts from Symposium held in Oslo 26 and 27 April 1988: Norsk Polarinstitutt Rapportserie, v. 46, p. 79–84.

Odell, N.E., 1927, Preliminary notes on the geology of the eastern parts of central Spitsbergen; with special reference to the problem of the Hecla Hook Formation: Quarterly Journal of the Geological Society, v. 83, p. 147–162.

Ohta, Y., 1988, Structure of Carboniferous strata at Tryghamna and along the SE margin of the Forlandsundet graben: Norsk Polarinstitutt Rapportserie, v. 46, p. 25–28.

Okulitch, A.V., 1991, Geology of the Canadian Arctic Archipelago, Northwest Territories and North Greenland, scale 1:2,000,000, *in* Trettin, H.P., ed., Geology of the Innuitian Orogen and Arctic Platform of Canada and Greenland, Geology of Canada: Geological Survey of Canada, v. 3.

Okulitch, A.V., and Trettin, H.P., 1991, Late Cretaceous - Early Tertiary deformation, Arctic Islands, *in* Trettin, H.P., ed., Geology of the Innuitian Orogen and Arctic Platform of Canada and Greenland, Geology of Canada: Geological Survey of Canada, v. 3, p. 469–490.

Orvin, A.K., 1940, Outline of the geological history of Spitsbergen; Skrifter om Svalbard og Ishavet, v. 78, p. 1–57.

Piepjohn, K., 1994, Tektonische Evolution der Devongräben (Old Red) in NW-Svalbard [PhD thesis]: Westfälische Wilhelms-Universität Münster, 170 p.

Piepjohn, K., 2000, The Svalbardian/Ellesmerian deformation of the Old Red Sandstone and the pre-Devonian basement in NW-Spitsbergen (Svalbard), *in* Friend, P.F., and Williams, B.P.J., eds., New Perspectives on the Old Red Sandstone: Geological Society, London, Special Publications, v. 180, p. 585–601.

Piepjohn, K., and Dallmann, W.K., 2014, Stratigraphy of the uppermost Old Red Sandstone of Svalbard (Mimerdalen Subgroup): Polar Research, v. 33, doi: org/10.3402/polar.v33. 19998.

Piepjohn, K., and von Gosen, W., 2001, Polyphase deformation at the Harder Fjord Fault Zone (North Greenland): Geological Magazine, v. 138, no. 4, p. 407–434.

Piepjohn, K., and von Gosen, W., 2017, Structural transect through Ellesmere Island (Canadian Arctic): superimposed Palaeozoic Ellesmerian and Cenozoic Eurekan deformation, *in* Pease, V., and Coakley, B., eds., Circum-Arctic Lithosphere Evolution: Geological Society, London, Special Publications, v. 460, p. 33–56, https://doi.org/10.1144/SP460.5.

Piepjohn, K., Brinkmann, L., Grewing, A., and Kerp, H., 2000a, New data on the age of the uppermost ORS and the lowermost post-ORS strata in Dickson Land (Spitsbergen) and implications for the age of the Svalbardian deformation, *in* Friend, P.F., and Williams, B.P.J., eds., New Perspectives on the Old Red Sandstone: Geological Society London, Special Publications, v. 180, p. 603–609.

Piepjohn, K., Tessensohn, F., Harrison, C., and Mayr, U., 2000b, Involvement of a Tertiary Foreland Basin in the Eurekan Foldbelt Deformation, NW Coast of Kane Basin, Ellesmere Island, Canada: Polarforschung, v. 68, p. 101–110.

Piepjohn, K., von Gosen, W., Tessensohn, F., and Saalmann, K., 2008, Ellesmerian fold-and-thrust belt (northeast Ellesmere Island, Nunavut) and its Eurekan overprint, *in* Mayr, U., ed., Geology of northeast Ellesmere Island adjacent to Kane Basin and Nares Strait, Nunavut: Geological Survey of Canada Bulletin, v. 592, p. 285–303.

Piepjohn, K., von Gosen, W., Läufer, A., McClelland, W.C., and Estrada, S., 2013, Ellesmerian and Eurekan fault tectonics at the northern margin of Ellesmere Island (Canadian High Arctic): Zeitschrift der Deutschen Gesellschaft für Geowissenschaften (German Journal of Geosciences), v. 164, no. 1, p. 81–105, doi: 10.1127/1860-1804/2013/0007.

Piepjohn, K., von Gosen, W., Tessensohn, F., Reinhardt, L., McClelland, W.C., Dallmann, W., Gaedicke, C., and Harrison, J.C., 2015, Tectonic map of the Ellesmerian and Eurekan deformation belts on Svalbard, North Greenland, and the Queen Elizabeth Islands (Canadian Arctic): arktos, v. 1, doi: 10.1007/s41063-015-0015-7.

Piepjohn, K., von Gosen, W., and Tessensohn, F., 2016, The Eurekan Deformation in the Arctic: an outline: Journal of the Geological Society, v. 173, doi: 10.1144/jgs2016-081.

Playford, G., 1962/63, Lower Carboniferous microfloras of Spitsbergen: Palaeontology, v. 5, no. 3-4, p. 550–678.

Riis, F., and Vollset, J., 1988, A preliminary interpretation of the Hornsund Fault Complex between Sørkapp and Bjørnøya, *in* Dallmann, W.K., Ohta, Y., and Andresen, A., eds., Tertiary Tectonics of Svalbard, extended abstracts from Symposium held in Oslo 26 and 27 April 1988: Norsk Polarinstitutt Rapportserie, v. 46, p. 91–92.

Ringset N., and Andresen, A., 1988, The Gipshuken Fault System – evidence for Tertiary thrusting along the Billefjorden Fault Zone, *in* Dallmann, W.K., Ohta, Y., and Andresen, A., eds., Tertiary Tectonics of Svalbard, extended abstracts from Symposium held in Oslo 26 and 27 April 1988: Norsk Polarinstitutt Rapportserie, v. 46, p. 67–70.

Saalmann, K., Tessensohn, F., Piepjohn, K., von Gosen, W., and Mayr, U., 2005, Structure of Palaeogene sediments in east Ellesmere Island: Constraints on Eurekan tectonic evolution and implications for the Nares Strait Problem: Tectonophysics, v. 406, p. 81–113.

Saalmann, K., Tessensohn, F., von Gosen, W., and Piepjohn, K., 2008, Structural evolution of Tertiary rocks on Judge Daly Promontory, *in* Mayr, U., ed., Geology of northeast Ellesmere Island adjacent to Kane Basin and Nares Strait, Nunavut: Geological Survey of Canada Bulletin, v. 592, p. 305–323.

Scheibner, C., Hartkopf-Fröder, C., Blomeier, D., and Forke, H., 2012, The Mississippian (Lower Carboniferous) in northeast Spitsbergen (Svalbard) and a re-evaluation of the

Billefjorden Group: Zeitschrift der Deutschen Gesellschaft für Geowissenschaften (German Journal of Geosciences), v. 163, no. 3, p. 293–308.

Schneider, D.A., Faehnrich, K., Majka, J., and Manecki, M., 2018, this volume, chapter 8, 40Ar/39Ar geochronologic evidence of Eurekan deformation within the West Spitsbergen Fold and Thrust Belt, *in* Piepjohn, K., Strauss, J.V., Reinhardt, L., and McClelland, W.C., eds., Circum-Arctic Structural Events: Tectonic Evolution of the Arctic Margins and Trans-Arctic Links with Adjacent Orogens: Geological Society of America, v. 541, Chapter 8, https://doi.org/10.1130/2018.2541(08).

Senger, K., Tveranger, J., Ogata, K., Braathen, A., and Planke, S., 2014, Late Mesozoic magmatism in Svalbard: A review: Earth-Science Reviews, v. 139, p. 123–144, http://dx.doi.org/10.1016/j.earscirev.2014.09.002.

Sigmond, E.M.O., 2002, Geological map, Land and Sea Areas of Northern Europe. Scale 1:4 million. Geological Survey of Norway.

Skilbrei, J.R., and Srivastava, S.P., 1993, Appendix: Greenland-Svalbard Plate Kinematics in the Tertiary and its relation to the west-Spitsbergen orogeny and structural highs in the western Barents Sea, *in* Interpretation of Geophysical Data from the Northwestern Barents Sea and Spitsbergen: Ph.D. thesis, Doktor Ing., 20 p.

Soper, N.J., and Higgins, A.K., 1987, A shallow detachment beneath the North Greenland fold belt: implications for sedimentation and tectonics: Geological Magazine, v. 124, no. 5, p. 441–-450.

Soper, N.J., and Higgins, A.K., 1991, Devonian - Early Carboniferous deformation and metamorphism, North Greenland). A. Deformation, *in* Trettin, H.P., ed., Geology of the Innuitian Orogen and Arctic Platform of Canada and Greenland, Geology of Canada: Geological Survey of Canada, v. 3, p. 283–288.

Soper, N.J., Dawes, P.R., and Higgins, A.K., 1982, Cretaceous-Tertiary magmatic and tectonic events in North Greenland and the history of adjacent oceanic basins, *in* Dawes P.R., and Kerr, J.W., eds., Nares Strait and the drift of Greenland: a conflict in plate tectonics: Meddelelser om Grønland, Geoscience, v. 8, p. 205–220.

Sømme, T.O., Doré, A.G., Lundin, E.R., and Tørudbakken, B.O., 2018, Triassic-Paleogene paleogeography of the Arctic: Implications for sediment routing and basin fill: AAPG Bulletin, v. 102, no. 12, p. 2481-2517, doi: 10.1306/05111817254.

Srivastava, S.P., 1978, Evolution of the Labrador Sea and its bearing on the early evolution of the North Atlantic: Geophysical Journal of the Royal Astronomical Society, v. 52, no. 2, p. 313–-357.

Srivastava, S.P., 1985, Evolution of the Eurasian Basin and its implications to the motion of Greenland along Nares Strait: Tectonophysics, v. 114, p. 29–53.

Srivastava, S.P., and Tapscott, C.R., 1986, Plate kinematics of the North Atlantic, *in* Vogt, P.R., and Tucholke, B.E., eds., The Geology of North America: Geological Society of America, Boulder, v. M., The Western North Atlantic Region, p. 379–405.

Steel, R.J., and Worsley, D., 1984, Svalbard's post-Caledonian strata – an atlas of sedimentational patterns and palaeogeographic evolution, *in* Spencer, A.M., Holter, E., Johnson, S.O., Mørk, A., Nysæther, E., Songstad, P., and Spinnangr, Å., eds., Petroleum Geology of the North European Margin: Graham & Trotman, London, p. 109–135.

Stephenson, R., Piepjohn, K., Schiffer, C. von Gosen, W., Oakey, G.N., and Anudu, G., 2017, Integrated crustal–geological cross-section of Ellesmere Island, *in* Pease, V., and Coakley, B., eds., Circum-Arctic Lithosphere Evolution. Geological Society, London, Special Publications, v. 460, https://doi.org/10.1144/SP460.12

Suess, E., 1888, Das Antlitz der Erde. Vol. I-III. Leipzig and Prague: F. Tempsky and G. Freytag, 778 p.

Talwani, M., and Eldholm, O., 1977, Evolution of the Norwegian - Greenland Sea: Geological Society of America Bulletin, v. 88, p. 969–999.

Tchalenko, J.S., and Ambraseys, N.N., 1970, Structural analyses of the Dasht-e Bayaz (Iran) earthquake fractures: Geological Society of America Bulletin, v. 81, p. 41–60.

Teben'kov, A.M., Ohta, Y., Balashov, J.A., and Sirotkin, A.N., 1996, Newtontoppen granitoid rocks; their geology, chemistry and Rb-Sr age: Polar Research, v. 15, p. 67–80.

Tegner, C., Storey, M., Holm, P.M., Thorarinsson, S.B., Zhao, X., Lo, C.-H., and Knudsen, M.F., 2011, Magmatism and Eurekan deformation in the High Arctic Large Igneous Province: ^{40}Ar-^{39}Ar age of Kap Washington Group volcanics, North Greenland: Earth and Planetary Science Letters, v. 303, no. 3-4, p. 203–214.

Tessensohn, F., ed., 2001, Intra-Continental Fold Belts. CASE 1: West Spitsbergen: Geologisches Jahrbuch (Polar Issue No. 7) B 91, p. 1–773.

Tessensohn, F., and Piepjohn, K., 2000, Eocene compressive deformation in Arctic Canada, North Greenland and Svalbard and its plate tectonic causes: Polarforschung, v. 68, p. 121–124.

Tessensohn, F., Henjes-Kunst, F., and Krumm, S., 2001, K/Ar Dating Attempts on Rocks from the West Spitsbergen Fold-and-Thrust Belt and the Central Basin, *in* Tessensohn, F., ed., Intra-Continental Fold Belts. CASE 1: West Spitsbergen: Geologisches Jahrbuch (Polar Issue No. 7) B 91, p. 719–728.

Tessensohn, F., von Gosen, W., Piepjohn, K., Saalmann, K., and Mayr, U., 2008, Nares transform motion and Eurekan compression along the northeast coast of Ellesmere Island, *in*

Mayr, U., ed., Geology of northeast Ellesmere Island adjacent to Kane Basin and Nares Strait, Nunavut: Geological Survey of Canada Bulletin, v. 592, p. 227–243.

Thorsteinsson, R., and Tozer, E.T., 1970, Geology of the Arctic Archipelago, *in* Douglass, R.J.W, ed., Geology and Economic Minerals of Canada: Geological Survey of Canada, Economic Geology Report, v. 1, p. 547–590.

Tsikalas, F., Faleide, J.I., and Eldholm, O., 2012, The North Atlantic conjugate margins, *in* Roberts, D.G., and Bally, A.W., eds., Principles of Phanerozoic Regional Geology. Phanerozoic Passive Margins, Cratonic Basins and Global Tectonic Maps. Elsevier, Amsterdam, p. 141–201.

Vink, G.E., 1982, Continental rifting and the implications for plate tectonic reconstructions: Journal of Geophysical Research, v. 87, p. 10677–10688.

Vogt, T., 1928, Den norske fjellkjedes revolusjonshistorie: Norsk Geologisk Tidsskrift, v. 10, p. 97–115.

von Gosen, W., and Piepjohn, K., 1999, Evolution of the Kap Cannon Thrust Zone (north Greenland): Tectonics, v. 18, no. 6, p. 1004–1026.

von Gosen, W., and Piepjohn, K., 2003, Eurekan transpressive deformation in the Wandel Hav Mobile Belt (northeast Greenland): Tectonics, v. 22, no. 4, p. 13–28.

von Gosen, W., Piepjohn, K., Tessensohn, F., and Saalmann, K., 2008, Eurekan fault tectonics on Judge Daly Promontory and their implications for displacements along Nares Strait, *in* Mayr, U., ed., Geology of northeast Ellesmere Island adjacent to Kane Basin and Nares Strait, Nunavut: Geological Survey of Canada Bulletin, v. 592, p. 325–346.

von Gosen, W., Piepjohn, K., and Reinhardt, L., 2012, Polyphase Eurekan deformation along the Vendom Fiord Fault Zone on south Ellesmere Island (Canadian Arctic) and its possible relation to the Wegener Fault: Zeitschrift der Deutschen Gesellschaft für Geowissenschaften (German Journal of Geosciences), v. 163, no. 3, p. 261–282.

von Gosen, W., Piepjohn, K., Gilotti, J.A., McClelland, W.B., and Reinhardt, L. 2018, this volume, chapter 18, Structural evidence for sinistral displacement on the Wegener Fault in southern Nares Strait, Arctic Canada, *in* Piepjohn, K., Strauss, J.V., Reinhardt, L., and McClelland, W.C., eds., Circum-Arctic Structural Events: Tectonic Evolution of the Arctic Margins and Trans-Arctic Links with Adjacent Orogens: Geological Society of America Special Paper, v. 541.

Wilcox, R.E., Harding, T.P., and Seely, D.R., 1973, Basic wrench tectonics: American Association of Petroleum Geologists Bulletin, v. 57, p. 74–96.

Woodcock, N.H., and Fischer, M., 1986, Strike-slip duplexes: Journal of Structural Geology, v. 8, p. 725-735.

FIGURE CAPTIONS

Figure 1: Tectonic map of northeastern Ellesmere Island, North Greenland, and Svalbard showing the sedimentary basins, the areas affected by the Caledonian, Ellesmerian, and Eurekan orogenies, and the most important fault zones (redrawn from Okulitch, 1991; Håkansson et al., 1991; Henriksen, 1992; Dallmann et al., 1993, 2002; Harrison et al., 2006; Piepjohn et al., 2013, 2015, 2016; Dallmann, 2015). BFZ–Billefjorden Fault Zone, HFFZ–Harder Fjord Fault Zone, KCTZ–Kap Cannon Thrust Zone, LFZ–Lomfjorden Fault Zone, and WHSSB–Wandel Hav Strike-Slip Belt.

Figure 2: (A) Simplified geological map of Svalbard (Hjelle, 1993; Dallmann, 2015) showing the locations of the West Spitsbergen Fold-and-Thrust Belt, the Billefjorden Fault Zone, and the Lomfjorden Fault Zone. Frame shows location of Fig. 2B, and the location of profile of Fig. 20 is also shown. (B) Simplified geological map of the Lomfjorden Fault Zone in eastern Spitsbergen

between Hinlopenstretet in the N and Agardhbukta in the south (redrawn from Miloslavskij et al., 1993a, b, 1996, and Dallmann et al., 2002, 2011). Frame shows location of Fig. 3.

Figure 3: Geological map of the northern and central segment of the Lomfjorden Fault Zone between Valhallfonna in the N and Andromedafjellet in the south, redrawn and simplified from Dallmann et al. (2002, 2009, 2010, 2011). Locations of cross-sections A–A' and B–B' of Figure 4 are shown. Locations of outcrop areas described in the text and figures are shown in Figure 6. BFR–Bjørnfjellet Reverse Fault, DRF–Dolerittfjellet Reverse Fault, LRF–Lomfjella Reverse Faults, SHF–Sillhøgda Fault, and UFA–Ursafonna Anticline.

Figure 4: Geological cross-sections across the Lomfjorden Fault Zone (A) from the Eolussletta Shear Zone through Lomfjella and southern Lomfjorden towards Lomfjordhalvøya, and (B) between Langfjellet and Vaigattbogen, based on Dallmann et al. (2009, 2011) as well as present fieldwork. Note the fault-dominated area of the Atomfjella Complex W of the Veteranen Fault and the km-scale fold structures with subvertical fold limbs in the Lomfjorden Supergroup to the E (for location of cross-sections see Fig. 3).

Figure 5: Caledonian structures: Lower hemisphere stereographic projections (equal area) of bedding planes S_0, cleavage planes S_1, δ_1-intersection lineations, and B_1-fold axes in Neoproterozoic sediments of the (A) Veteranen Group and (B) of the Akademikarbreen, Polarisbreen, and Oslobreen groups demonstrating the dominating architecture of Caledonian folding.

Figure 6: Map of the study area showing the locations of described outcrop areas and figures in the study (A) along the northern segment of the Lomfjorden Fault Zone between Kapp Fanshawe in the N and Andromedafjellet in the S and (B) along the central segment between Andromedafjellet in the N and Malte Brunfjellet in the S. The location of profile of Fig. 17B is shown. BFR–Bjørnfjellet Reverse Fault, DRF–Dolerittfjellet Reverse Fault, LRF–Lomfjella Reverse Faults, and SHF–Sillhøgda Fault.

Figure 7: (A) Geological map of the area SW of Kapp Fanshawe, redrawn from Dallmann et al. (2009). Red circle shows location of Fig. 7B. (B) Tectonic sketch map of the NNE–SSW striking fault in Neoproterozoic deposits of the Akademikarbreen Group SW of Kapp Fanshawe (for location see Figs. 6 and 7A). (C) Lower hemisphere stereographic projections (equal area) of fabric elements. Slickenside lineations are projected on the poles of the related planes, arrows indicate the relative sense of shear/displacement of the hanging wall units (Hoeppener, 1955).

Figure 8: Lower hemisphere stereographic projections (equal area) of fabric elements in (A) Neoproterozoic limestones of the Akademikarbreen Group and (B) Carboniferous limestones at the coast W of Mjølnerfjellet (for location see Fig. 6). Slickenside lineations are projected on the poles of the related planes, arrows indicate the relative sense of shear/displacement of the hanging wall units (Hoeppener, 1955). (C) NE-vergent fold structure and thrust fault in limestones of the Carboniferous Wordiekammen Formation at Mjølnerfjellet (for location see Fig. 6). (D) Diagram to an inferred tectonic scenario at Mjølnerfjellet showing ideal fault orientations in a N–S trending dextral strike-slip system. The diagram is based on Wilcox et al. (1973) and Christie-Blick and Biddle (1985); see text for explanation.

Figure 9: (A) Geological map of NE-dipping strata of the upper Veteranen, Akademikarbreen and lower Polarisbreen groups at the mountains Geren and Freken at the E-coast of Lomfjorden (for location see Fig. 6). The tilted rocks are truncated by NE–SW striking subvertical faults with a dextral sense of displacement that is documented by about 100 m of right-lateral offset of the boundary between the Veteranen and Akademikarbreen groups. (B) Lower hemisphere stereographic projections (equal area) of fabric elements in the Veteranen and Akademikarbreen groups at Geren and Freken. Slickenside lineations are projected on the poles of the related planes, arrows indicate the relative sense of shear/displacement of the hanging wall units (Hoeppener, 1955). (C) Diagrams to inferred tectonic scenarios demonstrated by a schematic pure shear-strain ellipse with ideal fault orientations in an E–W convergent system (C_1) and ideal fault orientations in N–S trending dextral (C_2) and sinistral (C_3) strike-slip systems. Diagrams are based on Wilcox et al. (1973) and Christie-Blick and Biddle (1985); see tect for explanation.

Figure 10: (A) The Eastern Lomfjella Reverse Fault at the W-coast of Lomfjorden N of Lomfjordbotnen (for location see Fig. 6). The reverse fault carries Neoproterozoic sedimentary rocks of the Veteranen Group westwards on top of Early Carboniferous deposits of the Billefjorden Group and Early Cretaceous dolerites. (B) Schematic block sketch of details of the reverse fault in (A). The floor thrust and back thrusts are marked in red colour. (C) Lower hemisphere stereographic projections (equal area) of fabric elements in the Veteranen Group in the hanging wall of the reverse faults. Slickenside lineations are projected on the poles of the related planes, arrows indicate the relative sense of shear/displacement of the hanging wall units (Hoeppener, 1955). (D) Diagram to an inferred tectonic scenario demonstrated by a schematic pure shear-strain ellipse with ideal fault orientations in an E–W convergent system. The diagram is based on Wilcox et al. (1973) and Christie-Blick and Biddle (1985); see tect for explanation.

Figure 11: W-dipping Bjørnfjellet Reverse Fault (A) E of Bjørnfjellet (view towards the NNE) and (B) at Løveryggen (view towards the S) carrying Neoproterozoic red beds of the Veteranen Group eastwards over horizontal middle Carboniferous to Early Permian limestones and Early Cretaceous dolerite sills (for location see Fig. 6). (C) Lower hemisphere stereographic projections (equal area) of fabric elements in the Veteranen sandstones from the outcrop group in the Bjørnfjellet area (for location see Fig. 6). Slickenside lineations are projected on the poles of the related planes, arrows indicate the relative sense of shear/displacement of the hanging wall units (Hoeppener, 1955).

Figure 12: Folded and thrust-faulted limestones and dolomites of the Carboniferous Wordiekammen and Gipshuken formations at Vinkelen/Chydenuisbreen (for location see Fig. 6). The thrust ramp is NNW-directed, and the F_2-folds are oriented NNE–SSW.

Figure 13: (A) WNW-directed thrust at Raudberget with Neoproterozoic deposits of the Lomfjorden Supergroup and unconformably overlying limestones of the Carboniferous Wordiekammen Formation in the hanging wall (for location see Fig. 6). (B) SW-vergent fold-structure in the hanging wall of the thrust (for location see Fig. 13A). (C) Lower hemisphere stereographic projections (equal area) of fabric elements in Carboniferous limestones at Raudberget. Slickenside lineations are projected on the poles of the related shear planes, arrows

indicate the relative sense of shear/displacement of the hanging wall units (Hoeppener, 1955). (D) Diagrams to inferred tectonic scenarios demonstrated by ideal fault orientations in N–S trending dextral (D_1) and sinistral (D_2) strike-slip systems. The diagrams are based on Wilcox et al. (1973) and Christie-Blick and Biddle (1985); see tect for explanation.

Figure 14: (A) Geological map of the Polarisbreen area (for location see Fig. 6). The offset of the boundaries of the Veteranen, Akademikarbreen, and Polarisbreen groups of the ENE-dipping Neoproterozoic Lomfjorden Supergroup proves the dextral sense of displacements along the NE–SW striking strike-slip faults. Location of profile of Fig. 14B is also shown. (B) Geological W–E cross-section of the Polarisbreen area (for location see Figure 14A). (C) Lower hemisphere stereographic projections (equal area) of fabric elements in Neoproterozoic and Carboniferous rocks at Grovtoppane SE of Chydeniusbreen, outcrops A925 and 946 (for locations see Figs.14A). Slickenside lineations are projected on the poles of the related planes, arrows indicate the relative sense of shear/displacement of the hanging wall units (Hoeppener, 1955). (D) Diagram to an inferred tectonic scenario demonstrated by a schematic pure shear-strain ellipse with ideal fault orientations in an E–W convergent system. The diagram is based on Wilcox et al. (1973) and Christie-Blick and Biddle (1985); see tect for explanation.

Figure 15: (A) Simplified profile across the Dolerittfjellet Reverse Fault and Sillhøgda Fault between Oslobreen and Ditlovtoppen (for location see Fig. 15B). (B) Geological map of the Oslobreen area (redrawn from own field data and Dallmann et al., 2011) (for location see Fig. 6). Note the parallel orientation of NNW–SSE striking normal faults and the Dolerittfjellet Reverse Fault. Note also the pattern of small-scale strike-slip faults between Kvitrevbreen and Oslobreen. The numbers refer to outrcops described in the text. Location of profile of Fig. 15A is also shown. ABF–Agardhbukta Fault. (C) Simplified profile across the Sillhøgda Fault S of Kirtonryggen (for location see Fig. 15B). (D) Lower hemisphere stereographic projections (equal area) of fabric elements in Cambrian and Carboniferous rocks, and Cretaceous dolerite sills at the Sillhøgda Fault S of Kyrtonryggen (outcrops A949–951, for locations see Fig. 15B). Slickenside lineations are projected on the poles of the related planes, arrows indicate the relative sense of shear/displacement of the hanging wall units (Hoeppener, 1955).

Figure 16: (A) Dolerittfjellet Reverse Fault carrying Neoproterozoic rocks to the ENE over horizontal Carboniferous limestones and Cretaceous dolerite sills at Dolerittfjellet. Lower hemisphere stereographic projections (equal area) of fabric elements in (B) Neoproterozoic rocks of the hanging wall (outcrops A932 and A934) and (C) in Carboniferous limestones and an Early Cretaceous dolerite sill in the footwall of the Dolerittfjellet Reverse Fault (outcrops A933 and A935, for locations see Fig. 15B). Slickenside lineations are projected on the poles of the related planes, arrows indicate the relative sense of shear/displacement of the hanging wall units (Hoeppener, 1955). (D) Diagrams to inferred tectonic scenarios demonstrated by a schematic pure shear-strain ellipse with ideal fault orientations in a local ENE–WSW convergent system in the vicinity of the Dolerittfjellet Reverse Fault (D_1) and by ideal fault orientations in N–S trending sinistral (D_2) and dextral (D_3) strike-slip systems. The diagrams are based on Wilcox et al. (1973) and Christie-Blick and Biddle (1985); see tect for explanation.

Figure 17: Lower hemisphere stereographic projections (equal area) of fabric elements in Carboniferous rocks at (A) Pachtusovfjellet and (C) in Neoproterozoic rocks at Vivienberget (for locations see Fig. 6B). Slickenside lineations are projected on the poles of the related planes, arrows indicate the relative sense of shear/displacement of the hanging wall units (Hoeppener, 1955). (B) Simplifiedc W–E profile through the monocline at Pachtusovfjellet and the Agardhbukta Fault. (D) Diagrams to inferred tectonic scenarios demonstrated by schematic pure shear-strain ellipse with ideal fault orientations in a local E–W convergent system at Pachtusovfjellet (D_1) and by ideal fault orientations in a NNE–SSW trending dextral strike-slip system at Vivienberget (D_2). The diagrams are based on Wilcox et al. (1973) and Christie-Blick and Biddle (1985); see tect for explanation.

Figure 18: Lower hemisphere stereographic projections (equal area) of fabric elements in Carboniferous to Permian sedimentary rocks at Malte Brunfjellet (for location see Fig. 6B). (A) Fabric elements interpreted as compatible with a dextral, and (B) with a sinistral strike-slip scenario in Carboniferous/Permian sedimentary rocks near the Agardhbukta Fault. Slickenside lineations are projected on the poles of the related planes, arrows indicate the relative sense of shear/displacement of the hanging wall units (Hoeppener, 1955). (C) Diagrams to inferred tectonic scenarios demonstrated by a schematic pure shear-strain ellipse with ideal fault

orientations in (C1) a W–E contractional scenario, and by ideal fault orientations (C2) in a sinistral N–S strike-slip scenario, and (C3) in a dextral N–S strike-slip scenario. The diagrams are based on Wilcox et al. (1973) and Christie-Blick and Biddle (1985); see tect for explanation.

Figure 19: Map of the Lomfjorden Fault Zone showing the left-stepping Lomfjorden and Agardhbukta faults wthin a dextral scenario with a contractional overstep (A) and within a sinistral scenario with an extensional overstep (B). The squares depict the main kinematics in the observed outcrops indicating the lateral movements by half-arrows and the corresponding shortening directions (yellow arrows) and extension directions (green arrows). The two insets show schematic sketches based on McClay (1987) with (A_1) left-stepping faults generating zones of compression with folds and thrusts in a dextral strike-slip system and (B_1) left-stepping faults generating zone of extension (normal faults) in a sinistral strike-slip system.

Figure 20: WSW–ENE cross section through the West Spitsbergen Fold-and-Thrust Belt, the Central Tertiary Basin, the southern segment of the Lomfjorden Fault Zone and the Ny-Friesland Block in the central part of Spitsbergen (redrawn and modified from Nøttvedt et al., 1988), two times exaggerated (for location of see Figure 2A). Note the detachment zones in the Triassic and Jurassic rocks and the assumed detachment in the pre-Devonian basement rocks.

Figure 21: Possible reconstruction of Svalbard, North Greenland, and the Queen Elizabeth Islands at approximately anomaly 21 (47 Ma) with the indication of the active faults during the phases of the Eurekan Orogeny (modified from Piepjohn et al., 2016, and citations therein). AFFZ–Archer Fiord Fault Zone, BFZ–Billefjorden Fault Zone, FFZ–Feilden Fault Zone, HFFZ–Harder Fjord Fault Zone, KCTZ–Kap Cannon Thrust Zone, LHFZ–Lake Hazen Fault Zone, LFZ–Lomfjorden Fault Zone, MRF–Mount Rawlinson Fault, PGT–Parrish Glacier Thrust, SEDL–Svartfjella-Eidembukta-Daudmannsodden Lineament, VFFZ–Vendom Fiord Fault Zone, and WHSSB–Wandel Hav Strike-Slip Belt.

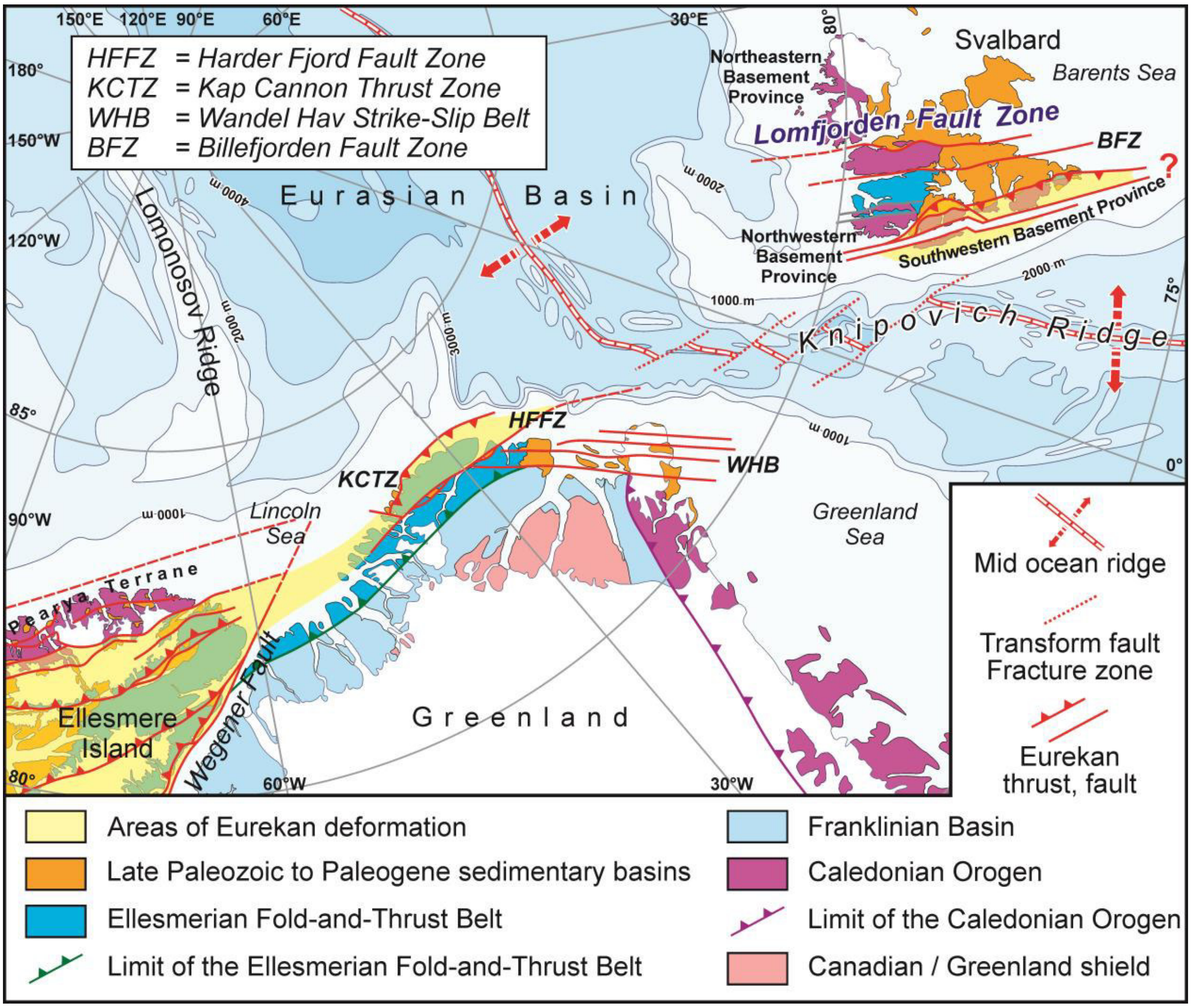
HFFZ = Harder Fjord Fault Zone
KCTZ = Kap Cannon Thrust Zone
WHB = Wandel Hav Strike-Slip Belt
BFZ = Billefjorden Fault Zone
Svalbard
Barents Sea
Northeastern Basement Province
Lomfjorden Fault Zone
BFZ
Northwestern Basement Province
Southwestern Basement Province
Eurasian Basin
Lomonosov Ridge
Knipovich Ridge
HFFZ
KCTZ
WHB
Lincoln Sea
Greenland Sea
Pearya Terrane
Ellesmere Island
Wegener Fault
Greenland
Mid ocean ridge
Transform fault Fracture zone
Eurekan thrust, fault
Areas of Eurekan deformation
Late Paleozoic to Paleogene sedimentary basins
Ellesmerian Fold-and-Thrust Belt
Limit of the Ellesmerian Fold-and-Thrust Belt
Franklinian Basin
Caledonian Orogen
Limit of the Caledonian Orogen
Canadian / Greenland shield

Figure 1

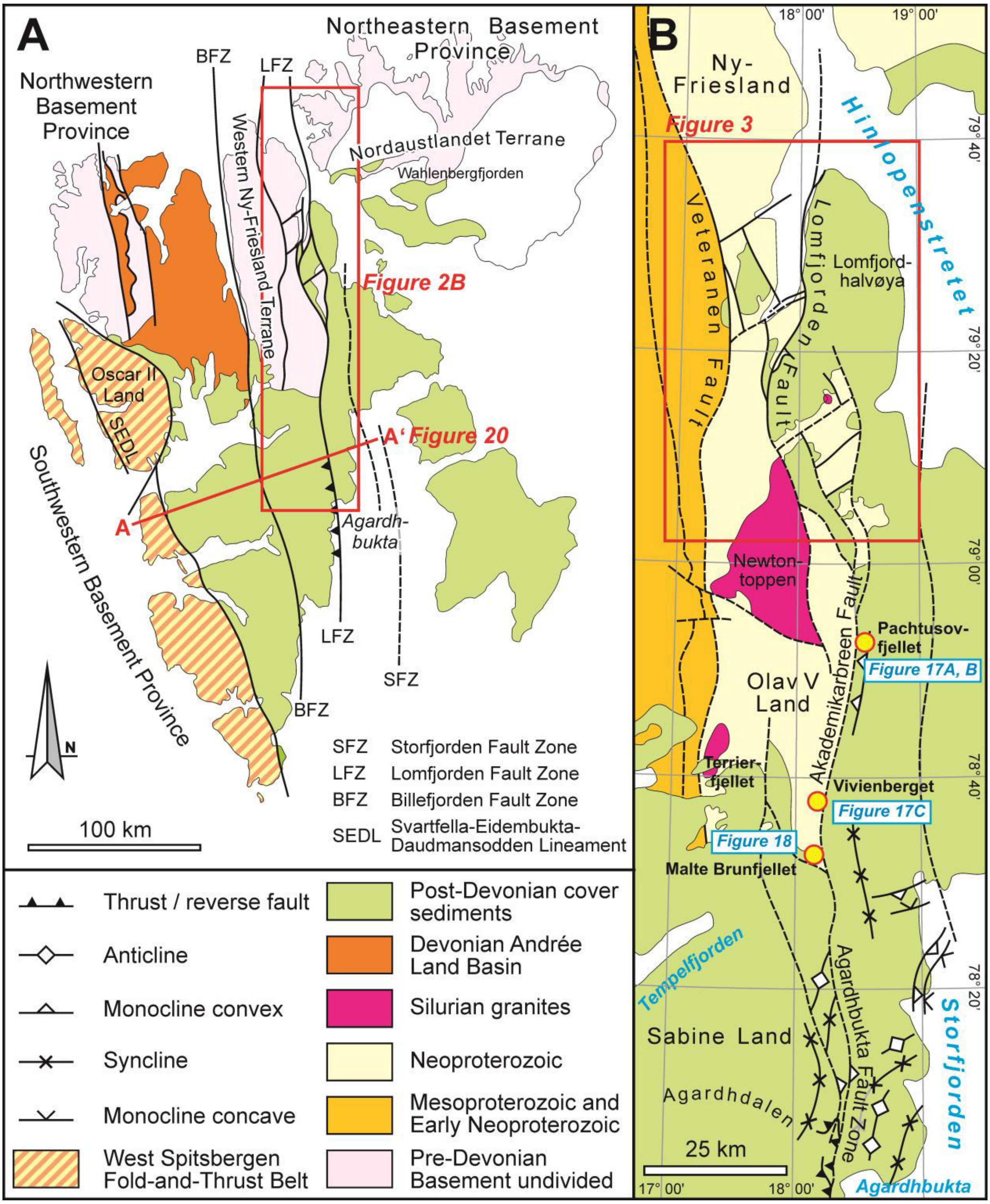

A
B
Northeastern Basement Province
Northwestern Basement Province
BFZ
LFZ
Nordaustlandet Terrane
Wahlenbergfjorden
Western Ny-Friesland Terrane
Figure 2B
Oscar II Land
SEDL
A' Figure 20
A
Agardh-bukta
Southwestern Basement Province
LFZ
SFZ
BFZ
N
100 km
SFZ Storfjorden Fault Zone
LFZ Lomfjorden Fault Zone
BFZ Billefjorden Fault Zone
SEDL Svartfella-Eidembukta-Daudmansodden Lineament
Thrust / reverse fault
Anticline
Monocline convex
Syncline
Monocline concave
West Spitsbergen Fold-and-Thrust Belt
Post-Devonian cover sediments
Devonian Andrée Land Basin
Silurian granites
Neoproterozoic
Mesoproterozoic and Early Neoproterozoic
Pre-Devonian Basement undivided
18° 00'
19° 00'
Ny-Friesland
Figure 3
Hinlopenstretet
79° 40'
Veteranen Fault
Lomfjorden Fault
Lomfjord-halvøya
79° 20'
Newton-toppen
79° 00'
Akademikarbreen Fault
Pachtusov-fjellet
Figure 17A, B
Olav V Land
Terrier-fjellet
Vivienberget
Figure 17C
Figure 18
Malte Brunfjellet
Tempelfjorden
78° 20'
Storfjorden
Sabine Land
Agardhbukta Fault Zone
Agardhdalen
25 km
17° 00'
18° 00'
Agardhbukta

Figure 2

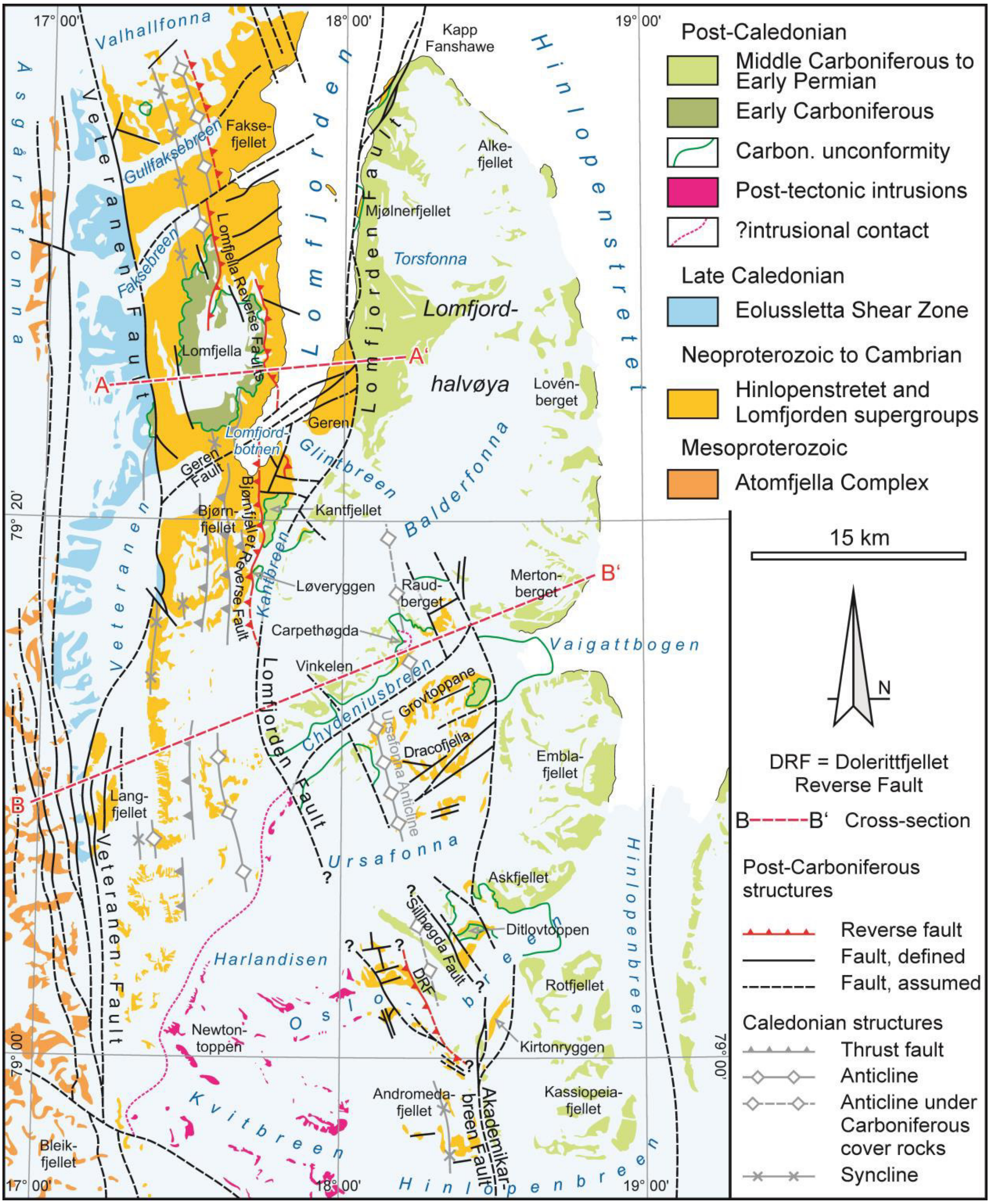

Post-Caledonian
Middle Carboniferous to Early Permian
Early Carboniferous
Carbon. unconformity
Post-tectonic intrusions
?intrusional contact
Late Caledonian
Eolussletta Shear Zone
Neoproterozoic to Cambrian
Hinlopenstretet and Lomfjorden supergroups
Mesoproterozoic
Atomfjella Complex
15 km
N
DRF = Dolerittfjellet Reverse Fault
B-----B‘ Cross-section
Post-Carboniferous structures
Reverse fault
Fault, defined
Fault, assumed
Caledonian structures
Thrust fault
Anticline
Anticline under Carboniferous cover rocks
Syncline
Valhallfonna
Kapp Fanshawe
Lomfjorden
Hinlopenstretet
Fakse-fjellet
Gullfaksebreen
Alke-fjellet
Mjølnerfjellet
Torsfonna
Lomfjord-halvøya
Lomfjorden Fault
Lomfjella Reverse Faults
Faksebreen
Veteranen Fault
Åsgårdfonna
Lomfjella
Lovén-berget
Geren
Geren Fault
Lomfjord-botnen
Glintbreen
Balderfonna
Bjørn-fjellet
Bjørnfjellet Reverse Fault
Kantfjellet
Kantbreen
Løveryggen
Raud-berget
Merton-berget
Carpethøgda
Vaigattbogen
Vinkelen
Chydeniusbreen
Grovtoppane
Ursafonna Anticline
Dracofjella
Embla-fjellet
Lang-fjellet
Veteranen
Ursafonna
Askfjellet
Sillhøgda Fault
Ditlovtoppen
Harlandisen
Oslobreen
DRF
Rotfjellet
Hinlopenbreen
Newton-toppen
Kirtonryggen
Kvitbreen
Andromeda-fjellet
Akademikarbreen Fault
Kassiopeia-fjellet
Bleik-fjellet
17° 00'
18° 00'
19° 00'
79° 20'
79° 00'
A
A‘
B
B‘

Figure 3 neu

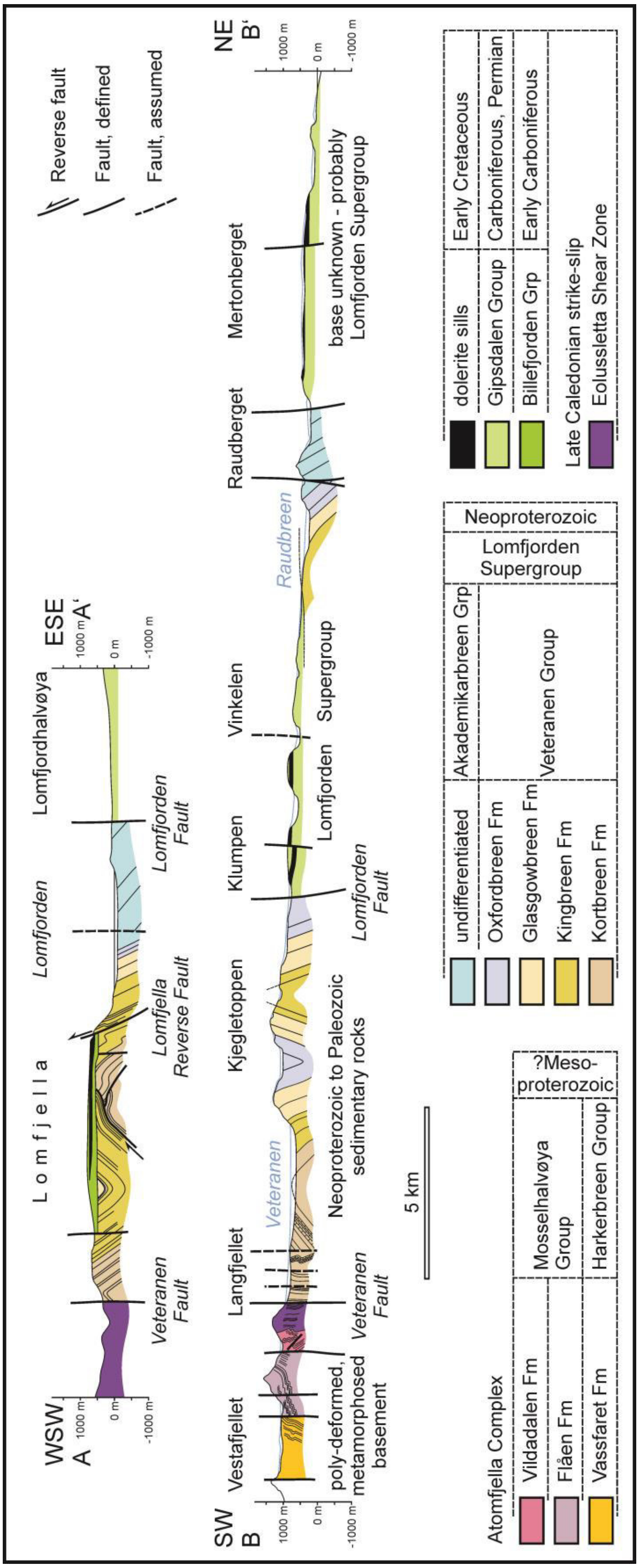
WSW
A
ESE
A'
SW
B
NE
B'
1000 m
0 m
-1000 m
Reverse fault
Fault, defined
Fault, assumed
Lomfjella
Lomfjorden
Lomfjordhalvøya
Veteranen Fault
Lomfjella Reverse Fault
Lomfjorden Fault
Vestafjellet
Langfjellet
Kjegletoppen
Klumpen
Vinkelen
Raudberget
Mertonberget
Veteranen
Raudbreen
poly-deformed, metamorphosed basement
Neoproterozoic to Paleozoic sedimentary rocks
Lomfjorden Supergroup
base unknown - probably Lomfjorden Supergroup
5 km
Atomfjella Complex
Vildadalen Fm
Flåen Fm
Vassfaret Fm
Mosselhalvøya Group
Harkerbreen Group
?Meso-proterozoic
undifferentiated
Oxfordbreen Fm
Glasgowbreen Fm
Kingbreen Fm
Kortbreen Fm
Akademikarbreen Grp
Veteranen Group
Lomfjorden Supergroup
Neoproterozoic
dolerite sills
Gipsdalen Group
Billefjorden Grp
Early Cretaceous
Carboniferous, Permian
Early Carboniferous
Late Caledonian strike-slip
Eolussletta Shear Zone

Figure 4

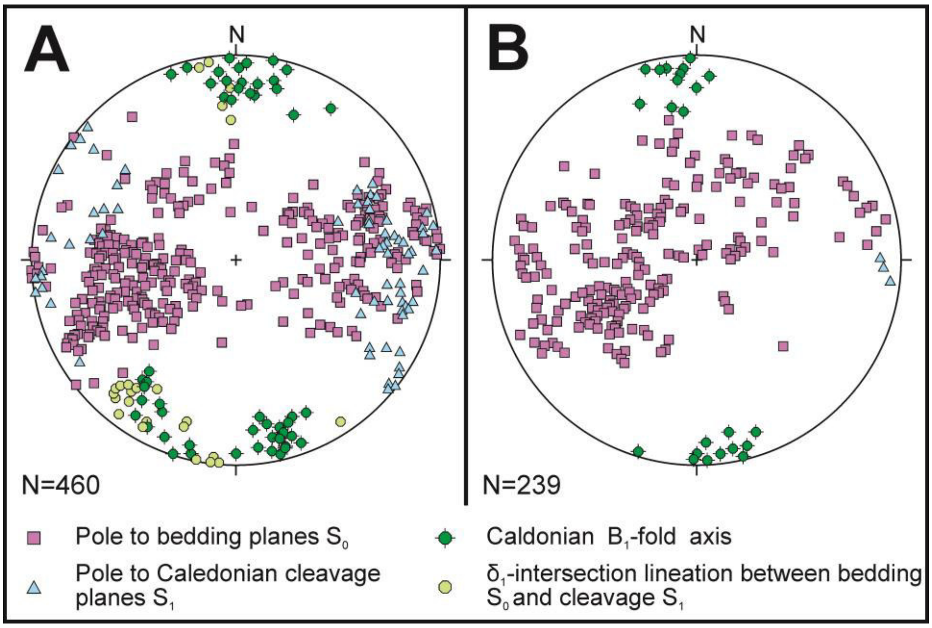
A
N
N=460
B
N
N=239
Pole to bedding planes S_0
Pole to Caledonian cleavage planes S_1
Caldonian B_1-fold axis
δ_1-intersection lineation between bedding S_0 and cleavage S_1

Figure 5

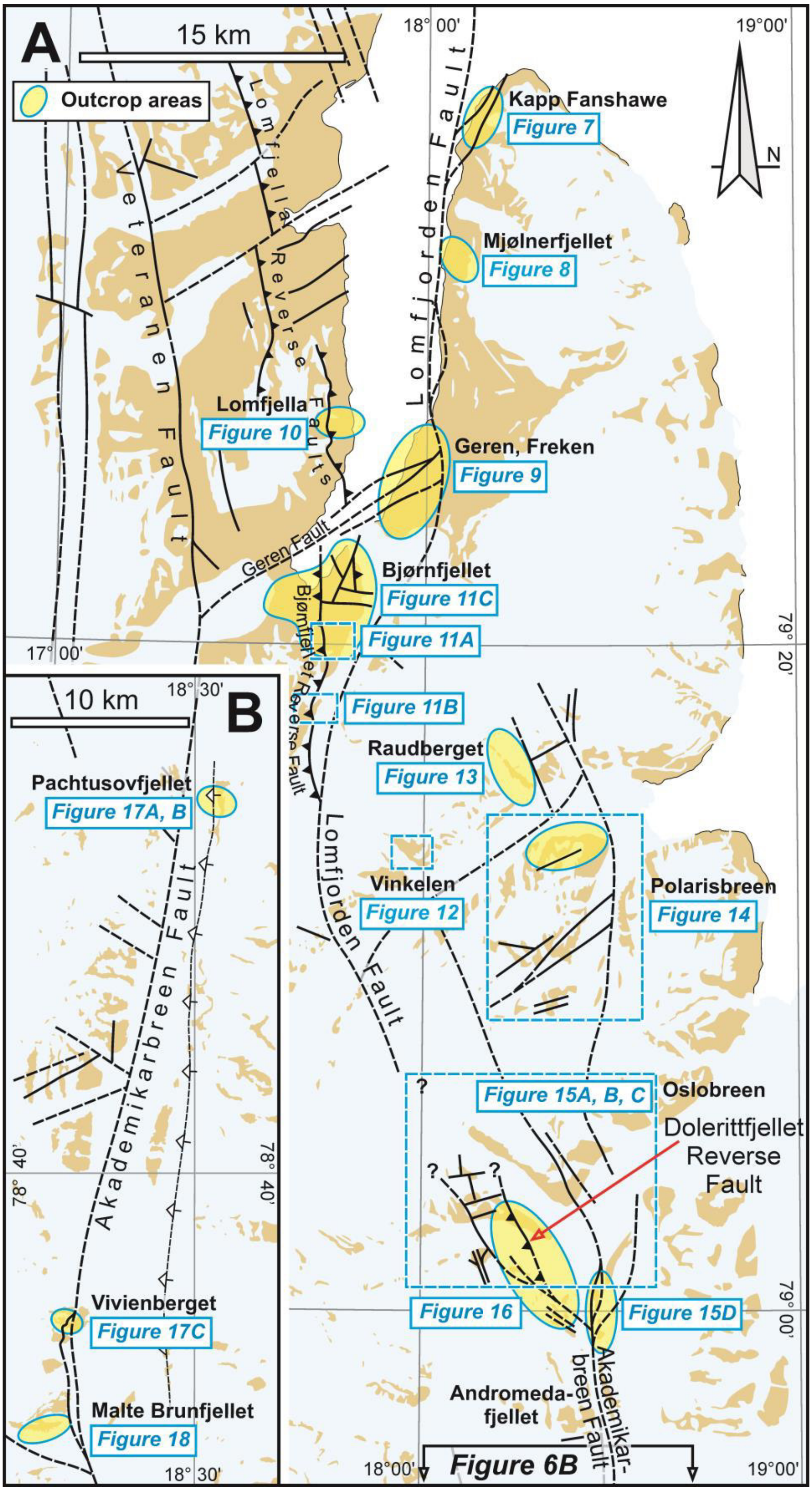
A
15 km
Outcrop areas
18° 00'
19°00'
N
Kapp Fanshawe
Figure 7
Mjølnerfjellet
Figure 8
Lomfjella Reverse Faults
Veteranen Fault
Lomfjorden Fault
Lomfjella
Figure 10
Geren, Freken
Figure 9
Geren Fault
Bjørnfjellet
Figure 11C
Figure 11A
Bjørnfjellet Reverse Fault
17° 00'
79° 20'
B
10 km
18° 30'
Figure 11B
Raudberget
Figure 13
Pachtusovfjellet
Figure 17A, B
Vinkelen
Figure 12
Polarisbreen
Figure 14
Akademikarbreen Fault
Lomfjorden Fault
Figure 15A, B, C
Oslobreen
Dolerittfjellet Reverse Fault
78° 40'
Figure 16
Figure 15D
79° 00'
Vivienberget
Figure 17C
Andromeda-fjellet
Akademikar-breen Fault
Malte Brunfjellet
Figure 18
18° 30'
18°00'
Figure 6B
19°00'

Figure 6 neu

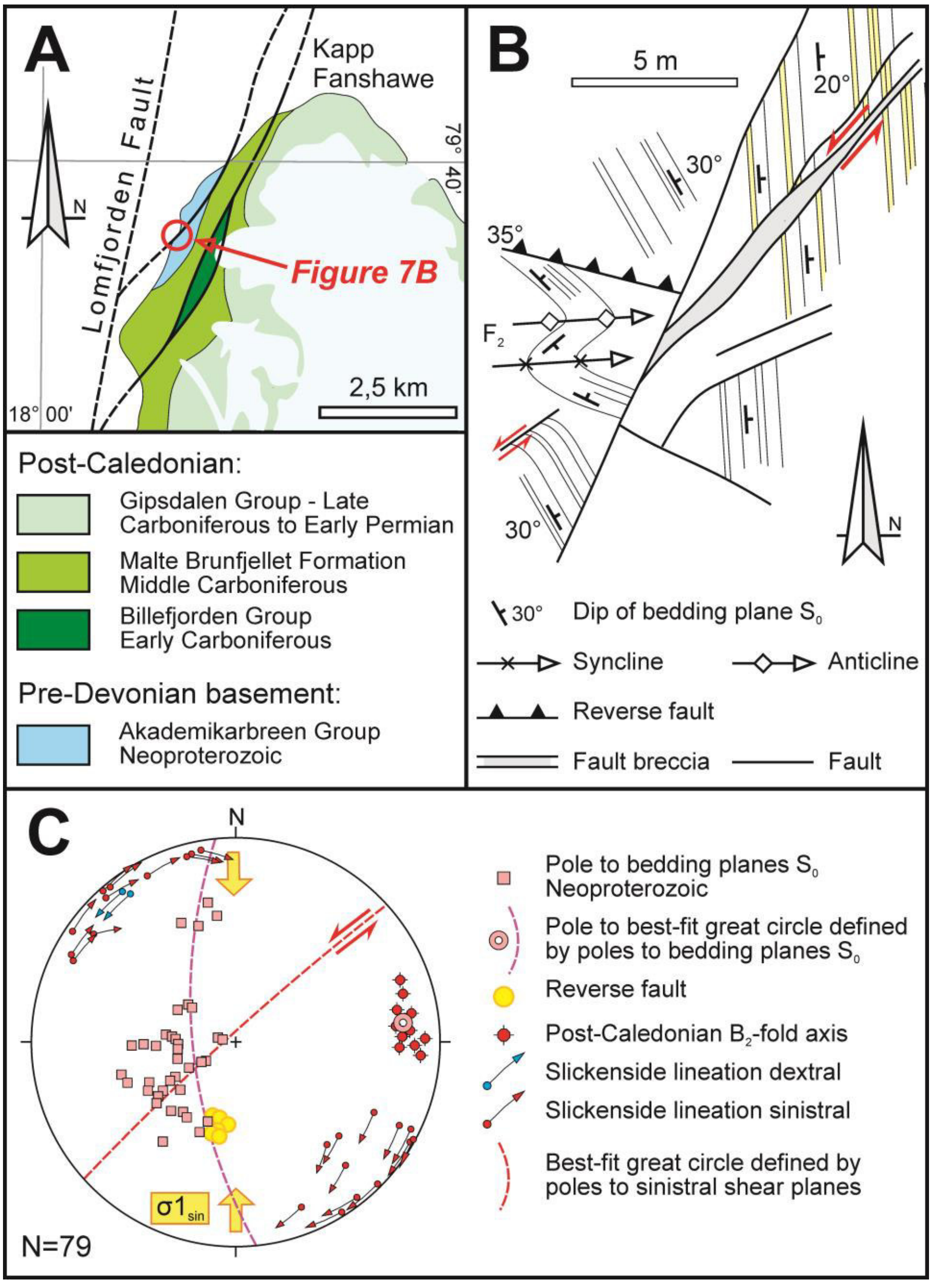

A
Kapp
Fanshawe
Lomfjorden Fault
79° 40'
N
Figure 7B
2,5 km
18° 00'
Post-Caledonian:
Gipsdalen Group - Late Carboniferous to Early Permian
Malte Brunfjellet Formation Middle Carboniferous
Billefjorden Group Early Carboniferous
Pre-Devonian basement:
Akademikarbreen Group Neoproterozoic
B
5 m
20°
30°
35°
F2
30°
N
30° Dip of bedding plane S0
Syncline
Anticline
Reverse fault
Fault breccia
Fault
C
N
σ1sin
N=79
Pole to bedding planes S0 Neoproterozoic
Pole to best-fit great circle defined by poles to bedding planes S0
Reverse fault
Post-Caledonian B2-fold axis
Slickenside lineation dextral
Slickenside lineation sinistral
Best-fit great circle defined by poles to sinistral shear planes

Figure 7 neu

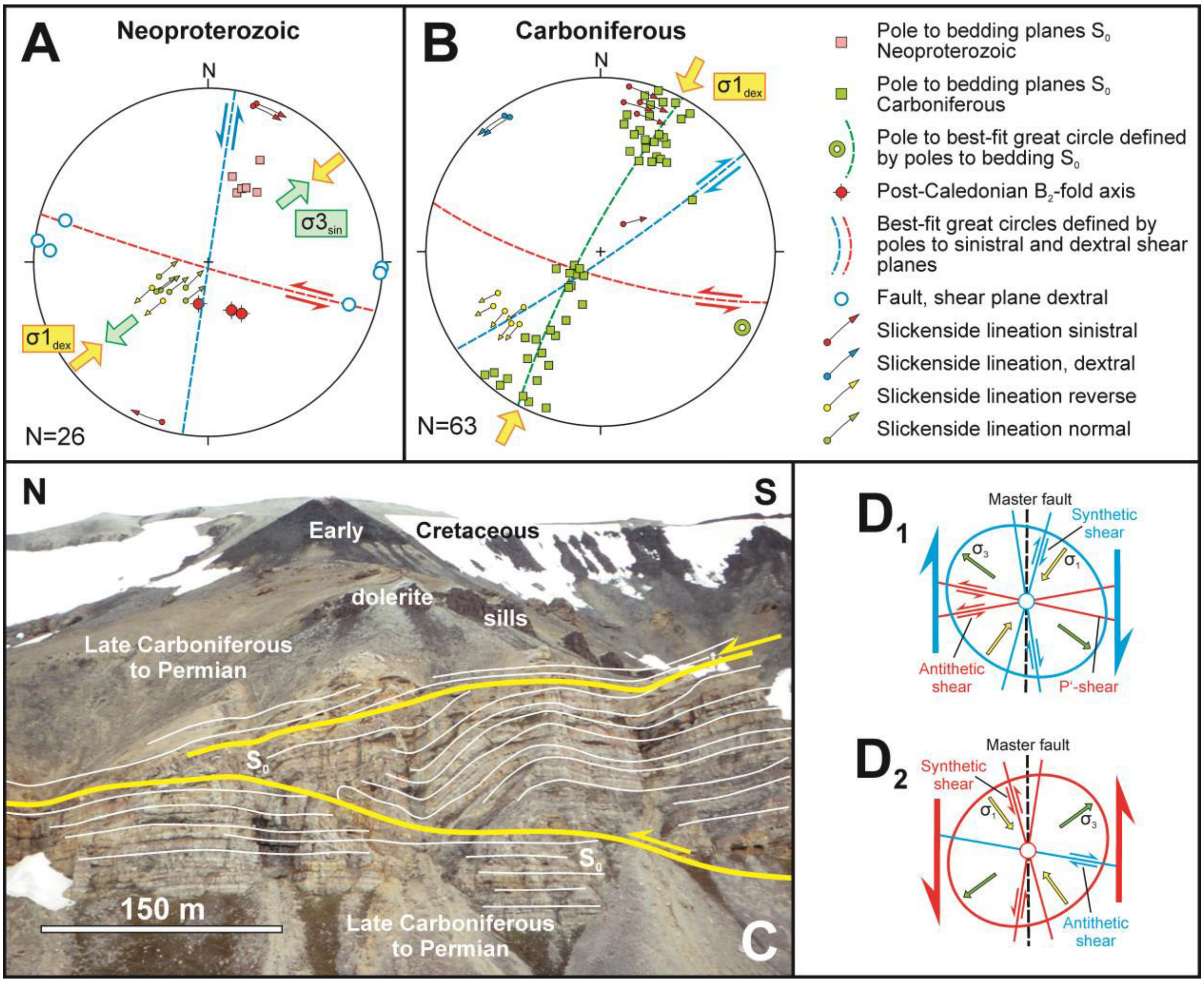
A
Neoproterozoic
N
σ3sin
σ1dex
N=26
B
Carboniferous
N
σ1dex
N=63
Pole to bedding planes S0
Neoproterozoic
Pole to bedding planes S0
Carboniferous
Pole to best-fit great circle defined
by poles to bedding S0
Post-Caledonian B2-fold axis
Best-fit great circles defined by
poles to sinistral and dextral shear
planes
Fault, shear plane dextral
Slickenside lineation sinistral
Slickenside lineation, dextral
Slickenside lineation reverse
Slickenside lineation normal
N
S
Early
Cretaceous
dolerite
sills
Late Carboniferous
to Permian
S0
S0
150 m
Late Carboniferous
to Permian
C
D1
Master fault
Synthetic
shear
σ3
σ1
Antithetic
shear
P'-shear
D2
Master fault
Synthetic
shear
σ1
σ3
Antithetic
shear

Figure 8

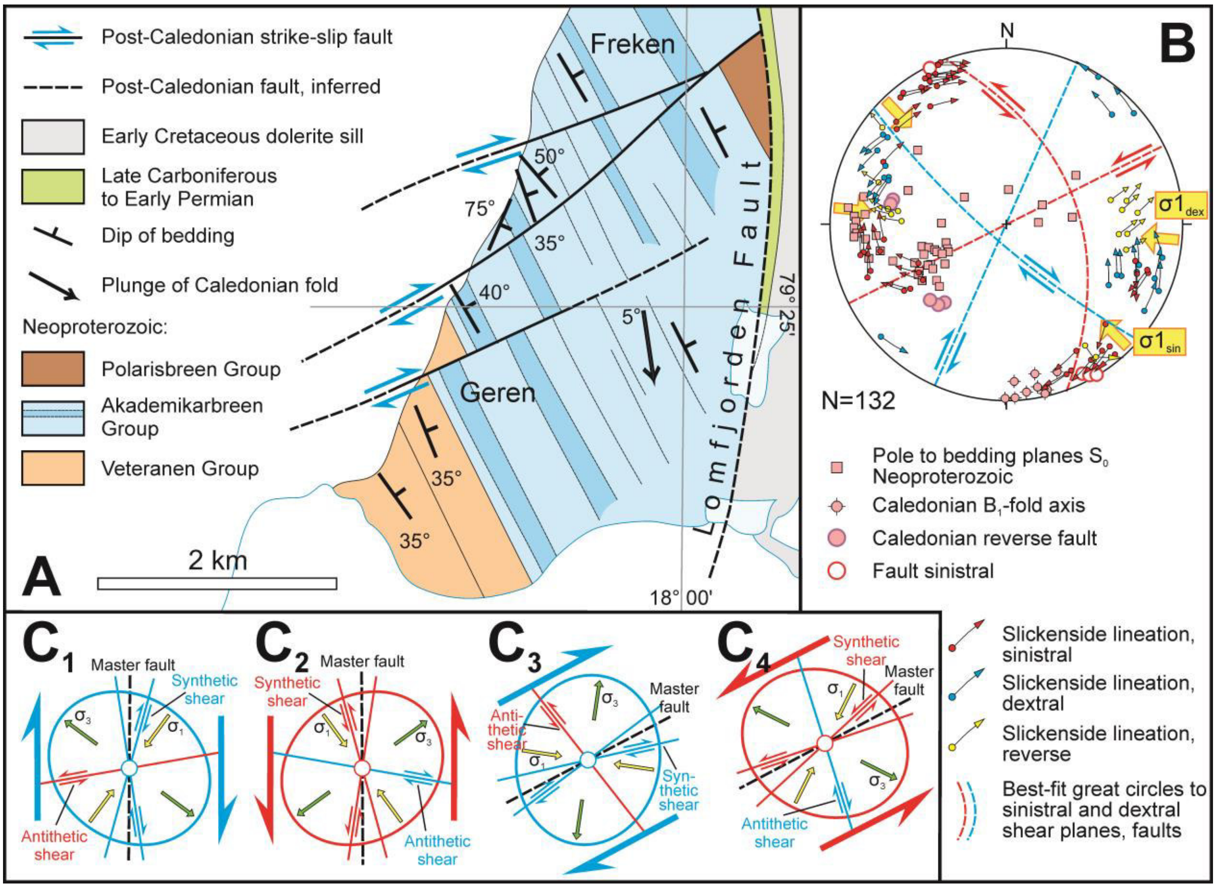

Post-Caledonian strike-slip fault
Post-Caledonian fault, inferred
Early Cretaceous dolerite sill
Late Carboniferous to Early Permian
Dip of bedding
Plunge of Caledonian fold
Neoproterozoic:
Polarisbreen Group
Akademikarbreen Group
Veteranen Group
Freken
Geren
Lomfjorden Fault
79° 25'
18° 00'
2 km
A
B
N
N=132
σ1dex
σ1sin
Pole to bedding planes S0 Neoproterozoic
Caledonian B1-fold axis
Caledonian reverse fault
Fault sinistral
C1
C2
C3
C4
Master fault
Synthetic shear
Antithetic shear
Slickenside lineation, sinistral
Slickenside lineation, dextral
Slickenside lineation, reverse
Best-fit great circles to sinistral and dextral shear planes, faults

Figure 9

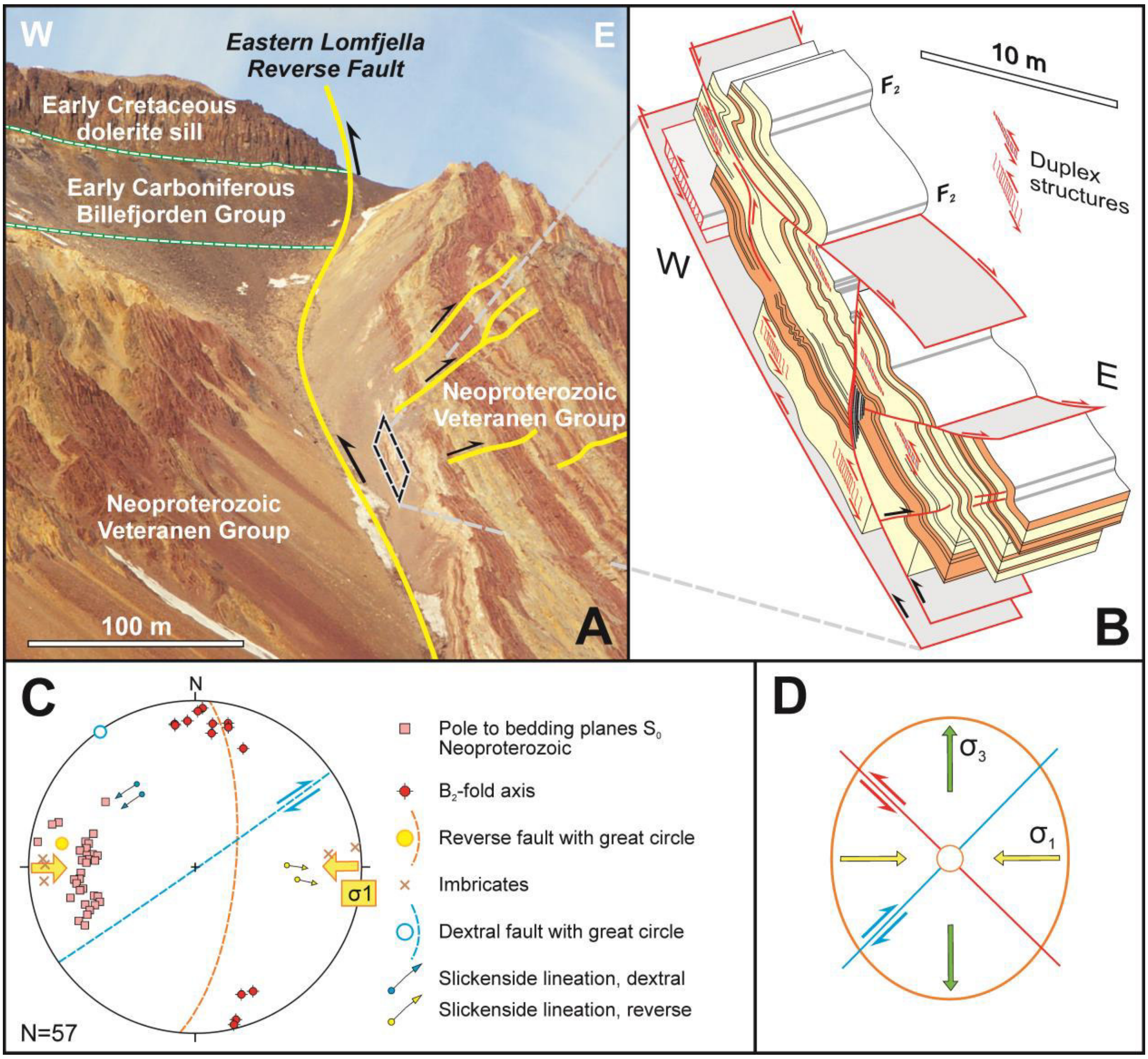
W
E
Eastern Lomfjella
Reverse Fault
Early Cretaceous
dolerite sill
Early Carboniferous
Billefjorden Group
Neoproterozoic
Veteranen Group
Neoproterozoic
Veteranen Group
100 m
A
10 m
F2
F2
Duplex
structures
W
E
B
C
N
σ1
N=57
Pole to bedding planes S0
Neoproterozoic
B2-fold axis
Reverse fault with great circle
Imbricates
Dextral fault with great circle
Slickenside lineation, dextral
Slickenside lineation, reverse
D
σ3
σ1

Figure 10

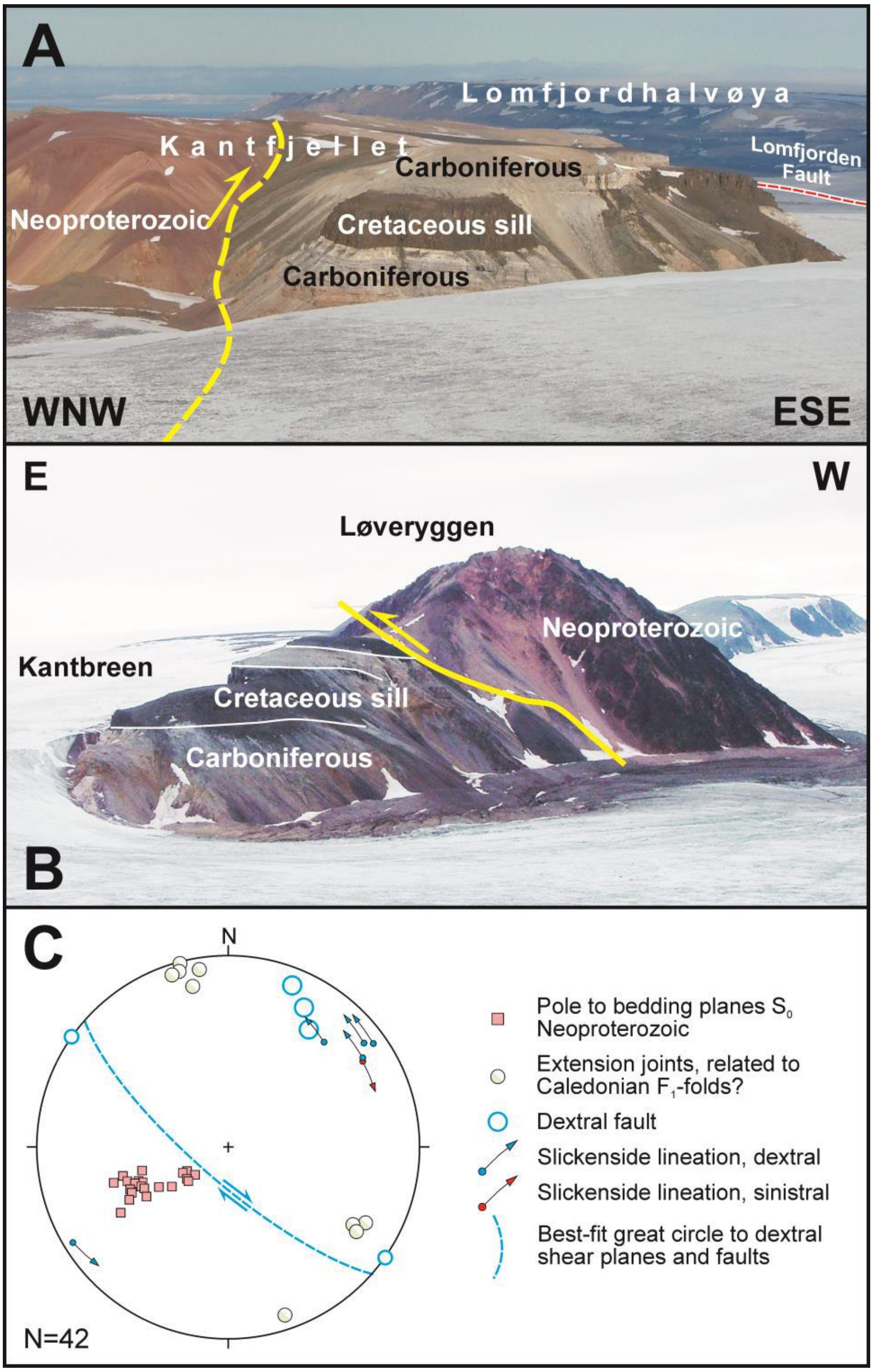
A
Lomfjordhalvøya
Kantfjellet
Lomfjorden Fault
Carboniferous
Neoproterozoic
Cretaceous sill
Carboniferous
WNW
ESE
E
W
Løveryggen
Neoproterozoic
Kantbreen
Cretaceous sill
Carboniferous
B
C
N
Pole to bedding planes S_0 Neoproterozoic
Extension joints, related to Caledonian F_1-folds?
Dextral fault
Slickenside lineation, dextral
Slickenside lineation, sinistral
Best-fit great circle to dextral shear planes and faults
N=42

Figure 11

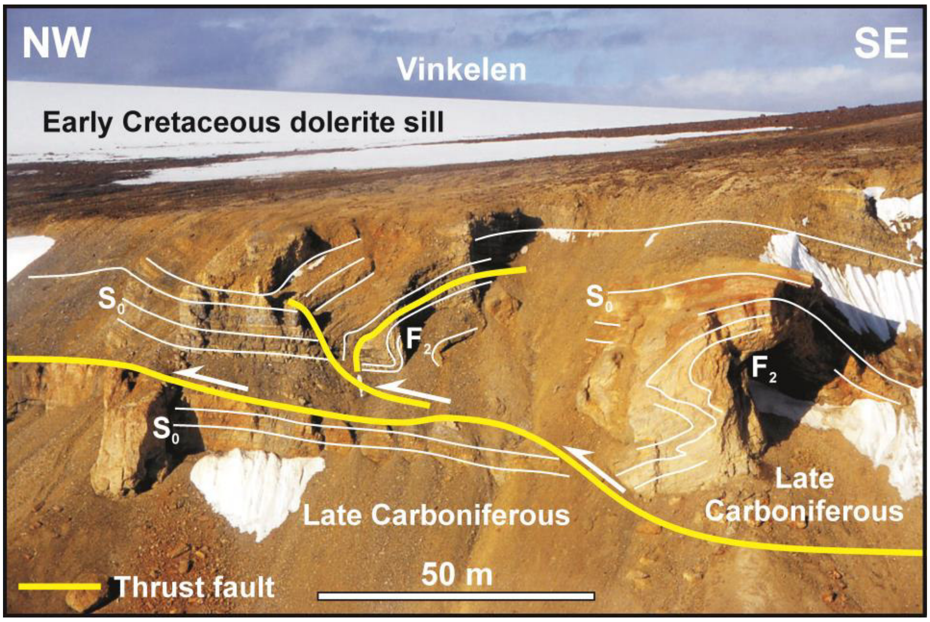
NW
SE
Vinkelen
Early Cretaceous dolerite sill
S_0
F_2
S_0
F_2
S_0
Late Carboniferous
Late Carboniferous
Thrust fault
50 m

Figure 12

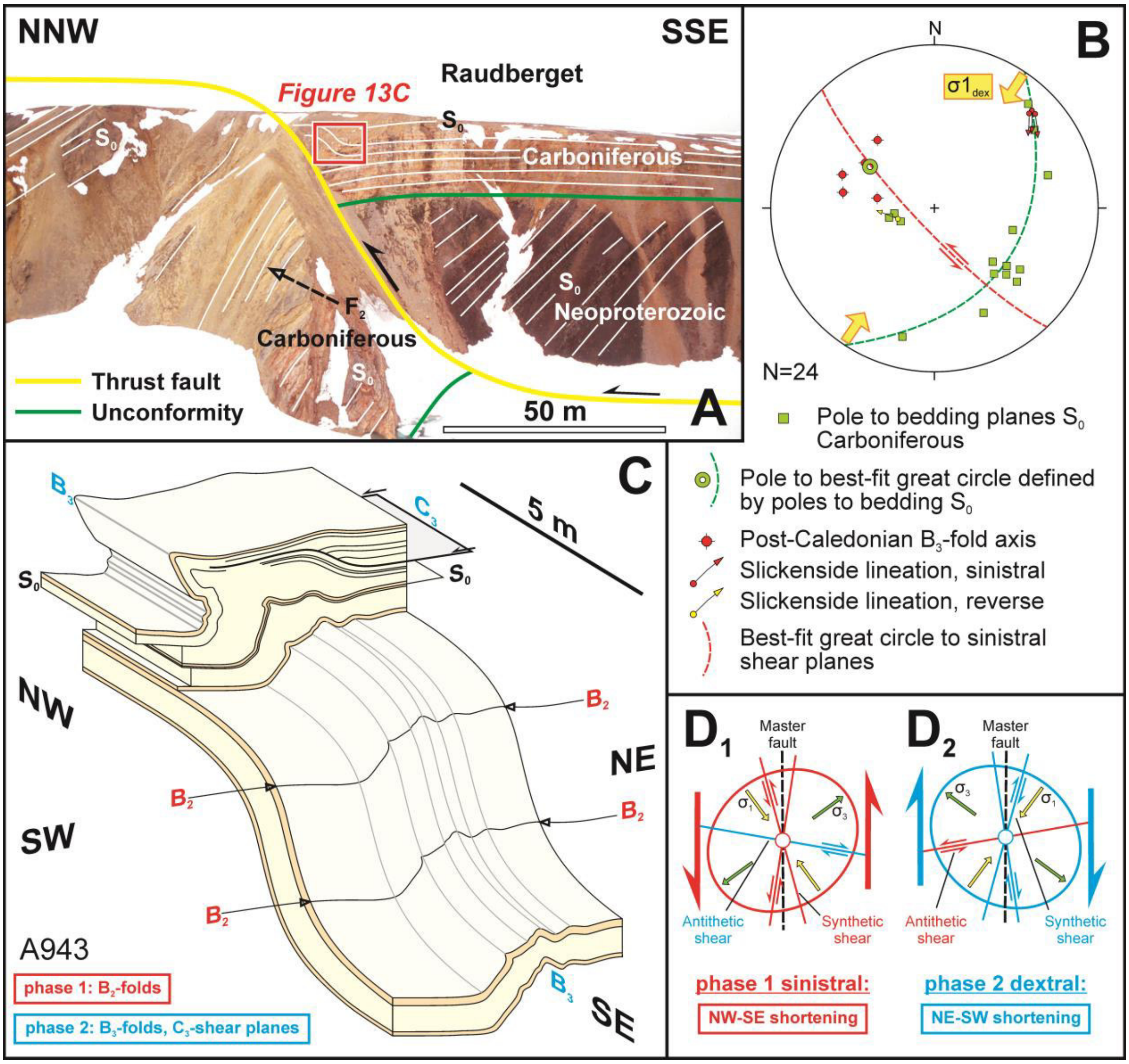

Figure 13 neu

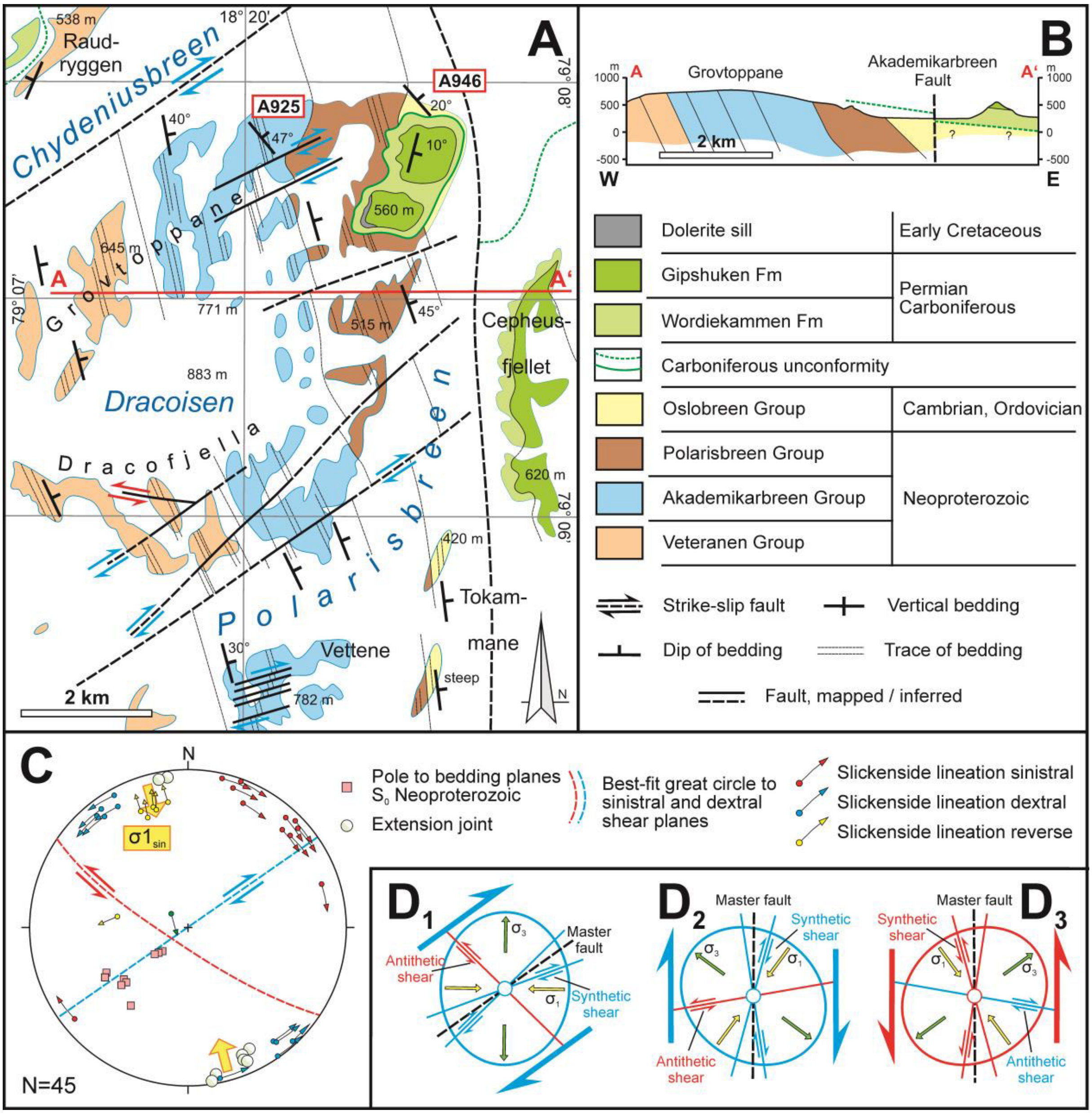

Figure 14 neu

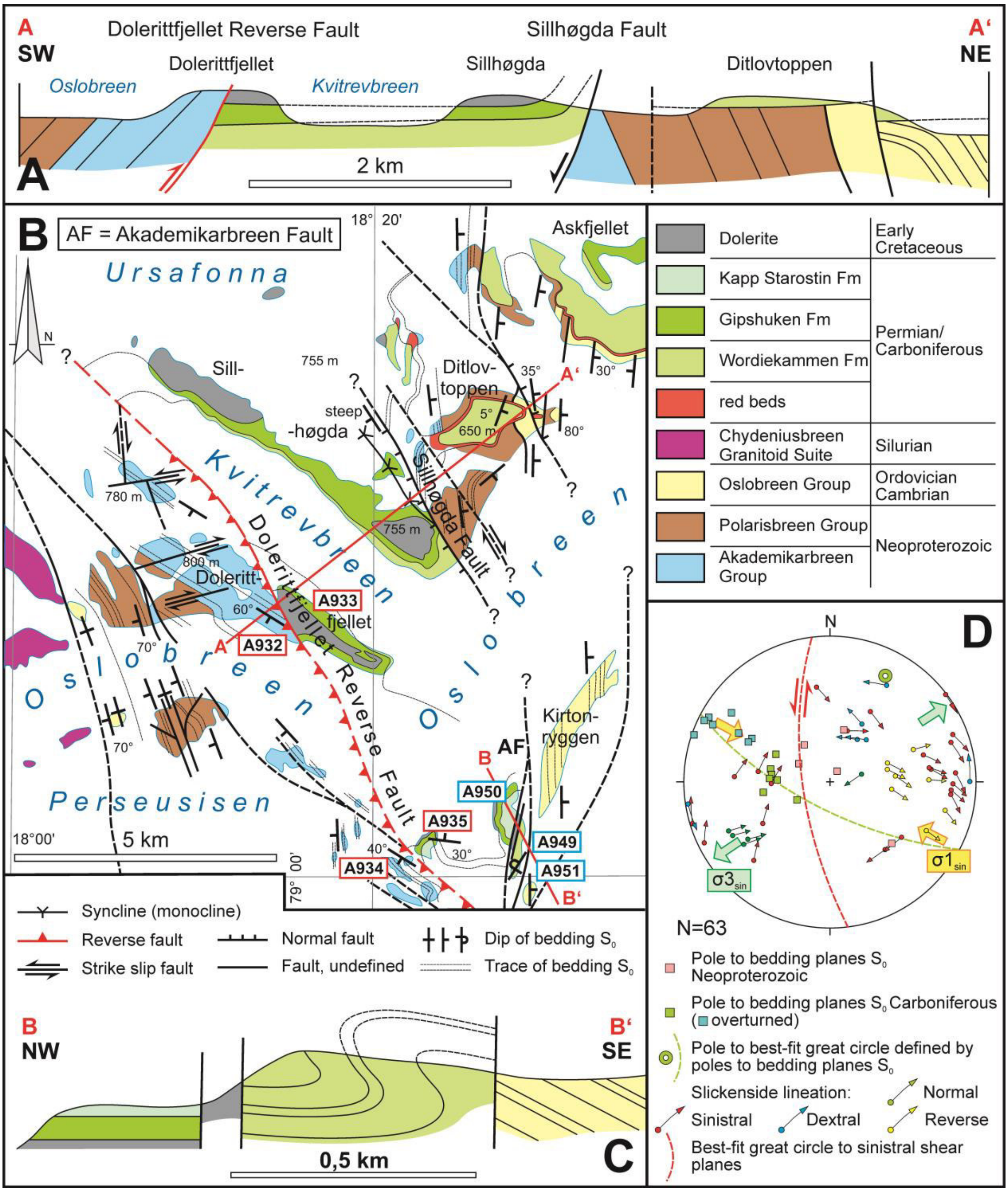

Figure 15 neu

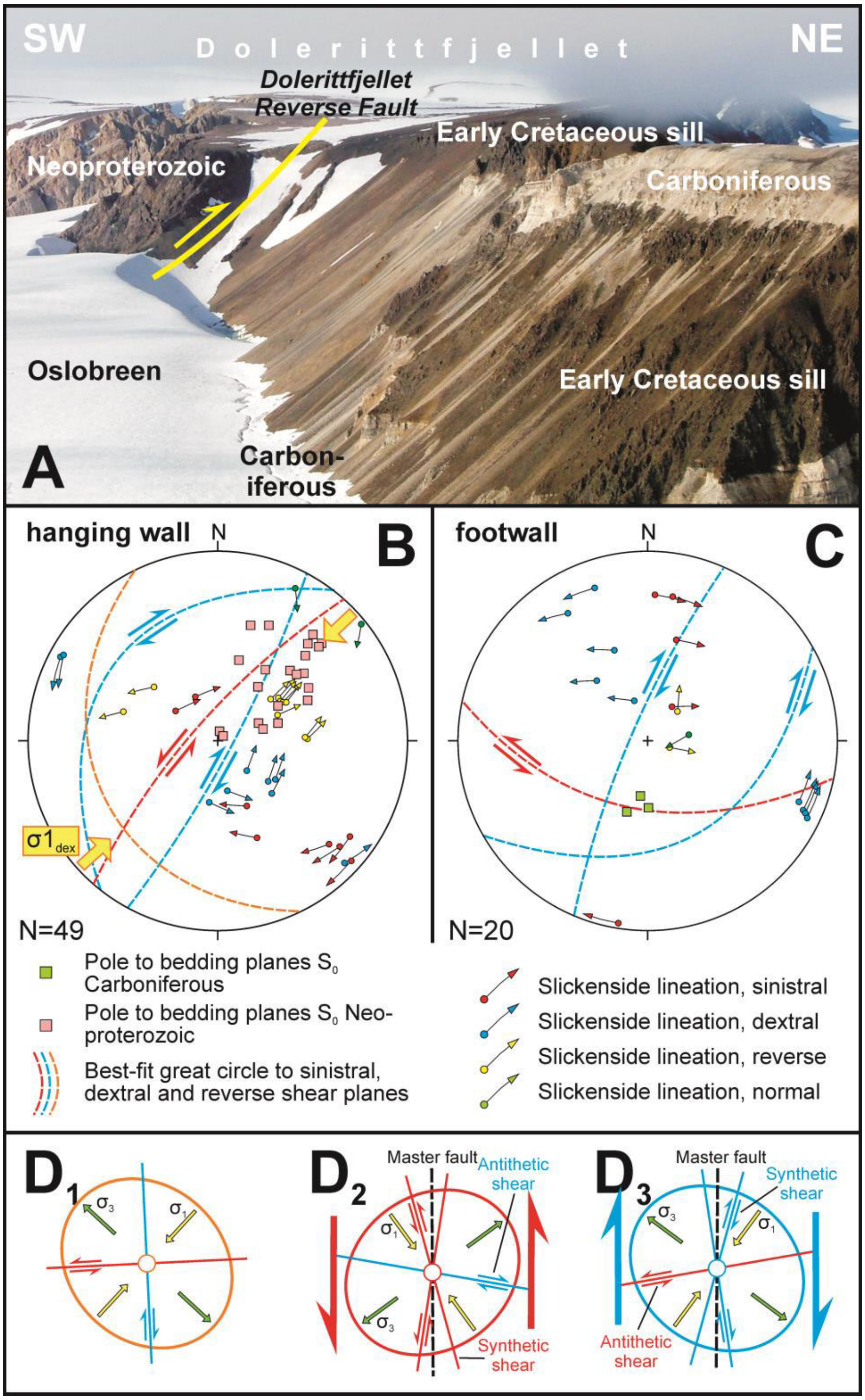
SW
Dolerittfjellet
NE
Dolerittfjellet Reverse Fault
Early Cretaceous sill
Neoproterozoic
Carboniferous
Oslobreen
Early Cretaceous sill
A
Carbon-iferous
hanging wall
N
B
footwall
N
C
σ1dex
N=49
N=20
Pole to bedding planes S0 Carboniferous
Pole to bedding planes S0 Neo-proterozoic
Best-fit great circle to sinistral, dextral and reverse shear planes
Slickenside lineation, sinistral
Slickenside lineation, dextral
Slickenside lineation, reverse
Slickenside lineation, normal
D1
σ3
σ1
D2
Master fault
Antithetic shear
σ1
σ3
Synthetic shear
D3
Master fault
Synthetic shear
σ3
σ1
Antithetic shear

Figure 16

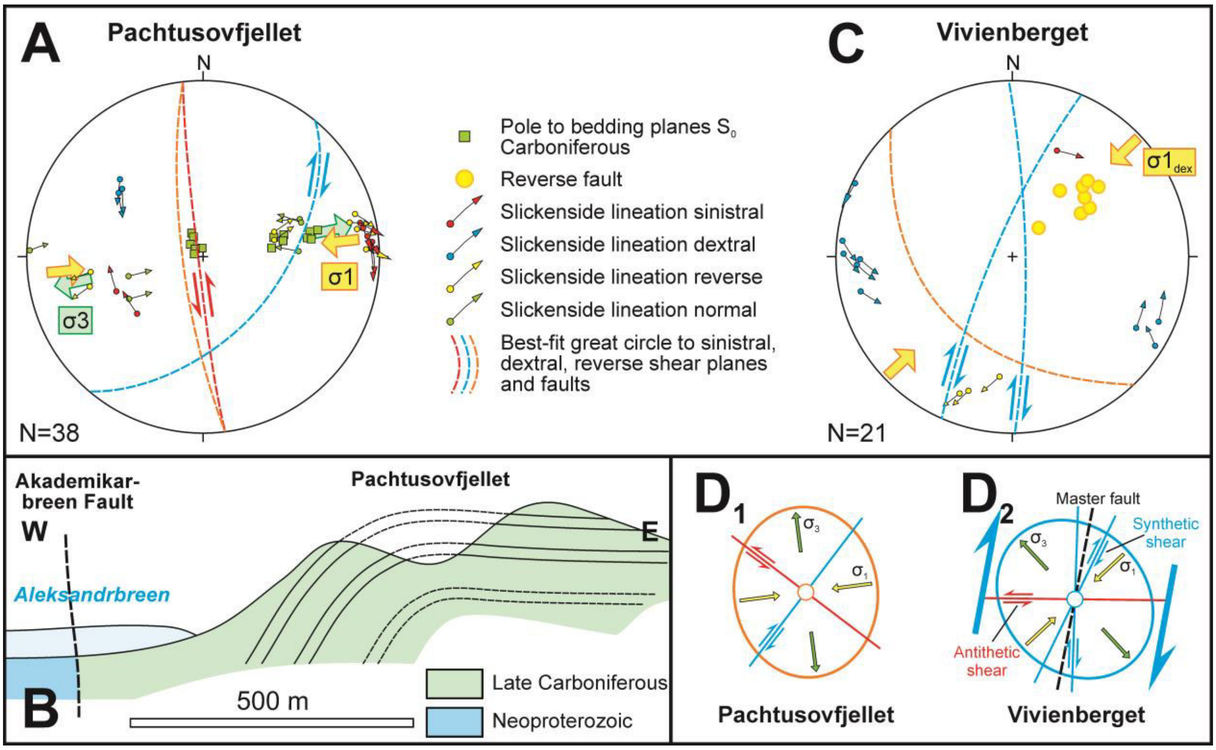

Figure 17 neu

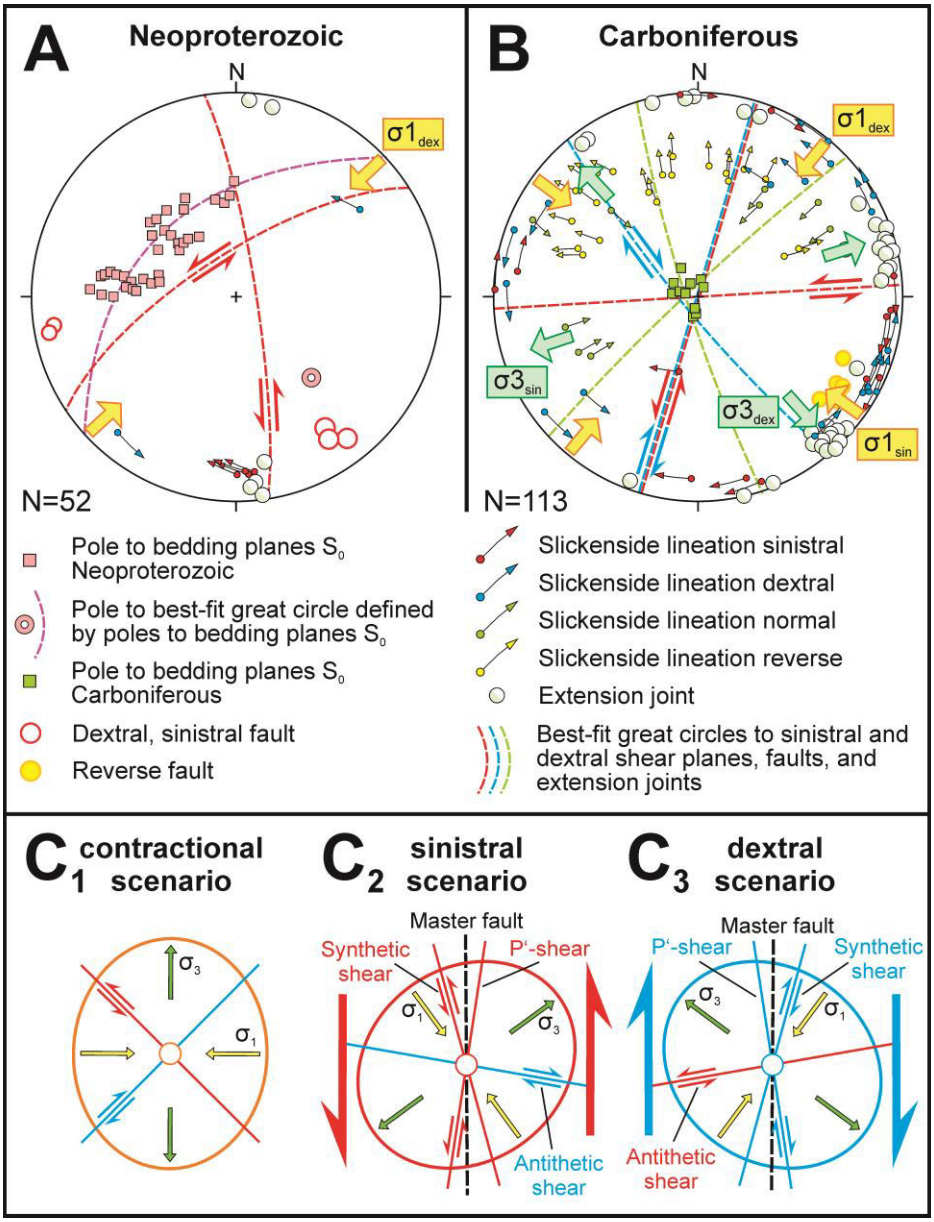

Figure 18 neu

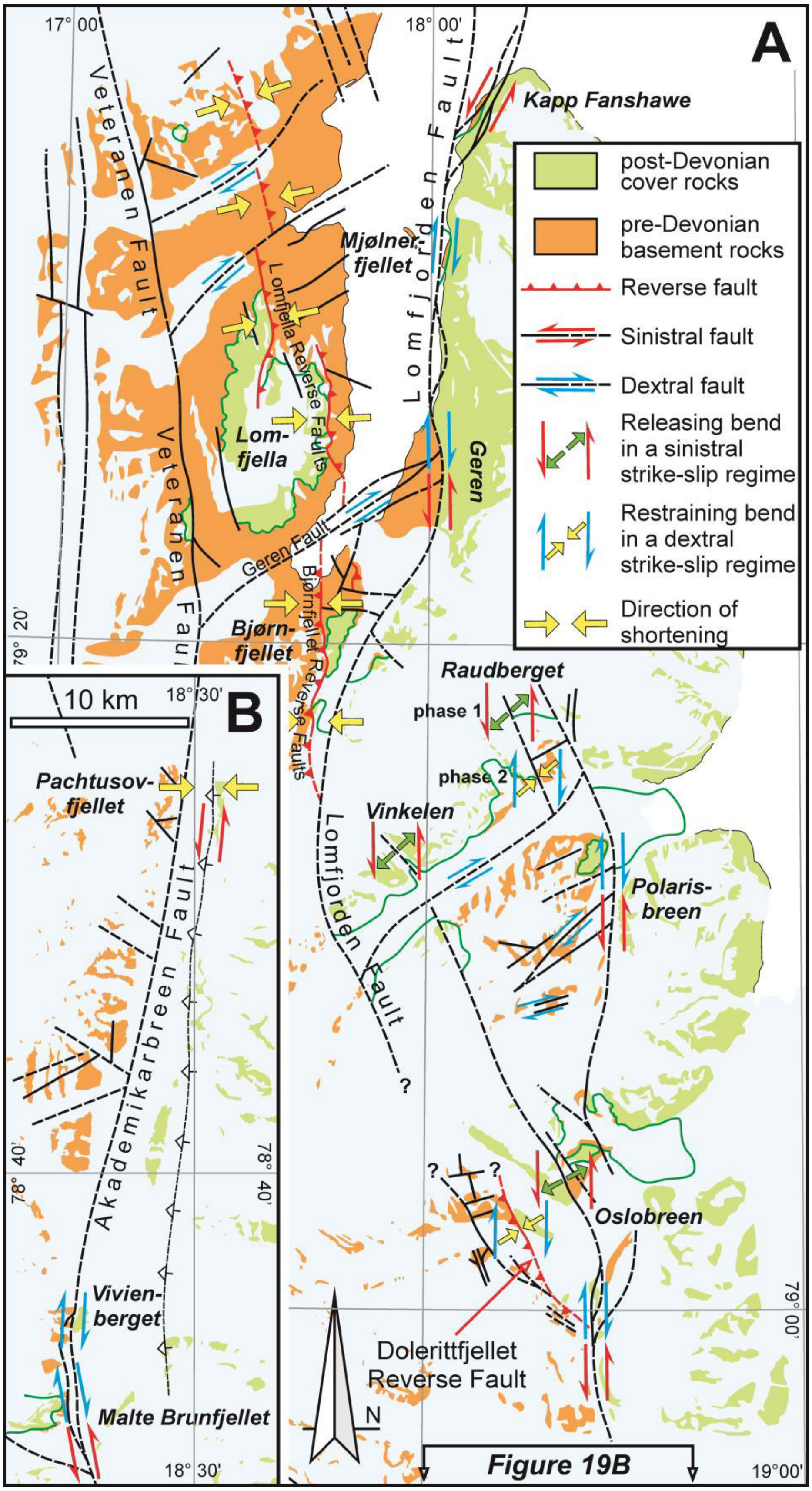

Figure 19 neu

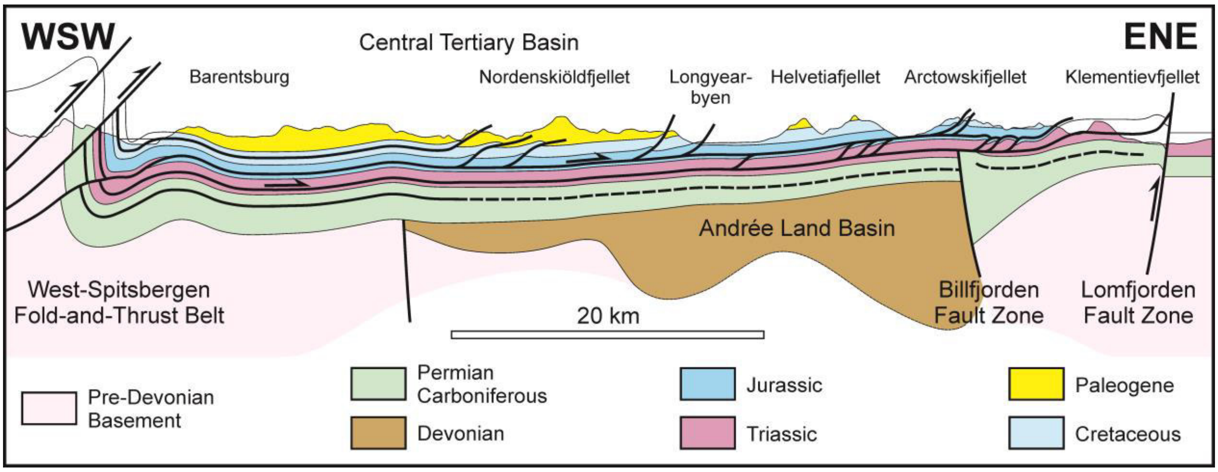
WSW
Central Tertiary Basin
ENE
Barentsburg
Nordenskiöldfjellet
Longyear-
byen
Helvetiafjellet
Arctowskifjellet
Klementievfjellet
Andrée Land Basin
West-Spitsbergen
Fold-and-Thrust Belt
20 km
Billfjorden
Fault Zone
Lomfjorden
Fault Zone
Pre-Devonian
Basement
Permian
Carboniferous
Devonian
Jurassic
Triassic
Paleogene
Cretaceous

Figure 20

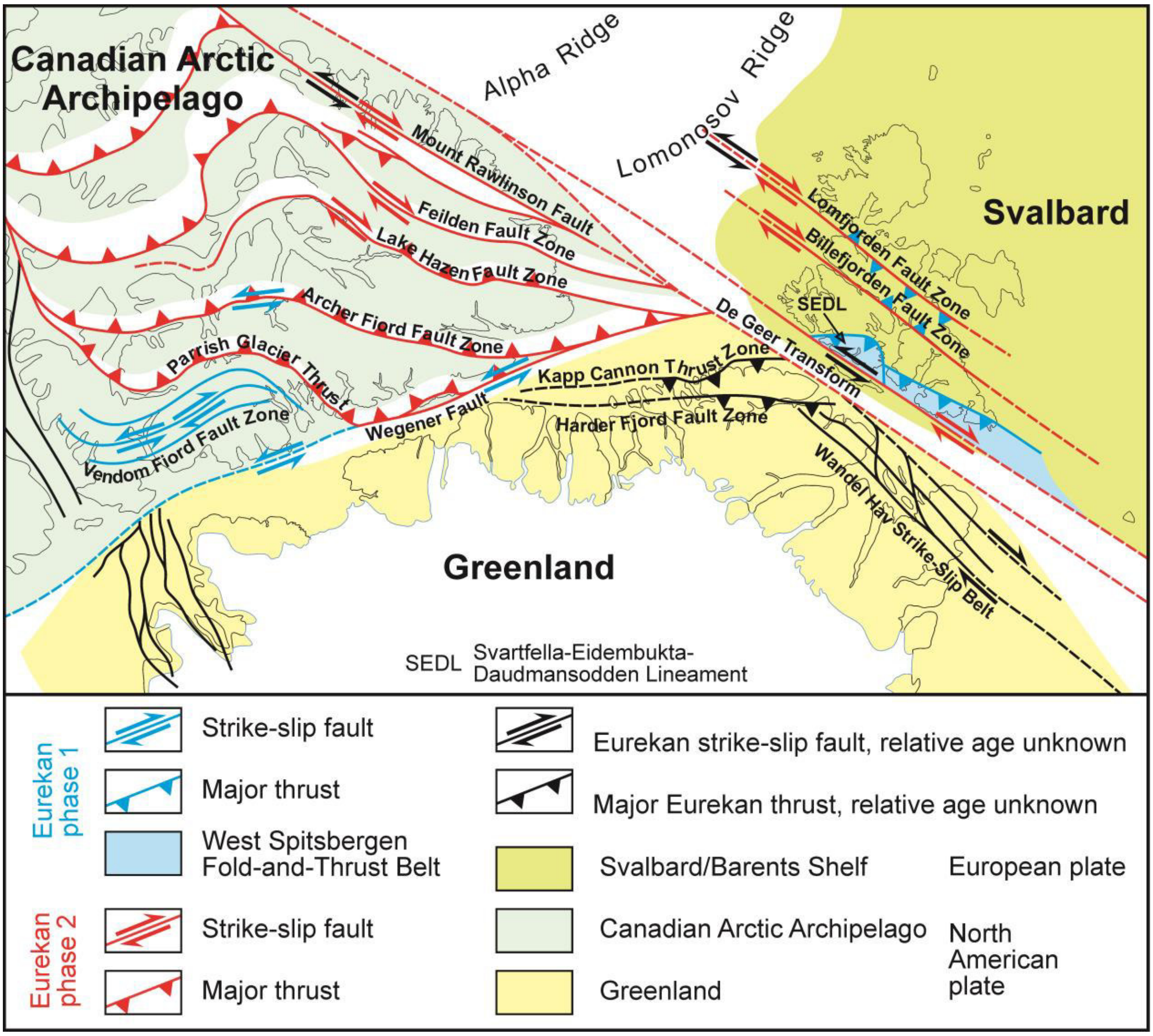
Canadian Arctic Archipelago
Alpha Ridge
Lomonosov Ridge
Svalbard
Mount Rawlinson Fault
Feilden Fault Zone
Lake Hazen Fault Zone
Archer Fiord Fault Zone
Parrish Glacier Thrust
Vendom Fiord Fault Zone
Wegener Fault
Kapp Cannon Thrust Zone
Harder Fjord Fault Zone
Wandel Hav Strike-Slip Belt
De Geer Transform
Lomfjorden Fault Zone
Billefjorden Fault Zone
SEDL
Greenland
SEDL Svartfella-Eidembukta-Daudmansodden Lineament
Eurekan phase 1
Strike-slip fault
Major thrust
West Spitsbergen Fold-and-Thrust Belt
Eurekan phase 2
Strike-slip fault
Major thrust
Eurekan strike-slip fault, relative age unknown
Major Eurekan thrust, relative age unknown
Svalbard/Barents Shelf
European plate
Canadian Arctic Archipelago
Greenland
North American plate

Figure 21